

# Novel insights in the function of the respiratory pump in ventilated ICU patients

A stylized, artistic illustration of the human respiratory system. The lungs are depicted in a soft, glowing purple and pink hue, with a network of branching bronchi visible. Below the lungs, the diaphragm is shown in a bright yellow color, with a central opening. The entire illustration is set against a dark blue background.

**Diana Jansen**

**RADBOD  
UNIVERSITY  
PRESS**

Radboud  
Dissertation  
Series

# **Novel insights in the function of the respiratory pump in ventilated ICU patients**

Diana Jansen

**Author:** Diana Jansen

**Title:** Novel insights in the function of the respiratory pump in ventilated ICU patients

**Radboud Dissertations Series**

ISSN: 2950-2772 (Online); 2950-2780 (Print)

Published by RADBOUD UNIVERSITY PRESS

Postbus 9100, 6500 HA Nijmegen, The Netherlands

[www.radbouduniversitypress.nl](http://www.radbouduniversitypress.nl)

Design: Proefschrift AIO | Manon de Snoo

Cover: Amy van den Berg

Printing: DPN Rikken/Pumbo

ISBN: 9789493296343

DOI: 10.54195/9789493296343

Free download at: [www.boekenbestellen.nl/radboud-university-press/dissertations](http://www.boekenbestellen.nl/radboud-university-press/dissertations)

© 2024 Diana Jansen

**RADBOUD  
UNIVERSITY  
PRESS**

This is an Open Access book published under the terms of Creative Commons Attribution-Noncommercial-NoDerivatives International license (CC BY-NC-ND 4.0). This license allows reusers to copy and distribute the material in any medium or format in unadapted form only, for noncommercial purposes only, and only so long as attribution is given to the creator, see <http://creativecommons.org/licenses/by-nc-nd/4.0/>.

# **Novel insights in the function of the respiratory pump in ventilated ICU patients**

Proefschrift ter verkrijging van de graad van doctor  
aan de Radboud Universiteit Nijmegen  
op gezag van de rector magnificus prof. dr. J.M. Sanders,  
volgens besluit van het college voor promoties  
in het openbaar te verdedigen op

donderdag 14 maart 2024  
om 10.30 uur precies

door

Diana Jansen  
geboren op 20 juli 1988  
te Bladel en Netersel

**Promotoren:**

prof. dr. L.M.A. Heunks

prof. dr. G.J. Scheffer

**Copromotoren:**

dr. C. Keijzer

dr. L.T. Van Eijk

**Manuscriptcommissie:**

prof. dr. H.F.M. van der Heijden

prof. dr. J. Horn

prof. dr. M.T.E. Hopman



# Table of contents

<b>Chapter 1</b>	General introduction and outline of this thesis Novel insights in ICU-acquired respiratory muscle dysfunction: implications for clinical care <i>Critical Care 2017</i>	Page 8 - 17
------------------	--	-------------

## **PART I: Physiological insights in inspiratory and expiratory muscle function**

<b>Chapter 2</b>	Positive end-expiratory pressure affects geometry and function of the human diaphragm <i>Journal of Applied Physiology 2021</i>	Page 18 - 43
<b>Chapter 3</b>	Expiratory muscle dysfunction in critically ill patients: towards improved understanding <i>Intensive Care Med 2019</i>	Page 44 - 61
<b>Chapter 4</b>	Respiratory muscle effort during expiration in successful and failed weaning from mechanical ventilation <i>Anesthesiology 2018</i>	Page 62 - 85

## **PART II: Monitoring diaphragm function in acutely ventilated patients**

<b>Chapter 5</b>	Estimation of the diaphragm neuromuscular efficiency index in mechanically ventilated critically ill patients <i>Critical Care 2018</i>	Page 86 - 103
<b>Chapter 6</b>	Monitoring patient-ventilator breath contribution in critically ill patients during neurally-adjusted ventilatory assist: reliability and improved algorithms <i>Journal of Applied Physiology 2019</i>	Page 104 - 123

### **PART III: Novel pharmacological interventions to modulate diaphragm function**

<b>Chapter 7</b>	Acetylcholine receptor antagonists in acute respiratory distress syndrome: much more than muscle relaxants <i>Critical Care 2018</i>	Page 124 - 131
<b>Chapter 8</b>	Neuromuscular blockers modulate inflammatory response and reactive oxygen production by peripheral blood mononuclear cells of healthy volunteers <i>Submitted</i>	Page 132 - 143

### **PART IV: Summary and future perspective**

<b>Chapter 9</b>	Summary	Page 144 - 149
<b>Chapter 10</b>	Discussion and future perspective	Page 150 - 157
<b>Chapter 11</b>	Nederlandse samenvatting	Page 158 - 163
	References	Page 164 - 175
	Research data management	Page 176
	Biografie	Page 177
	Publication list	Page 178
	Dankwoord	Page 179 - 185





## Chapter 1

### General introduction and outline of this thesis

---

## GENERAL INTRODUCTION

This is a modified version of our publication: A. Jonkman, D. Jansen and L.M.A. Heunks, chapter in 'Annual Update in Intensive Care 2017' entitled: 'Novel insights in ICU-acquired respiratory muscle dysfunction: implications for clinical care', dual publication in Critical Care. Crit Care. 2017 Mar 21;21(1):64.

The respiratory muscles drive ventilation. Under normal conditions, the diaphragm is the main muscle for inspiration, whereas expiration is largely passive driven by relaxation of the inspiratory muscles and elastic recoil pressure of the lung. A disturbance in the balance between loading and capacity of the respiratory muscles will result in respiratory failure. This may occur in the course of numerous disorders that increase loading of the diaphragm such as acute respiratory distress syndrome (ARDS), pneumonia, acute exacerbation of chronic obstructive airway disease (COPD) and ventilatory under-assist. On the other hand, the capacity of the respiratory muscles may be impaired due to (congenital) myopathies, acquired muscle dysfunction and ventilatory over-assist. Despite being life-saving, several studies have demonstrated that respiratory muscle function may further deteriorate by mechanical ventilation due to excessive unloading or unnoticed loading of the respiratory muscles. This is associated with prolonged duration of weaning, intensive care (re)admission and increased risk of complications [1-3]. Therefore, it is of critical importance to limit these ventilator-induced detrimental effects. In this introducing chapter we give an overview of the most relevant pathophysiologic pathways, monitoring tools and therapies for ventilator-induced diaphragm dysfunction.

### Effect on diaphragm structure

More than a decade ago, Levine et al. were the first to describe a rapid loss of diaphragm muscle mass in biopsies of 14 brain-dead organ donors on controlled mechanical ventilation for 18 to 69 hours before organ harvest [4]. The cross-sectional area (CSA) of diaphragm fibers was significantly lower (53% and 57% lower for fast- and slow-twitch fibers, respectively) compared to fibers obtained from patients referred for elective lung cancer surgery. This decrease in diaphragm fiber CSA was proportional to duration of mechanical ventilation (Pearson  $r^2 = 0.28$ )[5]. Interestingly, the severity of CSA atrophy was less pronounced in the pectoralis muscle, indicating that the diaphragm is much more sensitive to the effects of disuse. Hooijman et al. were the first to study these structural modifications in diaphragm biopsies obtained from living intensive care unit (ICU) patients on mechanical ventilation (mean duration MV: 7 days (range 14 to 607 hours))[6]. They confirmed

that, also in real ICU patients, both fast- and slow-twitch diaphragm fibers exhibited approximately 25% smaller CSA compared to diaphragm fibers from patients referred for elective surgery. As opposed to this well-known CSA atrophy characterized by a decrease in muscle fiber thickness, there is another form of structural adaptation, termed 'longitudinal fiber atrophy' [7], characterized by a shortening in diaphragm muscle fiber length. It is demonstrated in rats that prolonged mechanical ventilation with positive end-expiratory pressure (PEEP) results in diaphragm muscle fiber shortening, caused by the loss of sarcomeres in series [7]. The theory behind this adaptive response is that PEEP increase the end-expiratory lung volume (EELV) and thereby flatten the shape of the diaphragm dome (especially zone of apposition), which forces the muscle fibers to act at a shorter length during the respiratory cycle. However, at this shortened length the overlap of the myosin-based thick and actin-based thin filaments is not optimal and therefore less force can be generated. It seems that the rats in the previous mentioned study were able to reduce the number of sarcomeres in series in order to restore the optimal length for force generation. Thus, longitudinal fiber atrophy seems to be an adaptive response of muscles [8]. If similar adaptations develop in the human diaphragm is not yet known.

Besides the effects of mechanical ventilation on diaphragm structure, diaphragm inactivity may also lead to several biochemical and functional modifications as described by different studies in ventilated brain-dead patients [9, 10] and ICU patients [6]. Histological analysis demonstrated that the number of inflammatory cells including neutrophils and macrophages is significantly increased in the diaphragm of ICU patients [6]. In addition, van Hees et. al demonstrated that plasma of septic shock patients induces atrophy in (healthy) cultured skeletal muscle myotubes [11]. This supports a role for inflammatory mediators in the development of diaphragm atrophy or injury.

### **Effect on diaphragm function**

Structural modifications of the respiratory muscles as described above may have important functional implications. Single muscle fibers isolated from the diaphragm provide an excellent model to study contractile protein function *ex vivo*. It seems that the force generated by a single diaphragm fiber of ICU patients was reduced by more than 50% compared to non-ICU patients [6], resulting from the loss of contractile proteins (atrophy), but also contractile protein dysfunction. In clinical practice, the evolution of diaphragmatic thickness during mechanical ventilation and its impact on diaphragm function has been assessed with ultrasound [12]. It was found that both loss (44%) and gain (12%) of diaphragm thickness were observed during the first week of ventilation, which was significantly correlated ( $P=0.01$ ) with

the diaphragm thickening fraction (i.e. contractile activity of the diaphragm). The gold standard to evaluate *in vivo* diaphragm function is by measuring the change in airway pressure, or transdiaphragmatic pressure induced by magnetic stimulation of the phrenic nerves during an airway occlusion ( $P_{tr,magn}$  and  $P_{di,tw}$  respectively). It was demonstrated that 79% of the mechanically ventilated ICU patients developed diaphragm dysfunction (defined as a  $P_{tr,magn} < 11 \text{ cmH}_2\text{O}$ ) during their ICU stay [13]. Important to note was that 53% exhibited diaphragm dysfunction already at ICU admission, suggesting that besides mechanical ventilation other factors play a role [14]. Infection may be one of these factors, supported by the histological changes mentioned in the previous section. In addition, it seems that measures for *in vivo* contractile force are more affected in ventilated patients with infection compared to ventilated patients without infection [15], and that diaphragm dysfunction was independently associated with sepsis [13].

### Monitoring diaphragm function in ICU

As previously described, disuse is proposed to be an important risk factor for the development of diaphragm atrophy and dysfunction in ventilated patients. Therefore, a reasonable clinical goal is to limit the duration of respiratory muscle inactivity, by using partially assisted ventilatory modes as soon as feasible and safe. However, it should be mentioned that even in partially assisted ventilatory modes, complete unloading of the diaphragm may occur, which is often not recognized by clinicians when evaluating ventilator pressure and flow waveforms [16]. Thus there seems to be a role for more advanced respiratory muscle monitoring techniques [17, 18]. Today, the state of the art technique for monitoring diaphragm activity is the assessment of the transdiaphragmatic pressure ( $P_{di}$ ). This can be measured by simultaneous measurement of esophageal pressure ( $P_{es}$ ) and gastric pressure ( $P_{ga}$ ) as surrogate for the pleural and abdominal pressure, respectively. However, this technique is quite invasive and interpretation of waveforms may be complex [19, 20]. Diaphragm electromyography (EMG) is an alternative technique used to quantify breathing effort in ICU patients [17]. The electrical activity of the diaphragm ( $E_{adi}$ ) can be acquired using a dedicated nasogastric feeding tube with nine electrodes positioned at the level of the diaphragm muscle. The electrical activity is shown real-time on the ventilator screen (Servo-i/U, Maquet Sweden) and can be recorded in every ventilatory mode. There seems to be a strong correlation between  $E_{adi}$  and transdiaphragmatic pressure ( $P_{di}$ ) and esophageal pressure ( $P_{es}$ ) [21, 22]. In the literature there are two indices described that uses  $E_{adi}$  to estimate the patient's respiratory effort. The first index is the neuromechanical efficiency index (NME), defined by  $\Delta P_{aw} / \Delta E_{adi}$ , used to estimate the inspiratory effort breath-by-breath [22, 23]. The second index is the patient-ventilator breath contribution (PVBC) index, which

provides an estimation of the fraction of breathing effort that is generated by the patient compared to the total work of breathing (ventilator + patient). Liu et al. demonstrated that PVBC predicts the contribution of the inspiratory muscles versus the pressure delivered by the ventilator [24]. Today, both indices are only evaluated in small studies [22-26] and the repeatability, essential for any diagnostic tool, has not been investigated at all.

However, despite the known clinical relevance and the availability of several monitoring tools, clinicians do still not assess inspiratory effort as part of routine clinical care. Probably because additional nasogastric tubes and specific equipment are necessary and the interpretation of these measurements is quite complex and time consuming. For estimating the inspiratory drive during pressure support ventilation the P0.1 is a widely used tool [27], although it provides less information about the total dynamic lung stress generated by the ventilator and the patient's inspiratory effort. Recently, it was demonstrated that with the measurement of delta airway occlusion ( $\Delta P_{occl}$ ) both excessive inspiratory effort ( $P_{mus}$ ) and dynamic lung stress (delta transpulmonary pressure) can be detected [28]. They also showed that irrespective of depth of sedation or mode of ventilation, both inspiratory effort and dynamic lung stress frequently (89% and 69%, respectively) exceed safe thresholds, both underestimated by airway pressure values available on the ventilator.

### **Strategies to prevent diaphragm dysfunction**

Although respiratory muscle weakness may already be present at ICU admission [13], many patients develop weakness while in the ICU [14]. In the first phase of severe critically illness partially assisted ventilatory modes are often not feasible, and the patient is ventilated in controlled ventilatory modes with full unloading of the respiratory muscles. An interesting intervention in this category of patients is electrical activation of the diaphragm ("pacing") by stimulation of the phrenic nerves to keep the muscles 'active' and thereby limit the development of diaphragm weakness. Just like pacing of the quadriceps in COPD patients improve muscle performance and exercise capacity [29]. However, phrenic stimulation might not be feasible for therapeutic purposes, as prolonged transcutaneous pacing is uncomfortable for patients and proper positioning of the stimulator is cumbersome in an ICU setting. Earlier studies suggest that early transvenous phrenic nerve pacing can yield diaphragm contractions which reduce the positive pressure required for a ventilator to deliver breaths [30]. Another method that is currently being explored is bilateral phrenic nerve stimulation by the use of transcutaneous magnetic stimulation [31]. Sotak et al. showed that pacing of the phrenic nerve induced

contraction of the diaphragm and reduces both the rate of atrophy during mechanical ventilation and even increases its thickness [32].

## **Our study**

In partially assisted ventilatory modes, both disuse atrophy resulting from ventilator over-assist [4, 5, 12] and high respiratory muscle effort resulting from ventilator under-assist [3, 33] may induce diaphragm dysfunction. Therefore, a strong rationale exists to monitor diaphragm effort and titrate ventilatory support to maintain respiratory muscle activity within physiological limits [33] and thereby prevent development of diaphragm dysfunction. Recently, we demonstrated that partial neuromuscular blockade of the respiratory muscles could facilitate lung protective ventilation by reducing the physical forces applied to the lung while maintaining respiratory muscle activity [34]. However, many questions remain unanswered, due to the small number of patients, the relatively short duration (2 hours) and absence of a control group. Further studies should evaluate the feasibility of this intervention.

Sepsis is a recognized risk factor for the development of respiratory muscle weakness [14], but besides appropriate treatment of sepsis, no specific interventions can be applied to protect the respiratory muscles. Certain drugs have been associated with the development of respiratory muscle weakness, in particular corticosteroids and neuromuscular blockers. However, the effect of both drugs, together or separately, on muscle dysfunction is complex and beyond the scope of this paper. We refer to an excellent recent review on this subject [35].

## **Strategies to restore diaphragm dysfunction**

Loss of muscle mass plays an important role in the development of ICU-acquired respiratory muscle dysfunction [4]. Therefore, strategies that improve respiratory muscle strength are of potential clinical importance. Surprisingly, very few studies have evaluated strategies to enhance respiratory muscle function in these patients. Martin et al. demonstrated that inspiratory muscle strength training in 69 weaning-patients improved inspiratory muscle strength (primary outcome) and fastened liberation from the ventilator, without development of side effects. However in a trial a few years later no clinical benefits (such as length of stay or risk of readmission) were found despite respiratory muscle strength was significantly improved [36]. In addition, pharmacological interventions that restore muscle strength are discussed earlier by our group [37]. Although the effect of high-dose antioxidants, specific feeding strategies or anabolic steroids demonstrates encouraging results in animal models, no data support beneficial effects ICU patients with respiratory muscle weakness.

In addition to atrophy, dysfunction of the remaining muscle fibers has been demonstrated in critically ill patients [6, 12, 14]. Accordingly, optimizing contractility using positive inotropes seems a reasonable approach in these patients. Levosimendan is a relatively novel cardiac inotrope, that enhances the binding of calcium to troponin and improves contractile efficiency of the muscle fibers. Levosimendan has been shown to enhance contractile efficiency of muscle fibers isolated from the diaphragm of healthy subjects and patients with COPD [38]. In another study with healthy subjects it was demonstrated that levosimendan reverses fatigue and improves neuromechanical efficiency of the diaphragm *in vivo* [39]. Future studies should evaluate the effects of levosimendan on respiratory muscle function in difficult to wean patients.

## RATIONALE AND OUTLINE OF THIS THESIS

Diaphragm weakness is highly prevalent in ICU patients and associated with adverse outcomes such as prolonged duration of weaning, increased risk of ICU mortality and (re)admission. In the last decade, our understanding of the pathophysiology of ICU-acquired respiratory muscle dysfunction has importantly improved. However, this has also raised new questions which will be investigated and discussed in the following parts of this thesis.

### Part I: Physiological insights in inspiratory and expiratory muscle function

It is striking that most of previous studies have focused mainly on the effect of different ventilatory modes and levels of assist, on the inspiratory muscles, while the effect of other frequently used ventilatory settings, like PEEP, and the effect on and/or contribution of the expiratory muscles has been largely neglected.

Experimental data of our group showed that rats on mechanical ventilation with PEEP developed longitudinal fiber atrophy, by the loss of sarcomeres in series [7]. It would be of interest to know whether these long-term diaphragm adaptations also occur in ventilated ICU patients. However, first the acute effects of PEEP on the *in vivo* human diaphragm should be assessed, as acute changes in diaphragm geometry and function are a prerequisite for development of longitudinal atrophy. In **Chapter 2** we show our results of a study we performed in healthy subjects, in which we studied the acute effects of PEEP on the *in vivo* human diaphragm.



The impact of the expiratory muscles on the pathophysiology of diaphragm dysfunction is discussed in **Chapter 3** and **4**. **Chapter 3** represents a narrative review on the current knowledge on the (patho)physiology of expiratory muscle function in ICU patients. It seems that the expiratory muscles exhibit tonic activity during normal tidal breathing to counteract gravitational forces and maintain the diaphragm at optimal length for pressure generation. When the respiratory load increases or the inspiratory muscle capacity decreases, the expiratory muscles becomes active, likely to enhance inspiratory muscle capacity. In **Chapter 4** we investigate whether the expiratory muscle effort is indeed greater in patients with impaired inspiratory muscle capacity who fail to wean from mechanical ventilation.

## **Part II: Monitoring diaphragm function in acutely ventilated patients**

Despite the number of respiratory monitoring tools has increased significantly, assessment of inspiratory effort is still not part of routine clinical care, because most of them require dedicated equipment and skills and are time-consuming. Since most of the ICU patients already have a nasogastric tube in place, we decided to assess the repeatability of two indices that use the electrical activity of the diaphragm (measured by a specific nasogastric tube) to measure respiratory effort. In **Chapter 5** we investigate the neuromechanical index and in **Chapter 6** we discuss the usefulness of the patient-ventilator breath contribution (PVBC) index.

## **Part III: Novel pharmacological interventions to modulate diaphragm function**

As the underlying cause of diaphragm dysfunction is multifactorial, it is difficult to find one solution that can prevent or restore diaphragm dysfunction. One of our pillars lies in the effort to reduce excessive respiratory muscle activity by the administration of partial neuromuscular blockade. **Chapter 7** provides an overview of the mechanism of action of the neuromuscular blocking agent (NMBA) itself, which goes beyond neuromuscular blockade only. Several studies, in a selected group of patients, have demonstrated that non-depolarizing NMBAs itself might protect against the development of ventilator-induced lung injury through a direct, dose-dependent anti-inflammatory effect. Most of these studies were performed with cisatracurium, while in our country rocuronium and succinylcholine are more frequently used. In **Chapter 8** we demonstrate the immunomodulatory effects of these NMBAs in healthy volunteers.

In **Chapter 9 and 11** we present a summary of this thesis and in **Chapter 10** the results of our research are discussed in a broader scientific context. In addition, recommendations for future research are made.

## REFERENCES

See page 166.

**PART I:**  
**Physiological insights in inspiratory  
and expiratory muscle function**

## Chapter 2

# Positive end-expiratory pressure affects geometry and function of the human diaphragm

---

**Diana Jansen\*** and Annemijn H. Jonkman\*

Heder J. de Vries, Myrte Wennen, Judith Elshof, Maud A. Hoofs, Marloes van den Berg, Angelique M.E. de Man, Christiaan Keijzer, Gert-Jan Scheffer, Johannes G. van der Hoeven, Armand Girbes, Pieter Roel Tuinman, J. Tim Marcus, Coen A.C. Ottenheijm, Leo M.A. Heunks

*\* Both authors contributed equally to this manuscript*

*Journal of Applied Physiology 2021: doi:10.1152/jappphysiol.00184.2021*

## ABSTRACT

### Introduction

Positive end-expiratory pressure (PEEP) is routinely applied in mechanically ventilated patients to improve gas exchange and respiratory mechanics by increasing end-expiratory lung volume (EELV). In a recent experimental study in rats, we demonstrated that prolonged application of PEEP causes diaphragm remodeling, especially longitudinal muscle fiber atrophy. This is of potential clinical importance, as the acute withdrawal of PEEP during ventilator weaning decreases EELV and thereby stretches the adapted, longitudinally atrophied diaphragm fibers to excessive sarcomere lengths, having a detrimental effect on force generation. Whether this series of events occurs in the human diaphragm is unknown. In the current study we investigated if short-term application of PEEP affects diaphragm geometry and function, which are prerequisites for the development of longitudinal atrophy with prolonged PEEP application.

### Methods

Nineteen healthy volunteers were non-invasively ventilated with PEEP levels of 2, 5, 10 and 15 cmH<sub>2</sub>O. Magnetic resonance imaging was performed to investigate PEEP-induced changes in diaphragm geometry. Subjects were instrumented with nasogastric catheters to measure diaphragm neuromechanical efficiency (i.e., diaphragm pressure normalized to its electrical activity) during tidal breathing with different PEEP levels.

### Results

We found that increasing PEEP from 2 to 15 cmH<sub>2</sub>O resulted in a caudal diaphragm displacement (19 [14-26] mm,  $P<0.001$ ), muscle shortening in the zones of apposition (20.6% anterior and 32.7% posterior,  $P<0.001$ ), increase in diaphragm thickness (36.4 [0.9-44.1] %,  $P<0.001$ ) and reduction in neuromechanical efficiency (48 [37.6-56.6] %,  $P<0.001$ ).

### Conclusion

These findings demonstrate that conditions required to develop longitudinal atrophy in the human diaphragm are present with the application of PEEP.

### New and noteworthy

We demonstrate that PEEP causes changes in diaphragm geometry, especially muscle shortening, and decreases in vivo diaphragm contractile function. Thus, prerequisites for the development of diaphragm longitudinal muscle atrophy are present with

the acute application of PEEP. Once confirmed in ventilated critically ill patients, this could provide a new mechanism for ventilator-induced diaphragm dysfunction and ventilator weaning failure in the intensive care unit (ICU).

**Keywords:** Diaphragm contractile function, Diaphragm geometry, Positive end-expiratory pressure

## INTRODUCTION

Diaphragm weakness is highly prevalent in critically ill mechanically ventilated patients and may be associated with adverse outcomes such as difficult ventilator weaning, prolonged ICU stay, higher risk of complications, and mortality [3, 40, 41]. While many factors could contribute to the development and severity of diaphragm weakness [42], inappropriate inspiratory ventilator assist plays a prominent role, as over-assist is associated with diaphragm muscle fiber atrophy [4, 5, 43] and under-assist has been hypothesized to result in load-induced diaphragm injury [33, 44, 45]. In addition to inspiratory assist, expiratory assist (i.e., positive end-expiratory pressure (PEEP)) is applied to improve gas exchange and respiratory mechanics by increasing end-expiratory lung volume (EELV). Previous studies evaluated the effects of increased EELV on diaphragm geometry [46-49] and function [50, 51]. However, in those studies EELV was increased by active inspiration from functional residual capacity (FRC) up to total lung capacity (TLC), which might have different impact on diaphragm geometry and function, compared to a passive increase in EELV with the application of PEEP. Using two-dimensional ultrasound, we recently demonstrated that PEEP results in caudal movement of the diaphragm in ventilated ICU patients [7]. Moreover, our experimental study in rats demonstrates that prolonged application of PEEP induced shortening of the diaphragm muscle fibers and results in muscle fiber remodeling. This remodeling is mainly characterized by a reduced muscle length due to the loss of sarcomeres in series [7]. We termed this “longitudinal atrophy” [7], which is pathophysiologically different from the well-known cross-sectional atrophy that is characterized by a decreased muscle fiber thickness [4, 6, 52, 53]. Longitudinal atrophy is considered an adaptive response of muscles to restore their optimal length for force generation [8]. Whether PEEP-induced longitudinal fiber atrophy develops in the human diaphragm is unknown. This is of potential clinical importance during ventilator weaning: the acute release of PEEP upon patient-ventilator disconnection acutely decreases EELV and thereby stretches the adapted, longitudinally atrophied diaphragm fibers to excessive sarcomere lengths (for schematic, see **Fig.1**), having a detrimental effect on force generation.

Before investigating potential long-term diaphragm adaptations to PEEP in ICU patients, the acute short-term effects of PEEP on the *in vivo* human diaphragm should be assessed (i.e., the effects occurring at T1 in Fig.1), as acute changes in diaphragm geometry and function are a prerequisite for muscle remodeling associated with longitudinal atrophy. The current study tested the hypotheses that short-term application of PEEP 1) causes changes in diaphragm geometry, especially shortening and thickening of the diaphragm muscle in the zones of apposition (ZoA) and 2)

decreases *in vivo* contractile diaphragm function. We tested both hypotheses in healthy volunteers under non-invasive ventilation (NIV) with increasing levels of PEEP.

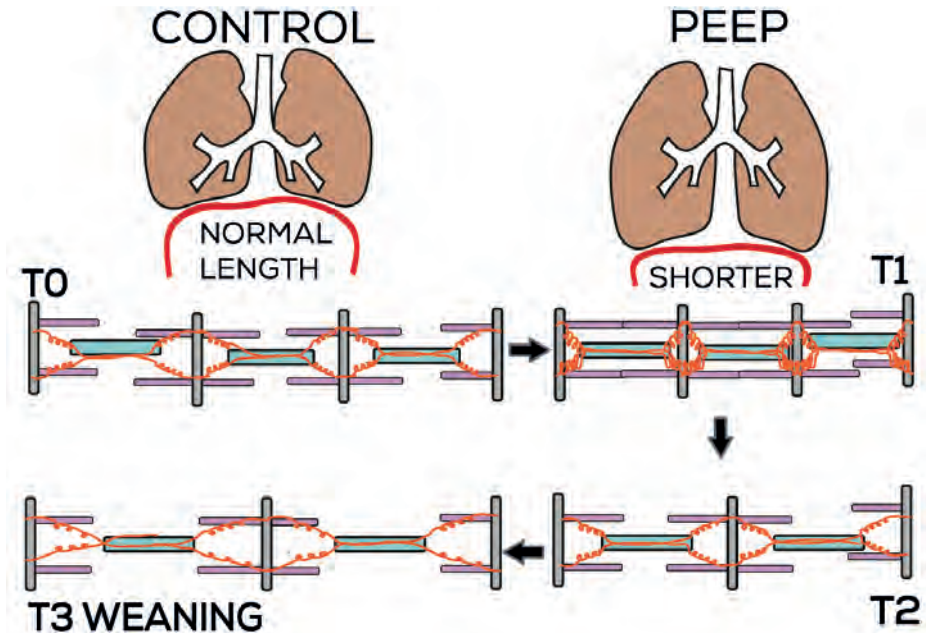


**Figure 1.** Schematic illustrating the hypothetical framework of the development of longitudinal atrophy in diaphragm fibers during mechanical ventilation with positive end-expiratory pressure (PEEP). Sarcomere absorption after long-term application of PEEP (T0 to T2) was demonstrated in previous experimental work (17). The current study investigates the geometrical and functional effect of acute changes in PEEP in the human diaphragm, i.e.: the effects occurring at T1. T0: Normal muscle resting length at end-expiration, without application of PEEP. For simplicity, only three sarcomeres were drawn. T1: The acute effect of PEEP on sarcomere length: application of PEEP results in a shorter muscle and more overlap of the thin (actin) and thick (myosin) filaments, i.e., a less optimal length for tension generation and that will acutely reduce diaphragm efficiency. T2: Long-term application of PEEP causes muscle remodeling: sarcomere absorption occurs to restore sarcomere length back to its original position for optimal tension generation. T3: The acute withdrawal of PEEP upon patient-ventilator disconnection acutely decreases end-expiratory lung volume and thereby stretches the adapted, longitudinally atrophied diaphragm fibers to excessive sarcomere lengths. At these lengths, overlap of the actin and myosin filaments within sarcomeres is suboptimal or even absent. This will substantially reduce the force generating capacity of the muscle fiber.



## MATERIALS AND METHODS

### Ethical Approval

This proof-of-principle study was performed at the Amsterdam UMC, location VUmc. The protocol was approved by the institutional research ethics board (ethics ref. 2017.590) and conducted in accordance with the Declaration of Helsinki and its later amendments.

### Study participants

We recruited 19 healthy volunteers. Exclusion criteria were contraindications for magnetic resonance imaging (MRI) (e.g., electrical/metallic implants, claustrophobia) and for placement of nasogastric catheters (e.g., esophageal varices, recent (<2 weeks) nasal bleeding, use of anticoagulants). Written informed consent was obtained.

### Study design

The protocol was divided into two parts: in healthy subjects we investigated PEEP-induced effects on diaphragm 1) geometry using MRI, and 2) contractile function using transdiaphragmatic pressure and electromyography.

### Part 1: Static MRI

Magnetic resonance (MR) imaging was performed with a 1.5 Tesla MR scanner (MAGNETOM Avanto, Siemens Medical Solutions, Erlangen, Germany) using a 6-channel phased-array coil. NIV was applied using a face mask (Nivairo RT046 NIV Mask, Fisher & Paykel Healthcare, Auckland, New Zealand) and an MRI-compatible ventilator (Servo-i, Getinge, Sweden). A leak test was performed and the face mask was fitted tightly and according to clinical protocols to minimize leaks (<15-20%). An oil-filled flexible tube was positioned around the subjects' costal margin to act as localization marker, as an estimator for the insertion of the diaphragm muscle into the thoracic wall during MRI [49]. Subjects were in supine position throughout the scanning protocol and randomized to a PEEP level of 5, 10 or 15 cmH<sub>2</sub>O (PEEP\_random); PEEP\_random was only used in step 1 and 2 of the experimental protocol. At baseline, PEEP was 2 cmH<sub>2</sub>O (a PEEP level below 2 cmH<sub>2</sub>O cannot be applied in NIV mode with the Servo-i ventilator for safety reasons), applied pressure support level 0 cmH<sub>2</sub>O, fractional inspired oxygen tension (FiO<sub>2</sub>) 0.21, inspiratory rise time 0.1 sec and inspiratory cycle off of 30%.

### Experimental protocol

The experimental protocol started after the subject was familiarized to NIV at 5 cmH<sub>2</sub>O PEEP for 5 minutes. The protocol was designed to obtain static MR images in different planes and PEEP levels of 2, 5, 10 and 15 cmH<sub>2</sub>O were applied to determine PEEP-induced changes in position, shape, length and thickness of the diaphragm; for MRI settings, see **Table 1**.

**Table 1.** Magnetic resonance imaging settings for 1) full coverage imaging in healthy subjects, and 2) high-resolution imaging in the sagittal right (SAG-R) plane in healthy subjects

	Static full coverage imaging	High resolution imaging SAG-R
Pulse sequence	Steady state free precession	T1-weighted turbo spin echo
Number of slices	35 to 45	1
Field of view <sup>1</sup>	400 x 400 mm (COR-mid) 280 x 340 mm (SAG-R)	280 x 340 mm
Slice thickness	8 mm	5 mm
Acquisition matrix (col x row)	168 x 256 (COR-mid) 108 x 256 (SAG-R)	250 x 384
Repetition time	285 ms	606 ms
Echo time	1.14 ms	25 ms
Turbo factor	Not applicable	12
Flip angle	80 degrees	180 degrees
Bandwidth	1149 Hz/pixel	303 Hz/pixel
Parallel imaging	Grappa, acceleration factor 2	Not applied

<sup>1</sup>This was the average field of view

All MRI measurements were performed during an end-expiratory breath hold of up to 30 seconds (i.e., for the duration of the image acquisition), to ensure that the observed effects were caused by passive lung volume increase solely and not by any inspiratory effort. The scanning protocol consisted of the following steps:

1. Full coverage imaging at baseline PEEP and PEEP\_random: the entire thorax was scanned in the sagittal and coronal orientations to obtain full coverage stacks. Images were used to plan the orientations used in step 2 and 3.
2. Static imaging at baseline PEEP and PEEP\_random: sagittal images were acquired through the top of the right hemidiaphragm dome (SAG-R, as planned on the COR full coverage stack) and coronal mid images were obtained through the top of both diaphragm domes (COR-mid, as planned on the SAG full coverage stack).

3. High spatial resolution imaging at all PEEP levels: images were obtained in the SAG-R plane, allowing a detailed assessment of diaphragm geometry, including the detection of muscle to tendon transition and diaphragm thickness. The left sagittal plane was not scanned as any tissue movement (i.e., heart motion) during the acquisition period would affect image quality.

### *Image analysis*

The following parameters were determined using XERO viewer (Agfa HealthCare GmbH, Bonn, Germany) and ImageJ (version 1.51; National Institutes of Health, USA).

### **High spatial resolution SAG-R images (see Fig. 2a and 5a/b)**

1. *Diaphragm displacement*: at the top of the dome (identified visually) and at 50% anterior and 50% posterior (i.e., the point on the dome halfway between its top and the inner anterior and posterior border of the thorax, respectively), a straight line was drawn to the upper edge of the image field of view, which was fixed during all measurements. Diaphragm displacement was calculated as the change in position relative to its baseline position.
2. *Diaphragm shape (posterior angle and K-dome)*: at the 50% posterior position a straight line was drawn through this point, in parallel to the diaphragm curvature. The posterior angle (alpha) was calculated between this line and the height axis. The larger alpha, the steeper the posterior diaphragm orientation. K-dome was determined as the length of the diaphragm dome divided by the diaphragm diameter (i.e., distance between the anterior and posterior diaphragm insertion into the thorax) [49].
3. *Anterior-posterior thoracic diameter*: maximal diameter measured from the inner anterior border to the inner posterior border of the thorax.
4. *Diaphragm length*: dome length was measured as the curved length from the anterior to the posterior diaphragm insertion into the thoracic wall. The distance from these insertion points to the localization marker was defined as the anterior and posterior zone of apposition (ZoA) length, respectively.

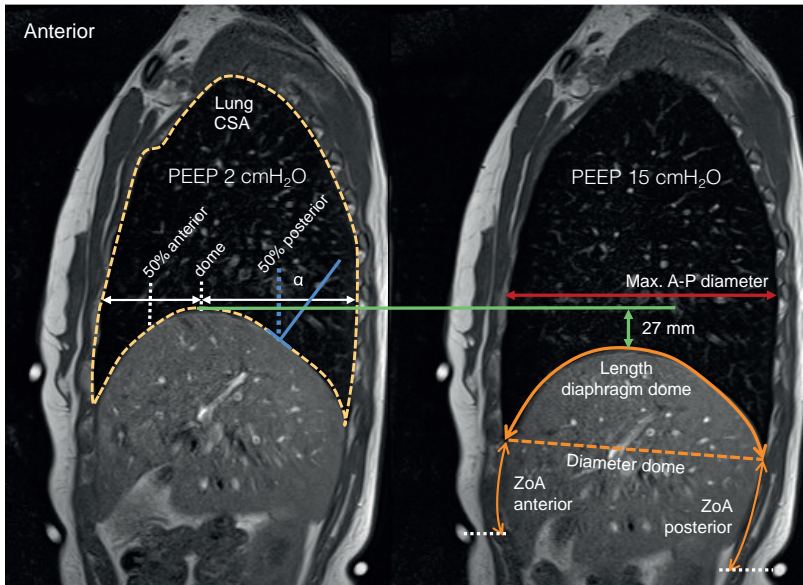


**Figure 2a.** Static high-resolution MRI at end-expiration (sagittal right plane) in a representative subject, with a PEEP of 2 cmH<sub>2</sub>O (left) and 15 cmH<sub>2</sub>O (right). The white dots on the subject's surface are from an oil-filled tube positioned around the costal margin acting as a localization marker. Measured parameters at all PEEP levels. *Left:* in white the determination of the top of the diaphragm dome, and at 50% anterior and 50% posterior. In blue the shape of the posterior diaphragm (angle). In light-yellow the lung cross sectional area. *Right:* in orange the measurement of the length of the anterior and posterior zone of apposition, the length of diaphragm dome and the diameter of the diaphragm (dashed line, to calculate K-dome (K-dome = length dome / diameter dome)). In red the maximum anterior-posterior thoracic diameter. In green the caudal displacement of the diaphragm due to PEEP, measured at the top of the diaphragm dome.

5. *Tendon length:* the tendon length was estimated indirectly. For those subjects in which the anterior and posterior muscular part of the diaphragm could be visualized, tendon length was measured as the distance between these two muscular parts, see also Figure 5a.
6. *Diaphragm thickness:* as muscle, liver and soft tissue have different gray values on MRI, diaphragm thickness could be measured using averaged gray intensity profile plots of a line drawn from the soft tissue (white pixels) to the liver (light gray pixels). Diaphragm (dark gray pixels) thickness was estimated as the distance between the transition in gray values.
7. *Lung cross-sectional area (CSA):* area within the outline of the inner thoracic cage and the diaphragm dome.

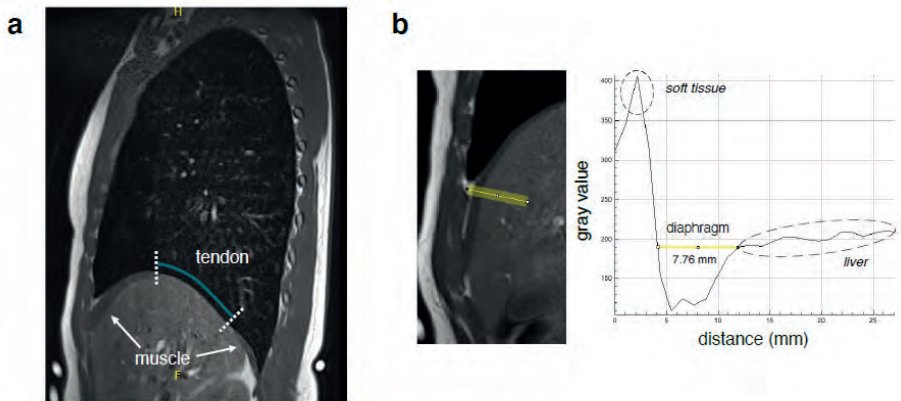


**Figure 5.** (a): Example of the visualization of the muscular part of the diaphragm. The green line denotes the tendon part. The white arrows point to the muscular parts. (b): Example of the measurement of the diaphragm thickness at PEEP level of 2 cmH<sub>2</sub>O (SAG-R), using gray value mapping. *Left*: a line was drawn from the soft tissue (white) to the liver (light gray) with the diaphragm (dark gray) in between. The corresponding averaged gray intensity profile plot is displayed on the right. The high gray values indicate the ‘white’ pixels (soft tissue), the lower gray values the ‘dark gray’ pixels (diaphragm) and the intermediate gray values the ‘light gray’ pixels (liver). Diaphragm thickness was estimated as the distance between the transition in gray values, as shown by the yellow line in the intensity plot.

### COR-mid images

8. *Left-right thoracic diameter*: maximal diameter from the inner left border to the inner right border of the thoracic wall.

### SAG-R full coverage stack

9. *Intrathoracic volume*: the lung CSA of twenty consecutive images of the right hemithorax was measured and multiplied by slice thickness (8 mm) [54]; values were summed to estimate right intrathoracic volume. These estimates allow assessment of volume differences related to PEEP, as well as to estimate whether changes in lung CSA as measured in the single SAG-R high resolution image are representative for changes in total right hemi-thoracic volume.

### Reliability of MRI parameters

Measurements for the main analysis were performed by one observer. Image analysis from a randomly chosen subject (66 measurements) was repeated by this observer for intra-rater reliability test. A second observer repeated the measurements from three random subjects (182 measurements) for assessment of inter-rater reliability.

## Part 2: Physiological measurements

### *Experimental protocol*

Subjects were in supine position while NIV was applied with the same ICU ventilator and the same face mask and ventilator settings as for the MRI protocol described above. Again, the experimental protocol started after the subject was familiarized to NIV at 5 cmH<sub>2</sub>O PEEP for 5 minutes. PEEP levels of 2 (baseline), 5, 10 and 15 cmH<sub>2</sub>O were applied in stepwise increments for 15 minutes each. In between these steps, PEEP was reduced to baseline for 5 minutes. PEEP of 5 cmH<sub>2</sub>O was applied twice to evaluate if measurements at the beginning and end of the protocol were consistent. Throughout the experiment, we recorded continuous data on ventilation, respiratory effort and diaphragm electromyography for offline time-series analysis. At each PEEP level, magnetic stimulation of the phrenic nerves was performed to measure diaphragm twitch strength (see below).

### *Nasogastric catheters, EMG electrodes, flow and airway pressure*

Gastric pressure (Pga) and esophageal pressure (Pes) were obtained with a nasogastric catheter equipped with two air-filled balloons (Nutrivent 16 Fr catheter, Sidam group, Mirandola, Italy). Transdiaphragmatic pressure (Pdi) was calculated as Pga - Pes. Correct catheter position and inflation of the balloons was confirmed using the end-expiratory occlusion test [55] and by observing cardiac oscillations and esophageal spasms in the Pes signal, whereas these artifacts were not visible in Pga tracings. At the same time of pressure measurement, diaphragm electromyography (EMGdi) was obtained with a nasogastric catheter (EAdi 12 Fr catheter, Getinge, Solna, Sweden) with nine stainless steel wire electrode rings. Prior to the experiment, the catheter was connected to the ventilator equipped with positioning software to confirm correct catheter placement [56]. Once positioned, the catheter was connected to a dedicated measurement setup (see below) to allow acquisition of the raw signals of all eight sequential electrode pairs. Electromyographic activity of the abdominal wall muscles (rectus abdominis (EMG<sub>RA</sub>) and external obliquus (EMG<sub>EO</sub>)) was obtained with Ag/AgCl surface electrodes that were positioned as described previously [57, 58] with position confirmed after volitional activation of the abdominal muscles. Flow and airway pressure (Paw) were measured with a pneumotachograph (Adult Flow Sensor, Hamilton Medical, Bonaduz, Switzerland) placed in line with the ventilator tubing, in between the face mask and the Y-piece. All signals were acquired synchronously at 2 kHz, using a dedicated measurement setup (MP 160, BIOPAC Systems inc., Goleta, California, USA).

### *Magnetic stimulation*

Supramaximal bilateral anterolateral stimulation of the phrenic nerves was performed to measure twitch Pdi (Pdi,tw). Two figure-of-eight coils were powered by a Magstim stimulator (MagStim 200, Magstim Co. Withland, Dyfed, UK). At each applied PEEP level, three Pdi,tw measurements were performed during short end-expiratory occlusions that were manually activated on the ventilator. Subjects were not aware of the exact time point of stimulation, to prevent anticipation. Before the experimental protocol, a ramp of stimulations (70-80-90-100% of maximal power output) was performed during NIV with baseline PEEP level to determine the power output for supra-maximal stimulations (usually at 90% or 100%). At least 30 seconds between repeated stimulations was implemented to prevent twitch potentiation [59, 60] and pressure tracings were rejected if the baseline Pes or Pdi was distorted, or when the twitch was imposed on a spontaneous breath.

### *Data analysis*

Offline breath-by-breath analysis was performed in a software routine developed for Matlab (Matlab, R2018b; Mathworks, USA). EMGdi signal processing was performed according to the method of Sinderby et al. [61-63], and as described previously [64]. Removal of artefacts was done prior to calculation of respiratory timing, mechanics and breathing effort. Prolonged periods with substantial noise (e.g., esophageal spasms) were removed as well as single breaths with potential artefacts and outliers based on physiological criteria defined prior to analysis (e.g., breaths < 0.5 seconds, substantial drift in baseline pressures, breaths with Pes increases during active inspiration).

At each PEEP level, the mean of two Pdi,tw measurements with the lowest variation was calculated, provided that this variation was < 20%. Mechanical inspiratory time (Ti), expiratory time (Te), total breath cycle (Ttot), respiratory rate and expiratory tidal volume (Vt) were derived from the flow recordings. Dynamic transpulmonary pressure during tidal breathing ( $PL_{dyn}$ ) was calculated as  $Paw - Pes$ . Inspiratory increase in  $PL_{dyn}$  ( $\Delta PL_{dyn}$ ; i.e.,  $PL_{insp} - PL_{exp}$ ) was calculated as a measure of lung driving pressure. Pes swing during inspiration ( $\Delta Pes_{insp}$ ) was calculated as the difference between the start of Pes decrease and its nadir.  $\Delta Pdi_{insp}$  was calculated as the increase in Pdi during inspiration. The inspiratory diaphragm pressure-time product ( $PTPdi_{insp}$ ) was defined as the inspiratory Pdi time-integral (i.e., from start of Pdi increase until end of inspiratory flow), per minute. Expiratory Pga increase ( $\Delta Pga_{exp}$ ) was calculated as the Pga difference between end-inspiration (based on flow zero-crossing) and the start of decrease in Pes (i.e. start of next inspiration) [64] to reflect expiratory muscle activity;  $\Delta Pga_{exp} > 2 \text{ cmH}_2\text{O}$  was arbitrarily considered as expiratory muscle recruitment and  $\Delta Pes_{insp}$  was corrected for  $\Delta Pga_{exp}$  of the preceding breath [65-67]. The diaphragm electrical activity (EAdi) inspiratory

amplitude ( $\Delta EAdi_{insp}$ ), an estimation of neural respiratory drive, was calculated as the peak root mean square of the inspiratory EMGdi. The ratio of  $\Delta Pdi_{insp}$  and  $\Delta EAdi_{insp}$  reflects diaphragm neuromechanical efficiency (NME) [22, 68]. As the amount of breaths at each PEEP level varied among subjects, only variables corresponding to the last ten adequate breaths at each PEEP level were included in the statistical analysis.

### Statistical analysis

Subjects and investigators were not blinded to the PEEP levels when applied and unblinded analysis was performed. Values are reported as mean (standard deviation (SD)), or median [quartile 1 – quartile 3] when appropriate. Statistical analysis was performed with IBM SPSS Statistics version 24 (IBM Corp., USA) and Graphpad Prism version 7 (GraphPad Software, Inc., USA). For all analyses,  $P < 0.05$  was considered significant; reported P-values represent the overall effect of PEEP, unless otherwise stated. Assumption of normality was tested using the Shapiro–Wilk test, histograms and Q-Q plots. Changes in MRI parameters with increasing PEEP levels were analyzed using one-way repeated measures ANOVA or its nonparametric equivalent the Friedman test; in the presence of a PEEP-effect with  $P < 0.05$ , pairwise comparison was performed using Tukey or Dunn's post hoc test for parametric and nonparametric data, respectively. Intra-rater and inter-rater reliability of MRI parameters was assessed with a one-way random and two-way random intraclass correlation model, respectively, with measures of consistency. Intraclass correlation coefficients (ICC) were reported as single measures ICC [95% confidence interval]. We calculated the required sample size assuming an ICC between two raters of  $\geq 0.70$  with 95% CI width of  $\leq 0.155$  and intra-rater ICC of 0.70 with 95% CI width of  $\leq 0.265$ . Under these assumptions, at least 170 measurements were required to evaluate inter-rater reliability and 60 measurements to evaluate intra-rater reliability.

For physiological parameters, a linear mixed model design was used with a fixed effect of PEEP level and random intercept per subject (i.e., change in parameter  $\sim$  PEEP + (1|subject)). A log-transformation was applied for those parameters in which the mixed model residuals did not fit a normal distribution. In the presence of a PEEP-effect with  $P < 0.05$ , pairwise comparison was performed after Bonferroni adjustment. Values are described as estimated means with 95% confidence interval (CI) [lower bound; upper bound].

Since no data is available on the effect of PEEP on the position and function of the human diaphragm, a valid a priori sample size calculation could not be performed. The number of subjects ( $n=19$ ) was considered an adequate sample size of the study based on previous respiratory physiological studies conducted in healthy volunteers [39, 69, 70].



## RESULTS

### *Study population*

Nineteen subjects (male/female, 9/10; age,  $28 \pm 5.5$  year; bodyweight,  $70 \pm 8.7$  kg; BMI  $22 \pm 2.3$  kg/m<sup>2</sup>) completed the study protocol without adverse events. Three subjects were excluded from physiological analysis due to inadequate data quality (esophageal spasms (n=1) or low signal-to-noise-ratio (n=2)). Additionally, EMGdi-derived parameters could not be obtained in three other subjects due to inadequate EAdi acquisition (technical problems EMG transducers (n=1) or low signal-to-noise ratio (n=2)). MRI parameters for diaphragm length could not be obtained in two subjects due to insufficient visualization of the localization marker. Diaphragm shape and diaphragm thickness could not be measured in two subjects due to insufficient image quality. MRI measurement of central tendon length was feasible in eight subjects.

The repeatability of MRI measurements was excellent; ICC values were 0.98800 [0.981-0.993] and 0.991 [0.988-0.993] for intra-rater and inter-rater reliability, respectively.

### *Diaphragm position, shape and chest wall configuration*

Application of PEEP resulted in a caudal displacement of the diaphragm, with a median caudal displacement of the dome of 19 [14-26] mm when increasing PEEP from 2 to 15 cmH<sub>2</sub>O ( $P < 0.001$ , **Fig.2b**). In addition, left-to-right thoracic diameter was not affected (mean (95% CI) 247 [242-252] mm vs. 244 [235-252] mm, respectively;  $P = 0.363$ ), while anterior-posterior thoracic diameter significantly increased (142 [131-158] mm vs. 150 [138-161] mm, respectively;  $P < 0.0001$ ) when comparing PEEP 2 versus 15 cmH<sub>2</sub>O. Lung cross-sectional area (CSA) significantly increased (185 [158-217] cm<sup>2</sup> to 228 [205-253] cm<sup>2</sup>, respectively,  $P < 0.0001$ ). This reflected an increase of 25.3 [12.2-31.1] %, which was representative for the increase in right hemithorax volume ( $R^2 = 0.95$ ,  $P < 0.0001$ ).

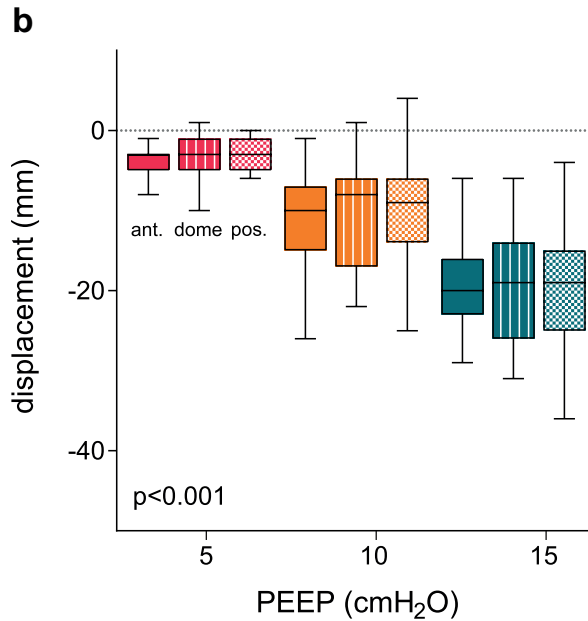


**Figure 2b.** PEEP-induced caudal displacement of the diaphragm, relative to a PEEP level of 2 cmH<sub>2</sub>O, measured at 50% anterior (ant., solid), top of the diaphragm dome (dome, stripes) and 50% posterior (pos., squares), obtained from the sagittal right plane.

The shape of the diaphragm was not affected by the increase of PEEP from 2 to 15 cmH<sub>2</sub>O (posterior angle; 25.0 [21.5-31.6] and 26.8 [22.1-31.5] degrees, respectively ( $P=0.2369$ ), and K-dome; 1.29 [1.24-1.32] and 1.26 [1.21-1.34], respectively ( $P=0.1132$ ) (**Fig.3a-b**).

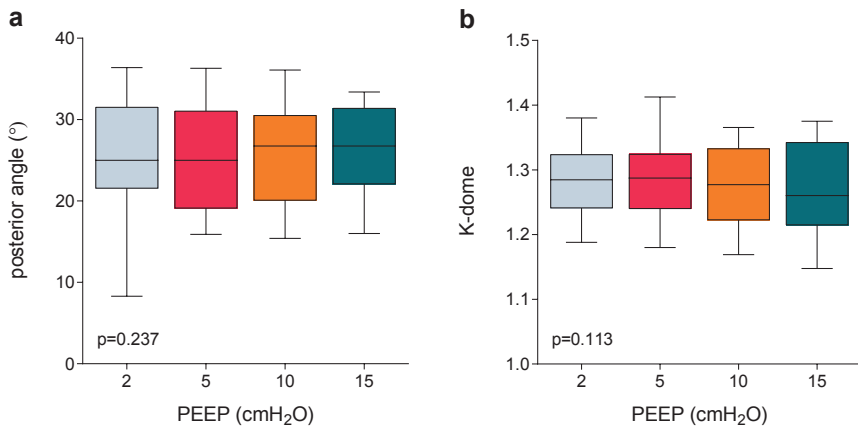


**Figure 3.** Effect of PEEP on diaphragm shape (posterior angle (**a**) and K-dome (**b**)). Data are presented as absolute values.

### Diaphragm length and thickness

Increasing PEEP from 2 to 15 cmH<sub>2</sub>O resulted in shortening of the ZoA ( $P<0.0001$ ); the posterior ZoA more pronounced than anterior ZoA (median shortening of 32.7 [20.8-46.7] % vs. 20.6 [18.1-32.6] %, respectively,  $P=0.0255$ ) (**Fig.4a**). While the length of the dome did not change ( $P=0.9941$ , **Fig.4b**), total diaphragm length (i.e., dome plus posterior and anterior ZoA) significantly decreased ( $P<0.0001$ , **Fig.4c**).

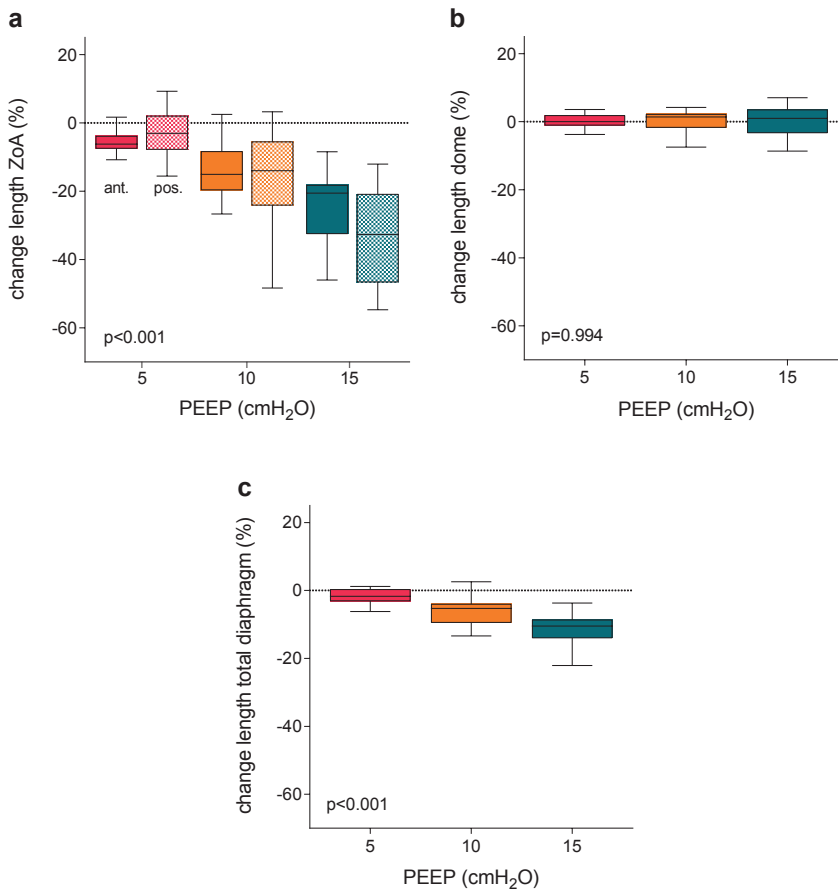


**Figure 4.** Effect of PEEP on diaphragm length in the zone of apposition (ZoA) anterior (solid) and posterior (squares) (**a**), length of the diaphragm dome (**b**), and total diaphragm length (**c**). Data are presented as percentage change from baseline (PEEP 2 cmH<sub>2</sub>O).

MRI measurement of central tendon length ( $n=8$ ) demonstrated that tendon length was not affected by PEEP ( $P=0.3125$ ; **Fig.5c**). **Fig.5d** shows that diaphragm thickness increased with 36.4 [0.9-44.1] % ( $P=0.0010$ ) when PEEP increased from 2 to 15 cmH<sub>2</sub>O.

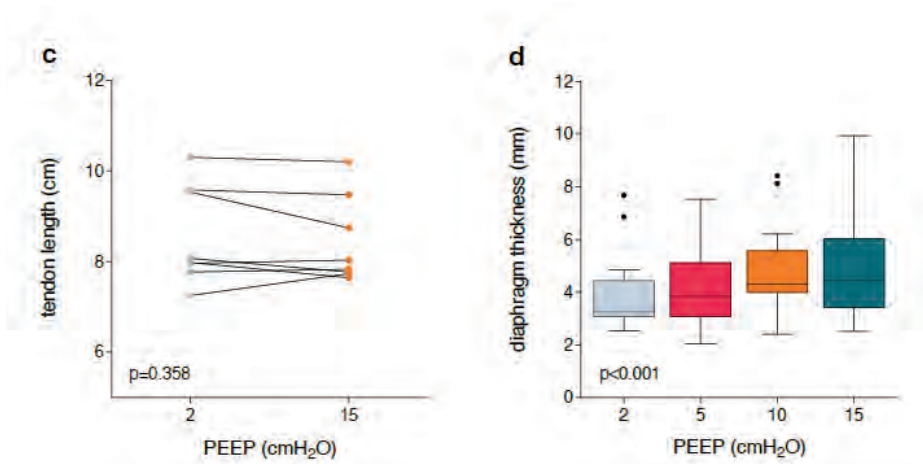


**Figure 5.** (c) Tendon length at PEEP level of 2 cmH<sub>2</sub>O and 15 cmH<sub>2</sub>O for those subjects in which the tendon could be measured at the two PEEP levels. (d) End-expiratory diaphragm thickness at different PEEP levels.

#### *Ventilation, respiratory timing, and lung mechanics*

Variables of ventilation, respiratory timing and lung mechanics are listed in **Table 2** and did not change with increasing PEEP levels.

**Table 2.** Variables of ventilation, respiratory mechanics and respiratory muscle function. Data are presented as mixed model estimates of the mean with 95% confidence interval [lower bound; upper bound]. \*P≤0.05, different from PEEP 2 cmH<sub>2</sub>O, †P≤0.05, different from PEEP 5 cmH<sub>2</sub>O

	PEEP			Main effect PEEP P-value
	2 cmH <sub>2</sub> O	5 cmH <sub>2</sub> O	10 cmH <sub>2</sub> O	15 cmH <sub>2</sub> O
<b>Ventilation and respiratory mechanics</b>				
Tidal volume (mL)	661 [516; 807]	628 [481; 774]	607 [461; 752]	684 [536; 833]
Respiratory rate (/min)	12.7 [10.6; 14.9]	12.5 [10.3; 14.7]	13.1 [10.9; 15.3]	14.3 [12.1; 16.5]
Minute ventilation (L/min)	8.1 [7.0; 9.1]	7.4 [6.4; 8.5]	7.4 [6.4; 8.5]	8.2 [7.1; 9.3]
Inspiratory time (s)	1.8 [1.5; 2.1]	2.0 [1.7; 2.3]	1.9 [1.6; 2.2]	1.8 [1.5; 2.1]
Expiratory time (s)	3.1 [2.7; 3.6]	3.2 [2.7; 3.7]	3.0 [2.5; 3.5]	2.9 [2.4; 3.4]
ΔP <sub>L,dyn</sub> (cmH <sub>2</sub> O)	9.5 [8.0; 10.9]	9.1 [7.6; 10.6]	8.5 [7.1; 10.0]	9.5 [8.0; 11.0]
<b>Respiratory muscle function</b>				
ΔPes <sub>insp</sub> (cmH <sub>2</sub> O)	-7.2 [-8.3; -6.2]	-6.8 [-7.9; -5.7]	-6.2 [-7.3; -5.1]	-6.9 [-8.0; -5.8]
ΔPdi <sub>insp</sub> (cmH <sub>2</sub> O)	9.7 [8.0; 11.5]	9.5 [7.7; 11.2]	8.2 [6.4; 9.9]	8.5 [6.8; 10.3]
PTPdi <sub>insp</sub> (cmH <sub>2</sub> O.s/min)	160.0 [127.4; 201.4]	142.2 [113.0; 179.1]	126.8 [100.5; 159.6]	126.2 [99.5; 160.0]
EAdi <sub>peak</sub> (uV)	12.6 [8.3; 19.2]	14.0 [9.2; 21.4]	15.6 [10.2; 24.0]	22.5* [14.5; 35.0]
NME (%)	100.0 [85.9; 116.4]	83.4 [71.1; 97.5]	70.0* [59.3; 82.4]	52.0* [43.4; 62.4]
Pdi,tw (cmH <sub>2</sub> O)	18.4 [14.7; 22.2]	18.5 [14.8; 22.1]	16.4 [12.8; 20.1]	15.3* [11.6; 19.0]
Subset (n=10) with no co-activation of abdominal muscles prior to Pdi,tw	18.5 [13.6; 23.4]	17.8 [13.0; 22.5]	15.6 [10.9; 20.4]	14.4* [9.6; 19.2]
Subset (n=5) with co-activation of abdominal muscles prior to Pdi,tw at ≥ one PEEP level	19.0 [10.8; 27.1]	19.8 [11.7; 27.9]	18.0 [9.8; 26.1]	16.9 [8.8; 25.0]

**Abbreviations:** EAdi<sub>peak</sub> peak of the electrical activity of the diaphragm; NME neuromechanically efficiency index; ΔPdi<sub>insp</sub> delta inspiratory transdiaphragmatic pressure; Pdi,tw twitch transdiaphragmatic pressure; PEEP positive end-expiratory pressure; ΔPes<sub>insp</sub> delta inspiratory esophageal pressure; ΔP<sub>L,dyn</sub> delta dynamic transpulmonary pressure; PTPdi<sub>insp</sub> inspiratory dia-phragm pressure-time product.

### Diaphragm effort and contractile efficiency

During tidal breathing with increasing PEEP levels,  $\Delta EAdi_{insp}$  significantly increased whereas  $\Delta Pdi_{insp}$  and diaphragm inspiratory pressure-time-product ( $PTPdi_{insp}$ ) decreased (**Table 2**), resulting in significantly reduced diaphragm NME ( $\Delta Pdi_{insp} / \Delta EAdi_{insp}$ ) (**Fig. 6a**). The release of PEEP immediately restored diaphragm efficiency as NME at both PEEP 5 cmH<sub>2</sub>O levels were not significantly different (mean difference 0.03 cmH<sub>2</sub>O/ $\mu$ V,  $P=0.597$ ). Bilateral phrenic nerve magnetic stimulation resulted in reproducible twitch pressures in fifteen subjects.  $Pdi_{tw}$  decreased with increasing PEEP levels (**Table 2**). Upon reviewing EMG recordings of the abdominal wall muscles, five subjects showed activation of the abdominal wall muscles during expiration prior to and during the magnetic twitch at one or more PEEP levels. This was reasoned to influence the effect of the twitch response and a subdivision was made between subjects with and without activation of their abdominal wall muscles during  $Pdi_{tw}$ ; the effect of PEEP on  $Pdi_{tw}$  was more pronounced in the latter subgroup ( $n=10$ ) (**Table 2**, **Fig. 6b**). Expiratory muscle recruitment during tidal breathing was observed in three subjects (defined by increase in  $Pga > 2$  cmH<sub>2</sub>O during expiration) at one or more PEEP levels.

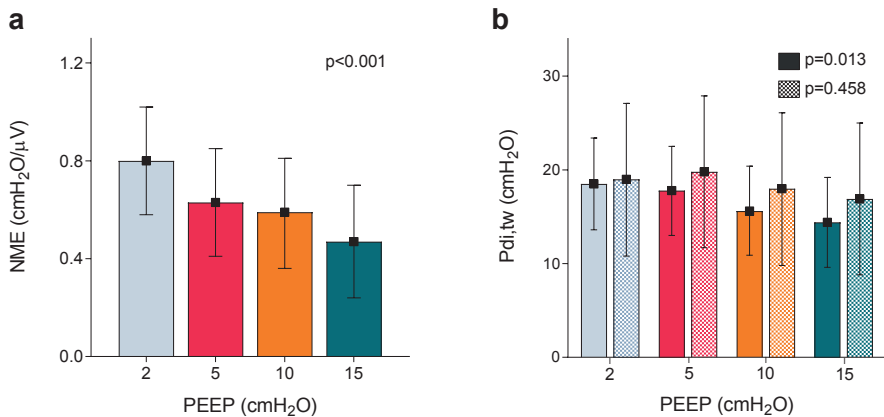


**Figure 6.** PEEP-induced changes in neuromechanical efficiency of the diaphragm (a) and twitch transdiaphragmatic pressure (b). Regarding twitch transdiaphragmatic pressure, a subdivision was made for those subjects that did (squares,  $P=0.458$ ) and did not show activation of their abdominal wall muscles just prior to the magnetic stimulus at one or more PEEP levels (solid,  $P=0.013$ ).

## DISCUSSION

In the current study we investigated the effects of short-term PEEP application on both geometry and contractile function of the healthy human diaphragm. The major findings can be summarized as follows: first, application of PEEP resulted in caudal displacement of the diaphragm and slight increase in anterior-posterior thoracic diameter. Second, PEEP shortened the diaphragm in the ZoA with a concomitant increase in diaphragm thickness. Third, PEEP decreased the contractile efficiency of the diaphragm. This sequence of events demonstrates that prerequisites for muscle remodeling are present with the acute application of PEEP (**Fig.1**, effects on T1). In recent experimental work, muscle remodeling has been described with prolonged application of PEEP, associated with longitudinal fiber atrophy [7]. Hence, the current study confirms the necessity to further explore the role of PEEP in the development of diaphragm weakness-related weaning failure in ICU patients (**Fig.1**).

### Effect of PEEP on diaphragm and thoracic geometry

Our study provides new and detailed insights on the impact of PEEP on diaphragm and chest wall geometry. We demonstrated that the PEEP-induced increase in EELV resulted in caudal diaphragm displacement and increased anterior-posterior thoracic diameter, with the first more pronounced. Thus, the diaphragm exhibits a “widening piston”-like behavior (i.e., the diaphragm acts as a piston, in which the “container” widens in the anterior-posterior direction as the piston descends). This concept was first described by Petroll et al. [71] and has important implications for diaphragm function. Gauthier and coworkers [49] investigated in non-ventilated healthy subjects changes in EELV (induced by active inspiration and subsequent relaxation at different lung volumes) on diaphragm shape. Using MRI, a caudal diaphragm displacement was demonstrated when lung volume was increased actively from residual volume (RV) to TLC. However, changes in diaphragm geometry induced by active inspiration and breath-holding are physiologically different, and may therefore not reflect changes in diaphragm geometry induced by mechanical ventilation with PEEP. During active inspiration and subsequent breath-holding, negative pleural pressure is created, while in case of breath-holding after tidal expiration during the application of PEEP the end-expiratory pleural pressure will be positive. This may have different impact on the distribution of lung volume and thus on diaphragm geometry. Therefore, the study by Gauthier [49] cannot be used to predict the effect of PEEP on the diaphragm. Furthermore, MRI techniques used in that study were less advanced as they are today and studying the effects of PEEP on diaphragm thickness and muscular length (distinguished from tendon length) was not feasible at that time. In a recent study [7], we reported that the *release* of PEEP results in

cranial movement of the diaphragm in invasively ventilated ICU patients. However, for imaging two-dimensional ultrasound was used, providing a limited view of the diaphragm. The MRI protocol used in the current study provides novel and detailed insights into diaphragm geometrical changes due to PEEP.

Gauthier et al. [49] reported that K-dome (dome shape) was progressively decreased (from 1.31 to 1.15) with increasing lung volumes (from RV to TLC), indicating flattening of the diaphragm dome. While our K-dome values at baseline PEEP were in line with those reported by Gauthier at RV, we did not find a reduction in K-dome with increasing PEEP. Gauthier [49] demonstrated that flattening of the diaphragm dome mainly occurred at very high lung volumes (up to TLC) and such volumes were not reached within the range of PEEP levels applied in our study. In addition, flattening of the diaphragm dome in Gauthier's study [49] might result from active inspiration.

### **Effect of increased PEEP on diaphragm length and thickness**

PEEP-induced caudal movement of the diaphragm was associated with diaphragm muscle shortening and increased thickness in the ZoA. The first is in line with previous work demonstrating significant reduction in diaphragm length ( $204 \pm 16$  mm vs  $91 \pm 13$  mm at FRC vs. TLC) when increasing lung volume by active inspiration [49]. Furthermore, rabbit studies demonstrated that PEEP acutely reduces *in vivo* end-expiratory costal diaphragm length [72]. By using high-resolution MRI techniques, we demonstrated that diaphragm shortening only occurred in the muscular parts (anterior and posterior ZoA), and that the length of the central tendon did not change. Shortening of the muscular part in the ZoA is the prerequisite for development of longitudinal atrophy (**Fig.1**, effect on T1). PEEP resulted in a more pronounced shortening of the posterior ZoA compared to anteriorly (32.7% and 20.5%, respectively) when increasing PEEP from 2 to 15 cmH<sub>2</sub>O. These findings are in line with Gauthier et al. [49] and likely indicate a posterior tilt of the diaphragm along the transversal axis. Furthermore, we demonstrated that with PEEP-induced passive diaphragm shortening the muscle thickens, consistent with previous experimental studies in dogs [48]. Diaphragm thickening due to PEEP was previously demonstrated in healthy subjects [73]. However, in that study, only one PEEP level (10 cmH<sub>2</sub>O) was evaluated and changes in diaphragm thickness were assessed by ultrasound. Since ultrasound has a limited field of view, it may provide a less detailed assessment of the effects of PEEP as compared to our high-resolution static MRI.

### **Effect of increased PEEP on diaphragm contractile efficiency**

We demonstrated a PEEP-induced decrease in diaphragm contractile efficiency, both during magnetic phrenic nerve stimulation (Pdi,tw) and spontaneous breathing (NME).



This is in line with Beck et al. [74] showing decreased maximum Pdi with actively increasing lung volume from FRC to TLC. In addition, Similowski et al. [51], reported reduced Pdi,tw after actively increasing lung volume from FRC to TLC in healthy volunteers and COPD patients. Interestingly, at comparable lung volumes, COPD patients showed higher Pdi,tw and inspiratory action of the diaphragm, as compared to the healthy controls. This could indicate that functional alterations in diaphragm muscle structure, including longitudinal atrophy, were already present in chronic hyperinflated COPD patients in order to restore sarcomere length and tension generating capacity [75, 76]. In addition, the clear relationship between PEEP (and thus EELV and diaphragm length) and Pdi,tw also highlights the importance of standardization of Pdi,tw measurements in clinical practice and research to describe and identify diaphragm dysfunction in the ICU population.

The PEEP-induced decrease in NME found in our study indicates that for the same pressure development (Pdi), a higher neural effort (EAdi) is required. This impaired NME could be explained by the fact that muscle fiber length has a major effect on muscle force generation [77, 78]. When considering the diaphragm as a curved membrane with specific tensions, Laplace's law would indicate a lower Pdi with widening of the thoracic cage and flattening of the diaphragm at high lung volumes [46, 79]. Indeed, Grassino et al. [50] described that the neuromechanical coupling of the diaphragm depends mainly on chest wall deformation in response to active increases in lung volume. Gauthier et al. [49] described that decreased diaphragm pressure with increasing lung volume could be entirely explained by decreases in muscle fiber length, which was earlier described in instrumented dogs [80]. Moreover, with PEEP a change in the direction of the force vector in the diaphragm may occur and fibers that were initially part of the ZoA become part of the diaphragm dome. This changes the force vector from a vertical vector to a more horizontal vector and could further reduce diaphragm contractility.

A small subset of subjects recruited their expiratory abdominal wall muscles in response to PEEP. Recruitment of expiratory muscles under mechanical ventilation is well-known and may limit the increase in EELV [81] through a physiological feedback mechanism involving proprioceptive influences and vagal pathways [82, 83]. Recruitment of expiratory muscles generates an increase in abdominal pressure moving the diaphragm to a more cranial position at end-expiration, thereby counteracting the effect of PEEP and improving neuromechanical coupling by placing the diaphragm at a more optimal length for tension generation [81, 84, 85]. It is unknown why only a subset of subjects recruited their expiratory muscles. Notably, in two subjects, PEEP resulted in a *cranial* displacement of the diaphragm shown by MRI (**Fig.2b**), which was reasoned to be the result of abdominal wall muscle activation.

## Strengths and limitations

We applied novel high-resolution MRI techniques and sophisticated functional techniques to assess PEEP-induced changes in diaphragm geometry and function. These techniques have not been applied earlier to evaluate the effects of PEEP on the diaphragm and chest wall, and provide novel insights.

Some limitations should be acknowledged. First, this physiological study was conducted in healthy subjects and the results should be extrapolated to ICU patients with caution. In general, ICU patients have lower lung compliance and thereby probably show less increase in EELV and caudal diaphragm displacement for the same PEEP level. However, it should be noted that in a previous pilot study in ICU patients using ultrasound, it was demonstrated that a change in PEEP of 10 cmH<sub>2</sub>O resulted in diaphragm displacement of  $\pm 10$  mm [7], corresponding to our findings in healthy subjects. We suggest that in ICU patients the PEEP-induced changes should be related to increases in EELV rather than to absolute PEEP. In the current study, we did not directly measure EELV, but estimated lung volume based on the lung cross sectional area obtained from twenty consecutive sagittal MR images, multiplied by the image slice thickness. This method has been used previously for measurements of thoracic volume [54]. State-of-the-art techniques such as nitrogen washout or gas dilution techniques to measure EELV are not reliable during NIV with increasing air leaks at higher levels of PEEP [86]. Third, MRI results are mainly based on images acquired in the SAG-R plane through the top of the diaphragm dome, which was considered the optimal image plane to assess the effects of PEEP under static conditions and with high resolution (e.g., not affected by the heart and its motion). However, this limits the assessment of PEEP-induced rotational movements of the dome and changes in muscle fiber direction, which requires three-dimensional modelling techniques, as used in previous studies [87, 88]. Fourth, length measurements of the ZoA with MRI depend on the assumption that the flexible tube marker reflects the insertion of muscle fibers at the rib cage. This is debatable [49], but probably has limited effects on the interpretation of the data and better techniques are not available. Fifth, for technical reasons we excluded some subjects from analysis of EMGdi parameters at one or more PEEP levels. Obtaining reliable EMGdi signals can be challenging at the acquisition and post-processing level, especially in the presence of multiple nasogastric catheters in healthy volunteers, cardiac and movement artifacts and changes in diaphragm position relative to the catheter electrodes. As the EMGdi signal was constructed during offline post-processing, we could not account for all factors influencing signal quality at the time of recordings. Although a linear mixed model design was used to account for missing data, EMGdi-based parameters ( $\Delta \text{EAdi}_{\text{insp}}$  and NME) should be

interpreted with some degree of caution. In addition, we did not perform maximum inspiratory or expiratory maneuvers during noninvasive ventilation with PEEP, precluding the assessment of maximum respiratory muscle strength. Finally, MRI and functional measurements were not performed at the same time, as MRI compatible equipment for diaphragm functional measurements is not available. Therefore, direct correlations between changes in diaphragm geometry and performance could not be tested.

In conclusion, PEEP-induced increase in EELV in healthy subjects led to a caudal diaphragm displacement and widening of the thorax, resulting in diaphragm shortening and thickening in the ZoA, and reduced contractile efficiency. This sequence of events confirms that prerequisites for development of diaphragm remodeling associated with longitudinal atrophy are present with the acute application of PEEP. If similar effects occur in ICU patients – with prolonged PEEP application leading to diaphragm remodeling – the acute release of PEEP upon ventilator weaning could overstretch the longitudinally atrophied fibers to excessive sarcomere lengths which could severely impact function. This may provide a new mechanism for diaphragm weakness-related ventilator weaning failure in ICU patients.

## REFERENCES

See page 166.



# Expiratory muscle dysfunction in critically ill patients: towards improved understanding

---

Zhong-Hua Shi, Annemijn H. Jonkman, Heder J. de Vries, **Diana Jansen**,  
Coen A.C. Ottenheijm, Armand Girbes, Angelique M.E. de Man, Jian-Xin Zhou,  
Laurent Brochard, Leo M.A. Heunks

*Intensive Care Med* 2019 <https://doi.org/10.1007/s00134-019-05664-4>

## ABSTRACT

### Introduction

This narrative review summarizes current knowledge on the physiology and pathophysiology of expiratory muscle function in ICU patients, as shared by academic professionals from multidisciplinary, multinational backgrounds, who include clinicians, clinical physiologists and basic physiologists.

### Results

The expiratory muscles, which include the abdominal wall muscles and some of the rib cage muscles, are an important component of the respiratory muscle pump and are recruited in the presence of high respiratory load or low inspiratory muscle capacity. Recruitment of the expiratory muscles may have beneficial effects, including reduction in end-expiratory lung volume, reduction in transpulmonary pressure and increased inspiratory muscle capacity. However, severe weakness of the expiratory muscles may develop in ICU patients and is associated with worse outcomes, including difficult ventilator weaning and impaired airway clearance. Several techniques are available to assess expiratory muscle function in the critically ill patient, including gastric pressure and ultrasound.

### Conclusion

The expiratory muscles are the "neglected component" of the respiratory muscle pump. Expiratory muscles are frequently recruited in critically ill ventilated patients, but a fundamental understanding of expiratory muscle function is still lacking in these patients.

**Keywords:** Expiratory muscles, Acute respiratory failure, Mechanical ventilation, Respiratory muscle weakness, Respiratory muscle monitoring

#### Take home message

The expiratory muscles are the "neglected component" of the respiratory muscle pump. This narrative review summarizes the physiology and pathophysiology of expiratory muscles in critically ill ventilated patients. Techniques to monitor expiratory muscle function in these patients are also discussed.

## INTRODUCTION

The respiratory muscle pump drives alveolar ventilation and is therefore of vital importance. The diaphragm, rib cage muscles and abdominal wall muscles are the most important components of the respiratory muscle pump [89]. Recruitment of each muscle depends on the (relative) load imposed on the respiratory system, lung volume, and the phase of the respiratory cycle. An acute imbalance between respiratory muscle load and capacity will result in respiratory failure and, ultimately, the need for mechanical ventilation. Many studies and reviews have focused on diaphragm structure and function in patients with acute respiratory failure, including critically ill patients [4, 5, 7, 12, 33, 41, 42, 53, 90, 91]. However, the role of expiratory muscles in the physiology of breathing in acute respiratory failure is largely neglected in the literature. This is surprising, given the important role of these muscles in respiration, especially in patients with impending respiratory failure. The aim of the current paper is to discuss the role of the expiratory muscles in respiration, in particular in critically ill patients in whom respiratory muscle weakness develops rapidly, and may thus have a large clinical impact. We will also describe techniques used to evaluate expiratory muscle function in intensive care unit (ICU) patients. We will not focus in detail on the role of the expiratory muscles in coughing or maintaining body position.

### Physiology of expiratory muscle recruitment

The expiratory muscles include those of the abdominal wall (transversus abdominis muscle, internal oblique muscle, external oblique muscle, and rectus abdominis muscle) and some of the rib cage ones (e.g., the internal intercostal muscles and the triangularis sterni muscle) [92-96] (**Figure 1**).

During tidal breathing, the expiratory muscles are largely inactive, although the transversus abdominis muscle may occasionally show some activity during quiet breathing [96]. Also, in the upright position, the abdominal wall muscles exhibit tonic activity to counteract the gravitational forces acting on the abdominal contents and thus to maintain the diaphragm at optimal length for pressure generation [97-99].



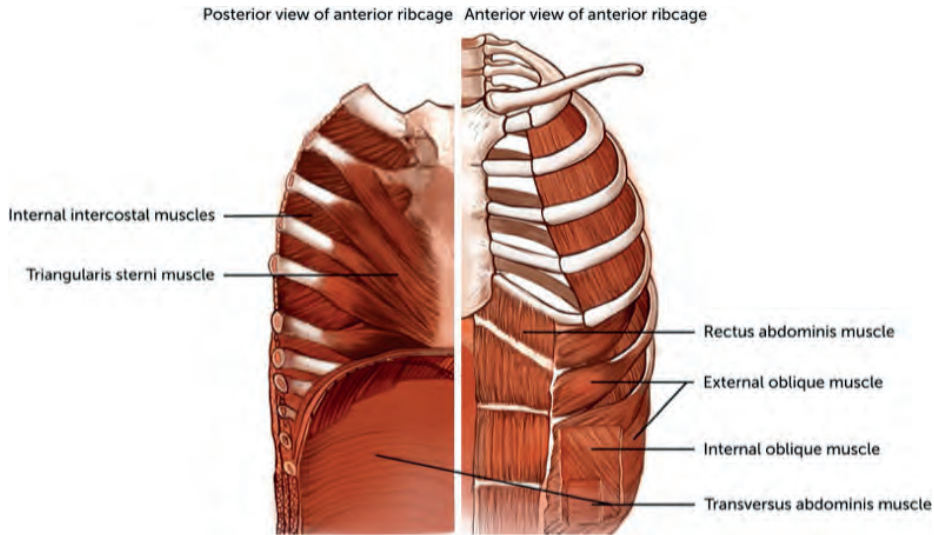


**Figure 1.** The expiratory muscles of the respiratory muscle pump. The respiratory muscle pump is a complex organ that involves a large number of muscles that contribute to inspiration or expiration. This figure schematically demonstrates the expiratory muscles. With the exception of the diaphragm, other inspiratory muscles are not shown.

**Figure 2** shows the physiology of expiratory muscle recruitment. Activation of the expiratory muscles during breathing occurs when the (relative) load imposed on the inspiratory muscles increases. High absolute respiratory loading may occur under different conditions, such as exercise, low respiratory system compliance, and intrinsic positive end-expiratory pressure (PEEPi). Low inspiratory muscle capacity (high relative load on inspiratory muscles) is common in ICU patients due to ICU-acquired respiratory muscle weakness [100]. In the presence of an imbalance between inspiratory muscle load and capacity, the abdominal wall muscles are recruited during expiration in a fixed hierarchy [64, 67, 101, 102]: initially the transversus abdominis muscle, followed by the internal oblique muscle and the external oblique muscle, and finally the rectus abdominis muscle [96, 97, 103]. Activation of the abdominal wall muscles increases abdominal pressure in the expiratory phase. As the diaphragm is relaxed during (most of the) expiratory phase, this increased abdominal pressure is transmitted to the pleural space, consequently reducing the expiratory transpulmonary pressure, which helps to deflate the lung (less pulmonary hyperinflation/lung strain). Furthermore, increased abdominal pressure enhances inspiratory muscle capacity via at least two mechanisms. First, increased abdominal pressure moves the diaphragm at end expiration to a more cranial position, which results in a more optimal length for tension generation [104, 105]; second, when the end-expiratory lung volume falls below functional residual capacity (FRC), elastic energy is stored in the respiratory

system. This stored energy facilitates the next inspiration (i.e., allows more rapid and greater development of negative pleural pressure) [106, 107]. In fact, during strenuous inspiratory loading up to 28% of tidal volume is generated below FRC, which can be attributed to expiratory muscle contraction [101].

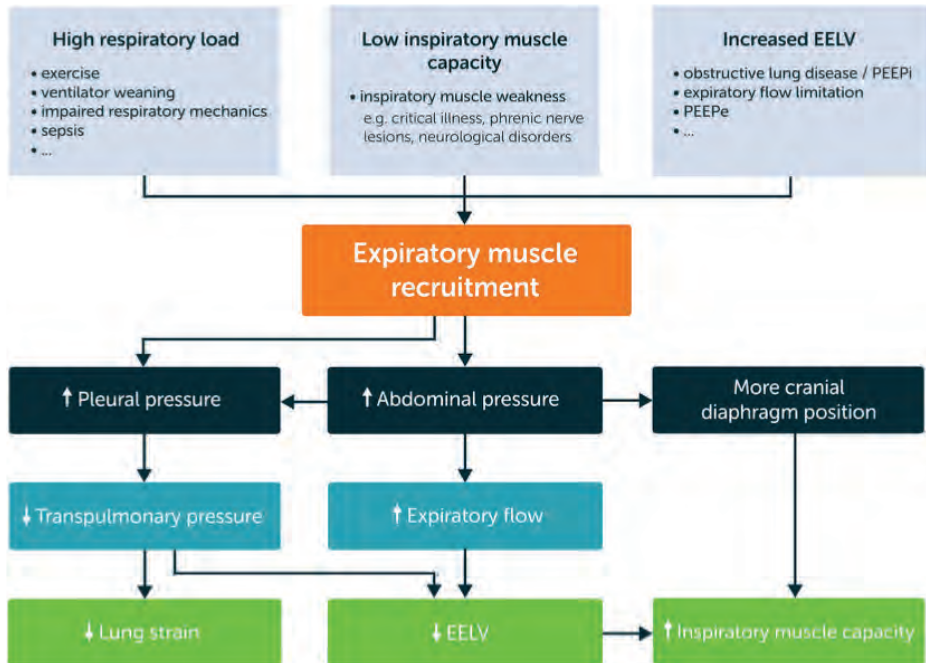


**Figure 2.** Physiology of expiratory muscle recruitment. Schematic illustration of the causes and consequences of expiratory muscle recruitment under physiological (healthy) conditions. All the consequences of expiratory muscle recruitment occur during expiration, except for the increased inspiratory muscle capacity (which occurs during the subsequent inspiration). See main text for explanation. *EELV* end-expiratory lung volume, *PEEPI* intrinsic positive end-expiratory pressure, *PEEPe* external positive end-expiratory pressure.

It should be recognized that isolated contraction of the abdominal expiratory muscles causing an increase in abdominal pressure and pleural pressure would result in chest wall distortion, in particular expansion of the lower rib cage. This would likely increase the elastic inspiratory work of breathing and flatten the diaphragm. To limit distortion of the lower rib cage during active expiration, the internal intercostal muscles are recruited to stabilize the rib cage [89].

In addition to an imbalance between inspiratory muscle load and capacity, an increased end-expiratory lung volume, as in application of positive end-expiratory pressure (PEEP), may also recruit the abdominal wall muscles (**Figure 2 and 3**) [108].

For example, in patients with normal respiratory system compliance (i.e., 80 mL/cmH<sub>2</sub>O), application of 10 cmH<sub>2</sub>O of PEEP would, theoretically, increase end-expiratory lung volume by 800 mL (in the absence of airway closure). However, a physiological feedback mechanism involving vagal pathways or proprioceptive influences limits the increase in end-expiratory lung volume by activation of the abdominal wall muscles during expiration, and thus protects against high lung strain [82, 83].

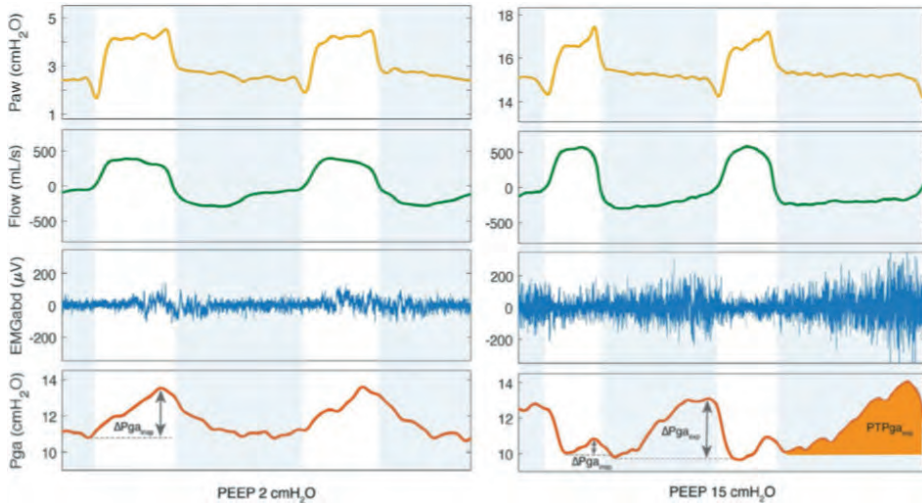


**Figure 3.** Activation of the abdominal muscles during high PEEP. Tracing of airway pressure (*Paw*), flow, EMG of the abdominal muscles (*EMGabd*) and gastric pressure (*Pga*) obtained from a healthy subject during non-invasive ventilation with PEEP levels of 2 cmH<sub>2</sub>O (left) and 15 cmH<sub>2</sub>O (right). At 2 cmH<sub>2</sub>O of PEEP there is no evidence of activation of the abdominal wall muscles (no *EMGabd* activity during expiration and no rise in *Pga* during expiration), however at 15 cmH<sub>2</sub>O of PEEP, the abdominal muscles are recruited during the expiratory phase, as shown by the presence of *EMGabd* activity during expiration and the rise in *Pga* during expiration. White column: inspiration; blue column: expiration. In the *Pga* tracing obtained during PEEP 15 cmH<sub>2</sub>O calculation of parameters to estimate expiratory muscle activity are shown: increase in gastric pressure during expiration ( $\Delta P_{gaexp}$ ); and the gastric pressure–time product during expiration (*PTPgaexp*) represented by the orange area. *EMGabd* electromyography of abdominal wall muscles, *Paw* airway pressure, *PEEP* positive end-expiratory pressure, *Pga* gastric pressure, *PTPgaexp* gastric pressure–time product during expiration.

Another fundamental role of the expiratory muscles is to develop effective cough pressure to facilitate airway clearance [109]. Contraction of the expiratory muscles against a closed airway may increase the intrathoracic pressure may increase to as high as 300 mmHg within 0.2 s. Once the glottis is open, a very high expiratory flow (up to 720 L/min) can be generated [109, 110]. Expiratory muscle weakness reduces cough strength and peak flow velocity, predisposing patients to pneumonia and atelectasis [109, 111, 112].

Undesirable effects of expiratory muscle recruitment

Recruitment of the expiratory muscles during expiration may have undesirable effects in critically ill patients (Figure 4 and Table 1).

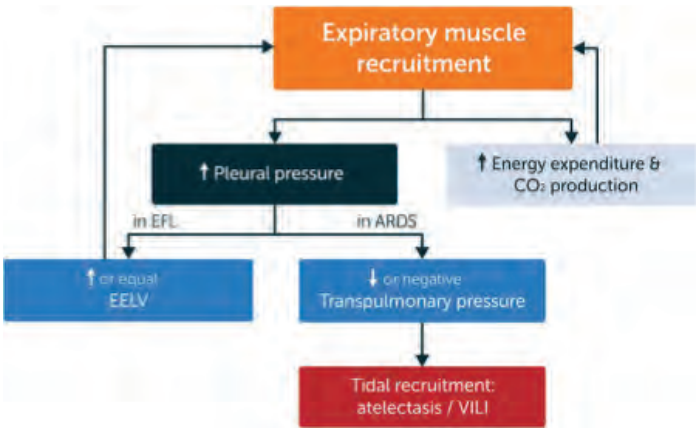


**Figure 4.** Pathophysiology of expiratory muscle recruitment. Schematic illustration of the pathophysiological consequences of expiratory muscle recruitment in critically ill patients. The depicted relationships are mostly hypothetical due to the low number of studies on expiratory muscle function in ICU patients. The elevated pleural pressure caused by expiratory muscle recruitment might lead to dynamic airway collapse, especially in patients who already have expiratory flow limitation (EFL). This leads to an equal or increased end-expiratory lung volume (EELV). On the other hand, elevated pleural pressure might lead to negative expiratory transpulmonary pressures, especially in diseases with an increased lung elastance such as in ARDS, which in turn leads to atelectasis and tidal recruitment. *EFL* expiratory flow limitation, *ARDS* acute respiratory distress syndrome, *VILI* ventilator-induced lung injury.

**Table 1** Clinical impact of expiratory muscle dysfunction

Clinical event	Expiratory muscles-related mechanisms
Weaning failure/extubation failure	Increased respiratory energy consumption, ineffective cough, inability to improve diaphragm efficiency
Atelectasis/pneumonia	Ineffective cough
Small airway and alveolar injury	Negative expiratory transpulmonary pressure resulting in alveolar collapse and/or airway closure
Pulmonary hyperinflation	Inability to increase expiratory flow

First, in patients with acute respiratory distress syndrome (ARDS) or atelectasis, increased pleural pressure during expiration resulting from expiratory muscle recruitment may result in negative transpulmonary pressure during expiration, leading to cyclic alveolar collapse or airway closure and thereby facilitating small airway and alveolar injury [113-116]. Consistent with this reasoning, a recent study in ARDS patients demonstrated a higher expiratory transpulmonary pressure in patients receiving neuromuscular blockers compared with control patients ( $1.4 \pm 2.7$  cmH<sub>2</sub>O versus  $-1.8 \pm 3.5$  cmH<sub>2</sub>O, respectively,  $p = 0.02$ ) [117]. Interestingly, neuromuscular blockers also abolish expiratory activity of the diaphragm (if present) [118] which is expected to decrease expiratory transpulmonary pressure. However, the pressure generated by the diaphragm in the expiratory phase is relatively low compared with that generated by the expiratory muscles. Therefore, the effects of neuromuscular blockers on expiratory transpulmonary pressure largely depend on the relaxation of the expiratory muscles.

Second, expiratory flow limitation is a condition in which expiratory flow cannot be increased, despite an increase in expiratory driving pressure (pressure difference between alveoli and mouth during expiration) [119]. Typically, this occurs in patients with emphysema, but it may also occur during tidal breathing in patients with expiratory muscle activity. The exact mechanism is unclear, but it has been proposed that dynamic airway compression plays an important role [120] (**Figure 5**).

Elevated pleural pressure during active expiration decreases the airway transmural pressure, which subsequently may compress the collapsible part of the airway. Total airway collapse is prevented as increased pleural pressure is also transmitted to the alveoli/airways (for an extensive discussion see also [119]). Expiratory airway compression may result in elevated end-expiratory lung volume and PEEPi [119], especially in patients with chronic obstructive pulmonary diseases (COPD) and in patients failing ventilator weaning [64, 121].

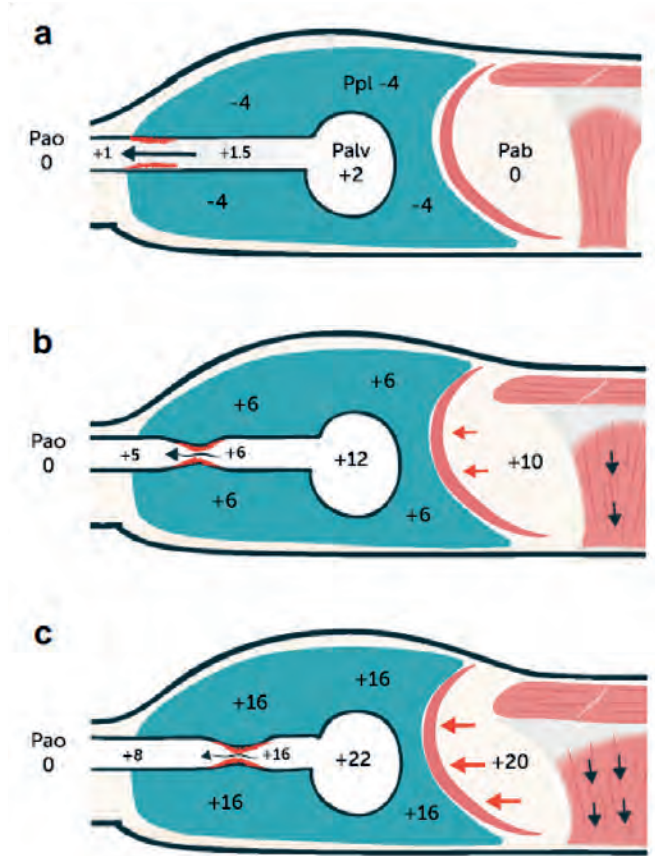


**Figure 5.** Role of expiratory muscle recruitment in the development of expiratory flow limitation (EFL). Schematic and simplified illustration demonstrating the role of expiratory muscle activation in EFL. **a–c** With activation of the expiratory muscles the abdominal pressure increases, also increasing pleural pressure during expiration. This decreases the transluminal pressure resulting in partial airway collapse and therefore EFL. With higher expiratory muscle pressure the flow-limiting site, or choking point, moves towards the alveoli. Note that gravitational forces are not considered in this illustration.  $P_{ab}$  abdominal pressure,  $P_{alv}$  alveolar pressure,  $P_{ao}$  airway opening pressure,  $P_{pl}$  pleural pressure.



Third, in patients weaning from mechanical ventilation, expiratory muscle recruitment is expected when an imbalance exists between the respiratory load and inspiratory muscle capacity. Indeed, activation of the expiratory muscles has been demonstrated during ventilator weaning, especially in patients failing a weaning trial [64, 67, 102]. We recently found that expiratory muscle effort progressively increased throughout the trial in such patients [64]. The neuromuscular efficiency of the diaphragm was lower in weaning failure patients compared with weaning success patients, which challenges the concept that expiratory muscle activation improves diaphragm contractile efficiency [64], although this requires further evaluation. Nevertheless, recruitment of the expiratory muscles during a weaning trial appears to be a strong marker of weaning failure.

Technically, expiratory muscle activity interferes with the assessment of PEEPi. PEEPi can be measured using different techniques. In patients with expiratory muscle activity, an end-expiratory occlusion will be highly influenced and exaggerated by the contraction of the expiratory muscles [65]. Similarly, the relaxation of the expiratory muscles at the beginning of the effort explains part of the initial drop in esophageal pressure, which is not entirely explained by so-called dynamic PEEPi. Either the drop in gastric pressure (Pga) or the rise in Pga during expiration must be subtracted from the esophageal drop in order to measure a reliable PEEPi [122].

### **Expiratory muscle strength in critically ill patients**

Several studies have demonstrated the development of expiratory muscle weakness in critically ill patients [48-63]. Most studies used the maximum expiratory pressure (MEP) as a marker of expiratory muscle strength [1, 123-131]. Despite the heterogeneity of the studies in terms of populations and measurement techniques, the MEP was lower than the reference values [132] in all studies that obtained MEP at the time of ventilator weaning [123-130, 133]. Patients failing extubation exhibit a lower MEP (mean decrease varying from 9 to 31 cmH<sub>2</sub>O) compared with extubation success patients [48-55, 64]. This indicates that expiratory muscle weakness is a potential predictor of weaning outcome. How expiratory muscle weakness affects weaning and extubation outcome is largely unknown. Potential explanations include inadequate secretion clearance and insufficient cough capacity resulting in atelectasis, reduced contractile efficiency of the diaphragm, or inadequate reduction of PEEPi. Remarkably, no studies have investigated the association between diaphragm weakness and expiratory muscle weakness.

## **Risk factors for expiratory muscle weakness in critically ill patients**

Risk factors for the development of ICU-acquired weakness of the peripheral muscles and diaphragm have been discussed recently [1, 4, 42, 134]. Whether these risk factors also have an impact on the expiratory muscles is largely unknown. We briefly discuss risk factors that may contribute to the development of expiratory muscle weakness.

### **Sepsis**

Sepsis and systematic inflammation have been linked to the development of muscle weakness, including weakness of the expiratory muscles [42, 134, 135]. Sepsis induces a severe and persistent increase in protein catabolism, resulting in muscle wasting and muscle weakness [136, 137]. Compared with non-septic surgical patients, the rectus abdominis muscle from surgical patients with sepsis showed significantly lower in vitro contractility [136]. In addition, the reduced MEP ( $\leq 30$  cmH<sub>2</sub>O) found at the time patients regained normal consciousness showed an independent association with septic shock [1].

### **Mechanical ventilation**

Mechanical ventilation plays an important role in the development of diaphragmatic dysfunction in critically ill patients [33, 42, 90, 138]. Potential mechanisms include disuse atrophy due to ventilator over-assist, or load-induced injury as a result of ventilator under-assist. The impact of mechanical ventilation on expiratory muscles has not been systematically investigated. However, as mentioned earlier, ventilator settings including PEEP and the level of inspiratory assist may have an impact on the activity of the expiratory muscles (**Figure 3**) [65, 139], although the ultimate impact of mechanical ventilation on expiratory muscle strength is largely unknown and should be further investigated.

### **Other risk factors**

Co-morbidities, such as COPD and myopathies, or complications such as intra-abdominal hypertension, may put patients at increased risk of ICU-associated expiratory muscle weakness [140, 141]. Drugs such as sedatives, neuromuscular blockers and corticosteroids have been shown to affect peripheral muscle function and diaphragm muscle function in ICU patients [42, 134, 142]. The effects of these drugs on expiratory muscle function have not been systematically studied.



### **Strategies to maintain or improve expiratory muscle strength**

Strategies that aim to improve diaphragm function [37, 42] may also benefit the expiratory muscles, although clinical studies are lacking. The feasibility of neuromuscular electrical stimulation to reduce expiratory muscle atrophy in ICU patients is under investigation (NCT 03453944).

### **Quantification of expiratory muscle effort in critically ill patients**

While visual inspection of the trunk and palpation of the abdominal wall may reveal activation of the expiratory muscles, they do not allow quantification of effort. In this section, we summarize the main clinical techniques that can be used to quantify expiratory muscle effort in ICU patients.

#### **Gastric pressure**

Activation of the abdominal wall muscles increases abdominal pressure. Changes in Pga during expiration reflect changes in abdominal pressure and can thus be used to quantify expiratory muscle effort [64, 67, 115, 132, 143]. Pga is measured using an air-filled balloon catheter inserted into the stomach. Bladder pressure has also been proposed as a means of quantifying intra-abdominal pressure [144, 145], and showed an acceptable correlation with Pga in supine position (bias = 0.5 mmHg, and precision = 3.7 mmHg (limits of agreement, – 6.8 to 7.5 mmHg)) [144]. To quantify the effort of expiratory muscles, Pga amplitude and the Pga pressure–time product (PTP) during expiration can be calculated (**Figure 3**).

#### **Amplitude of gastric pressure**

Both the rise in Pga over the course of expiration [65] and the drop in Pga at the onset of the next inspiration [146] have been used to quantify the activity of the expiratory muscles. However, only the expiratory increase in Pga showed a good correlation with the electromyographic amplitude of the transverse abdominis muscle (correlation coefficient ranging from 0.70 to 0.95) [147].

#### **Pressure–time product**

The PTP of the expiratory muscles has been quantified using the area enclosed by the esophageal pressure curve and the static chest-wall recoil pressure curve during expiration [148]. The PTP accounts for the energy expenditure during both the isometric and dynamic phases of expiration (independently of volume displacement). However, expiratory esophageal pressure only represents the pressure generated by the abdominal wall muscles when the diaphragm is completely relaxed [115, 149]. As diaphragm activity has been demonstrated during expiration [118, 139], abdominal wall muscle effort cannot be reliably quantified using the expiratory esophageal PTP alone.

Therefore, it is recommended to use the expiratory Pga in order to calculate the PTP of the expiratory muscles [150-153]. The gastric PTP can be obtained from the area under the expiratory Pga curve, in which the baseline is defined as the resting end-expiratory Pga from the preceding breath [64, 150, 151].

### **Work of breathing**

Traditionally, the Campbell diagram is used to quantify the inspiratory work of breathing [154], but it allows estimation of the expiratory work as well. The area of the esophageal pressure–volume loop at the right side of the chest wall relaxation curve represents expiratory muscle effort [20, 155]. By definition, work is performed only when there is volume displacement (work = pressure × volume). However, as explained above, during dynamic airway collapse part of the pressure generated by the expiratory muscles does not result in lung volume displacement, and therefore the Campbell diagram underestimates the total effort of the expiratory muscles [120, 156]. Under these circumstances, the PTP may better reflect expiratory muscle effort.

### **Volitional tests of expiratory muscle strength**

The MEP is the most widely used measure of expiratory muscle strength [132]. Standard procedures for non-intubated subjects have been established [132]. For intubated patients, the MEP can be measured using a unidirectional valve that allows inspiration but prevents expiration [123, 133, 157]. Some investigators coached subjects to perform an expiratory effort against an occluded airway for 25 to 30 s, and then recorded the most positive pressure developed [123, 133, 157]. Calculating the ratio of maximum inspiratory pressure to MEP is a simple way to assess the relative impairment of the inspiratory muscles versus the expiratory muscles [158]. As MEP measurement requires a voluntary patient effort, this might not be feasible in a proportion of ICU patients. As an alternative to MEP, cough pressure can be assessed to quantify expiratory muscle strength [109, 132, 143].

### **Cough test**

The cough test is a relatively easy-to-perform, complementary test for the diagnosis of expiratory muscle weakness. Both cough pressure measured via air-filled balloons in the stomach or esophagus, and cough peak expiratory flow measured at the opening of an endotracheal tube or using the ventilator flow sensor [159], are feasible in ICU patients. In patients unable to cooperate, a cough may be induced either by instilling physiological saline [111] or by advancing a suctioning catheter through the patient's tube [112].

### Abdominal wall muscle ultrasound

Ultrasound has become a popular tool for quantifying changes in the thickness and activity of the diaphragm in ICU patients [12, 43, 160], but few studies have used this technique to evaluate the expiratory muscles. Abdominal ultrasound allows direct visualization of the three layers of the abdominal wall muscles and the rectus abdominis muscle [161-164] (**Figure 6**). In our experience, the abdominal wall muscles are easy to visualize using ultrasound, and measurement of thickness is feasible in almost all patients. In healthy subjects, the thickness of individual abdominal wall muscles follows a certain pattern: transversus abdominis < external oblique < internal oblique < rectus abdominis [164].

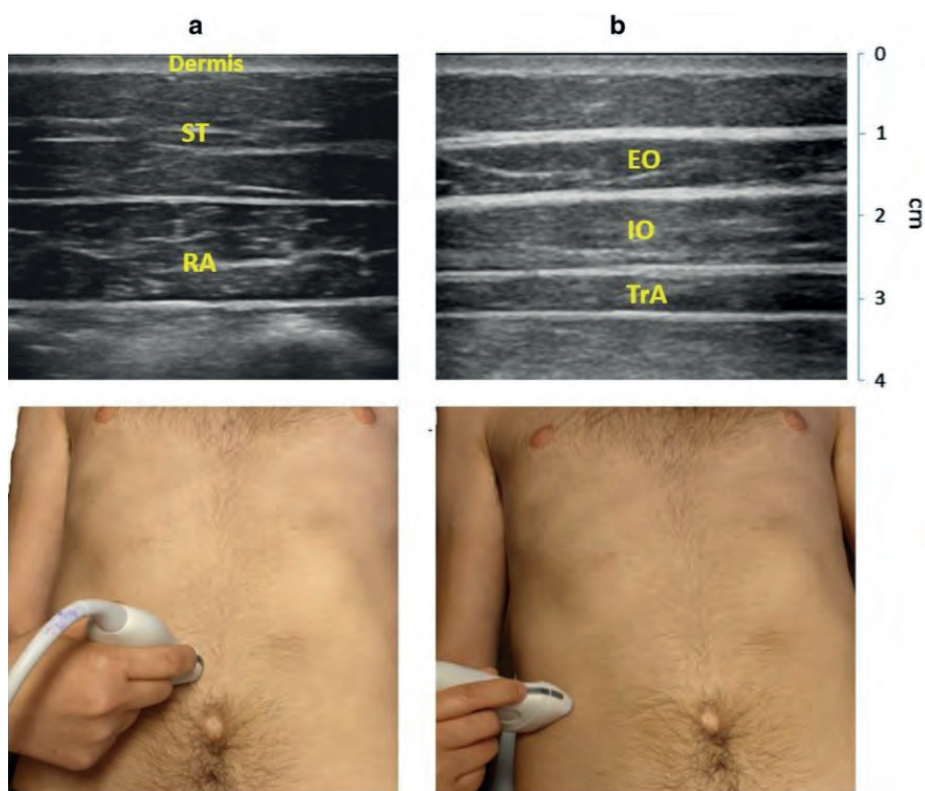


**Figure 6.** Ultrasound image of the abdominal muscles. Left: ultrasound image of the rectus abdominis muscle (RA) (top), obtained with the probe placed 2–3 cm above the umbilicus and 2–3 cm from the midline (bottom). Right: ultrasound image of the external oblique muscle (EO), internal oblique muscle (IO) and transversus abdominis muscle (TrA) (top), obtained with the probe placed midway between the costal margin and the iliac crest, along the anterior axillary line (bottom).

The thickness of the transversus abdominis muscle measured with ultrasound is strongly correlated with the pressure developed during an expiratory maneuver (assessed by the change in Pga) [162]. In addition, the transversus abdominis muscle thickness increase is significantly correlated with the muscle's electrical activity [161]. However, all these studies were performed in healthy subjects, and further studies are needed to determine the reliability and validity of ultrasound assessment of expiratory muscle thickness and function in ICU patients.

### **Other diagnostic tests**

Electrical and magnetic stimulation of the abdominal wall muscles are other methods used to quantify the strength of these muscles [103, 149, 151]. As these techniques are cumbersome and uncomfortable, they are rarely used either in clinical practice or for research purposes. Electromyography of the expiratory muscles has been used in research settings to study the timing of expiratory muscle recruitment during respiration [97, 147], but has not reached clinical implementation. Therefore, these techniques are beyond the scope of this review.

## **CONCLUSIONS**

The expiratory muscles are the “neglected component” of the respiratory muscle pump. Rather as the heart does not comprise only a left ventricle, but also a right one, the respiratory muscle pump is much more than just the diaphragm. In this paper, we have summarized the physiology and pathophysiology of expiratory muscles, with a special focus on critically ill patients. Expiratory muscles are frequently recruited in critically ill ventilated patients, but a fundamental understanding of expiratory muscle function is still lacking in these patients. Gastric pressure monitoring provides multiple bedside parameters for analysis of expiratory muscle effort, but their clinical implications need to be established.

## REFERENCES

See page 166.





## Chapter 4

# Respiratory muscle effort during expiration in successful and failed weaning from mechanical ventilation

---

Jonne Doorduyn, Lisanne H. Roesthuis, **Diana Jansen**, Johannes G. van der Hoeven, Hieronymus W. H. van Hees, Leo M. A. Heunks

*Anesthesiology* 2018 DOI: 10.1097/ALN.0000000000002256



## ABSTRACT

### Background

Respiratory muscle weakness in critically ill patients is associated with difficulty in weaning from mechanical ventilation. Previous studies have mainly focused on inspiratory muscle activity during weaning; expiratory muscle activity is less well understood. The current study describes expiratory muscle activity during weaning, including tonic diaphragm activity. The authors hypothesized that expiratory muscle effort is greater in patients who fail to wean compared to those who wean successfully.

### Methods

Twenty adult patients receiving mechanical ventilation (more than 72 h) performed a spontaneous breathing trial. Tidal volume, transdiaphragmatic pressure, diaphragm electrical activity, and diaphragm neuromechanical efficiency were calculated on a breath-by-breath basis. Inspiratory (and expiratory) muscle efforts were calculated as the inspiratory esophageal (and expiratory gastric) pressure–time products, respectively.

### Results

Nine patients failed weaning. The contribution of the expiratory muscles to total respiratory muscle effort increased in the “failure” group from  $13 \pm 9\%$  at onset to  $24 \pm 10\%$  at the end of the breathing trial ( $P = 0.047$ ); there was no increase in the “success” group. Diaphragm electrical activity (expressed as the percentage of inspiratory peak) was low at end expiration (failure,  $3 \pm 2\%$ ; success,  $4 \pm 6\%$ ) and equal between groups during the entire expiratory phase ( $P = 0.407$ ). Diaphragm neuromechanical efficiency was lower in the failure versus success groups ( $0.38 \pm 0.16$  vs.  $0.71 \pm 0.36$  cm H<sub>2</sub>O/ $\mu$ V;  $P = 0.054$ ).

### Conclusions

Weaning failure (vs. success) is associated with increased effort of the expiratory muscles and impaired neuromechanical efficiency of the diaphragm but no difference in tonic activity of the diaphragm.

## INTRODUCTION

Prolonged weaning from mechanical ventilation develops in 6 to 15% of mechanically ventilated patients and is associated with increased morbidity and mortality [165-168]. A major determinant of weaning failure is respiratory muscle dysfunction [42, 169, 170]. The respiratory muscles are profoundly affected by critical illness and mechanical ventilation [1, 4, 5, 12, 13, 52, 171, 172]. The respiratory muscle pump is made up of a number of muscles, but research in weaning failure has mainly focused on the inspiratory muscles, in particular the diaphragm [23, 102, 173-175]. The role of the expiratory muscles including the internal intercostals and abdominal wall muscles during weaning failure is less well understood.

Recruitment of the expiratory muscles has been demonstrated in patients with chronic obstructive pulmonary disease (COPD) during a failed weaning trial [67, 176]. Expiratory muscle recruitment may help inspiration because the active reduction in end-expiratory lung volume stores elastic energy, facilitating subsequent inspiration. In addition, active reduction in end-expiratory lung volume may help to limit hyperinflation [141]. However, recruitment of the expiratory muscles increases the energy expenditure of breathing, although the relative contribution of expiratory muscle effort to total breathing effort in patients weaning the ventilator is unknown. Expiratory muscles effort can be quantified as the pressure–time product of gastric pressure during expiration [153, 177]. Several studies have demonstrated that the diaphragm exhibits tonic activity during expiration [178-183]. Recently, Pellegrini et al. [118] have demonstrated in pigs with mild acute respiratory distress syndrome that the diaphragm acts as a brake during expiration to prevent lung collapse. In weaning-failure patients, tonic activity of the diaphragm during expiration might prevent airway closure and consequently limit intrinsic positive end-expiratory pressure (PEEP).

Accordingly, the aim of the current physiologic study was to quantify the expiratory pressure–time product and the expiratory activity of the diaphragm in weaning-success and weaning-failure patients. In addition, we studied respiratory muscle activity effort during inspiration. We hypothesized that expiratory muscle effort is higher in weaning-failure patients compared to successfully weaned patients.

## MATERIALS AND METHODS

### Study design and population

This cross-sectional physiologic study was conducted in the intensive care unit of the Radboud University Medical Center, Nijmegen, The Netherlands. We recruited 20 adult patients invasively ventilated for at least 3 days and considered ready for a spontaneous breathing trial. A priori sample size calculation was not performed, but the number of required subjects was based on previous physiologic studies in mechanically ventilated patients [34, 184-186]. The decision to extubate or resume mechanical ventilation was made solely by the clinical team, blinded to the study data. Exclusion criteria were a past medical history of neuromuscular disorders, upper airway or esophageal pathology (e.g., recent surgery, esophageal varices, diaphragmatic hernia), and recent (less than 1 month) nasal bleeding.

The protocol was approved by the local ethics review committee (approval number 2010-058) and conducted in accordance with the Declaration of Helsinki and its later amendments. Written informed consent was obtained in patients that were not already instrumented with the dedicated nasogastric catheter.

### Study protocol

All patients were ventilated with the SERVO-i ventilator (Maquet Critical Care, Sweden). Per clinical protocol, sedatives were discontinued before the spontaneous breathing trial, and patients were verified to be responsive and adequate. If not already in situ, a nasogastric catheter with multiple electrodes and two balloons (NeuroVent Research, Inc., Canada) was inserted nasally. Catheter characteristics and positioning techniques have been described previously [55, 187, 188]. Baseline data were acquired while patients were ventilated in pressure support mode with an inspiratory support of 8 cmH<sub>2</sub>O and a PEEP level of 5 cmH<sub>2</sub>O for 10 min. Subsequently, a spontaneous breathing trial with T-tube and supplemental oxygen was performed for up to 60 min, according to our clinical protocol. The criteria for spontaneous breathing trial failure were tachypnea (more than 35 breaths/min), low peripheral capillary oxygen saturation (less than 90%), tachycardia (more than 140 beats/min), systolic hypertension (more than 180 mmHg), systolic hypotension (less than 90 mmHg), agitation, diaphoresis, and anxiety during the spontaneous breathing trial. Patients were extubated after a successful spontaneous breathing trial. Weaning failure was defined as a failed spontaneous breathing trial or reintubation within 48h after extubation. Arterial blood samples were collected before disconnection from the ventilator and at the end of the spontaneous breathing trial before reinstitution of ventilator support.

## Data acquisition

Flow was measured with a Fleisch pneumotachograph (Hans Rudolph, USA) placed at the endotracheal tube or cannula. The pneumotachograph was connected to a differential pressure transducer (range  $\pm 50$  kPa; Freescale, USA).

The air-filled esophageal balloon and gastric balloon of the nasogastric catheter were connected to differential pressure transducers (range  $\pm 50$  kPa; Freescale). Pressure and flow signals were digitized (Porti 16, 22 bits,  $1.4 \mu\text{V}$ /least significant bit; TMSi, The Netherlands) at a sampling frequency of 2 kHz. Transdiaphragmatic pressure was calculated as esophageal pressure subtracted from gastric pressure.

Electrical activity of the diaphragm recorded from the electrodes of the nasogastric catheter were amplified and digitized (Porti 16, 22 bits,  $71.5 \text{ nV}$ /least significant bit; TMSi) at a sampling frequency of 2 kHz. Signal processing of the electrical activity of the diaphragm was performed according to the method of Sinderby et al. [61–63]. Details are provided in the Supplemental Digital Content (<http://links.lww.com/ALN/B717>).

Flow, esophageal pressure, gastric pressure, and diaphragm electrical activity were acquired synchronously (maximal 0.5-ms delay between mechanics and diaphragm electrical activity) using dedicated software (NeuroVent Research, Inc.) and stored on a hard disk for offline analysis in a software routine developed for Matlab (R2014b; Mathworks, USA).

## Data analysis

The data were analyzed on a breath-by-breath basis. For the period of mechanical ventilation, a 2-min epoch at the end was selected for analysis. The duration of the spontaneous breathing trial varied from patient to patient. Therefore, data were analyzed at seven points in time: the first and last minute and five epochs of at least 1 min taken at equal time intervals in between. The epochs were visually inspected for artefacts, such as movement and esophageal and gastric contractions. In the presence of artefacts, an adjacent artefact-free epoch was selected. In **Figure 1**, the acquired signals (flow, diaphragm electrical activity, esophageal pressure, gastric pressure, and transdiaphragmatic pressure) are shown with the calculated variables.

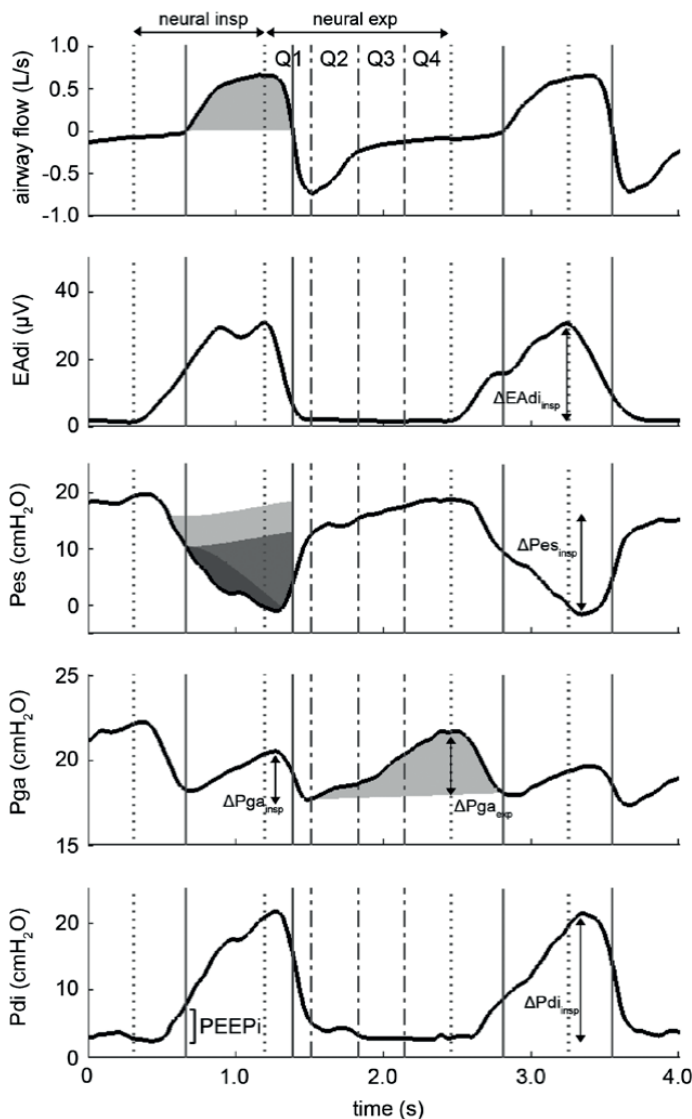


**Figure 1.** Example of calculation of the different variables from the recorded signals from a weaning-failure patient during the end of the spontaneous breathing trial. The *dotted vertical lines* represent the start and end of neural inspiration, and the *solid vertical lines* represent the start and end of inspiratory flow. The neural expiratory phase was divided into four quartiles (Q1–Q4, *dotted and dashed lines*) to calculate the mean signal per quartile for diaphragm electrical activity (EAdi), transdiaphragmatic pressure (Pdi), and gastric pressure (Pga). Different areas under the curves are shown. The *gray area* in the flow signal represents tidal volume. The area with three shades of gray in the esophageal pressure (Pes) signal represents the different components of the esophageal pressure–time product during inspiration (PTPes<sub>insp</sub>): intrinsic positive end-expiratory pressure (PEEPi: *light gray*), elastic (*medium gray*), and resistive (*dark gray*). The components of PTPes<sub>insp</sub> are defined by the recoil pressures of the chest wall and the lung. The gray area in the Pga signal represents the gastric pressure time product during expiration (PTPes<sub>exp</sub>).

Mechanical inspiratory time, expiratory time, total breath cycle time, and respiratory rate were derived from the flow signal. Tidal volume (VT) was calculated as the integral of inspiratory flow. Neural inspiration was defined as the period between the onset of diaphragm electrical activity and the peak of diaphragm electrical activity, and neural expiration was defined as the period between peak of diaphragm electrical activity and the onset of the next diaphragm electrical activity [118, 178].

The rise in expiratory gastric pressure ( $\Delta Pga_{exp}$ ) was calculated as the difference in gastric pressure between end-inspiration and the start of decrease in esophageal pressure (i.e., start of inspiration). As described previously [118, 178], expiratory diaphragm electrical activity ( $\Delta EAdi_{exp}$ ) was calculated as the mean signal during ongoing neural expiration divided into four equally sized quartiles ( $Q1EAdi_{exp}$ ,  $Q2EAdi_{exp}$ ,  $Q3EAdi_{exp}$ ,  $Q4EAdi_{exp}$ ). The mean  $\Delta EAdi_{exp}$  of each quartile was expressed as the percentage of the peak diaphragm electrical activity of that breath during inspiration after the subtraction of the noise level. Quartile 4 was considered the index closest to the tonic diaphragmatic activity. Details on the noise level calculation are provided in the Supplemental Digital Content (<http://links.lww.com/ALN/B717>). Analogous analysis was performed on the transdiaphragmatic pressure and gastric pressure signal, resulting in  $Q1Pdi_{exp}$ ,  $Q2Pdi_{exp}$ ,  $Q3Pdi_{exp}$ ,  $Q4Pdi_{exp}$ ,  $Q1Pga_{exp}$ ,  $Q2Pga_{exp}$ ,  $Q3Pga_{exp}$ , and  $Q4Pga_{exp}$ .

During inspiration, the drop in esophageal pressure ( $\Delta Pes_{insp}$ ) was calculated as the difference between the start of decrease in esophageal pressure and the negative peak value of esophageal pressure.  $\Delta Pga_{insp}$  was calculated as the difference between the start of increase in gastric pressure and the positive (or negative) peak value of gastric pressure during inspiration.  $\Delta Pdi_{insp}$  was calculated as the difference between the start of increase in transdiaphragmatic pressure and the positive peak value of transdiaphragmatic pressure during inspiration.  $\Delta Pes_{insp}$  and  $\Delta Pga_{insp}$  were corrected for  $\Delta Pga_{exp}$  in the preceding breath. The physiologic base for these corrections have been described in detail [65-67]. In short, expiratory muscle activity can increase the end-expiratory alveolar pressure, leading to an overestimation of the decrease in esophageal pressure during inspiration. In the case of expiratory muscle recruitment, part of the decrease in esophageal pressure preceding inspiration is actually due to relaxation of the expiratory muscles rather than contraction of the inspiratory muscles. Therefore, the amount of pressure due to expiratory muscle activity should be subtracted from the decrease in esophageal pressure. Intrinsic PEEP was calculated as the rise in transdiaphragmatic pressure until the start of inspiratory flow and thus corrected for a drop in gastric pressure at the start of inspiration.  $\Delta EAdi_{insp}$ , an estimation of neural respiratory drive, was calculated as the peak root

mean square per 50 samples of the diaphragm electrical activity during inspiration. Neuromechanical efficiency of diaphragm during inspiration ( $\text{NMEdi}_{\text{insp}}$ ) was computed as  $\Delta \text{Pdi}_{\text{insp}} / \Delta \text{EAdi}_{\text{insp}}$ .

The effort of the inspiratory muscles was quantified by calculating the esophageal pressure–time product ( $\text{PTPes}_{\text{insp}}$ ).  $\text{PTPes}_{\text{insp}}$  was calculated as the time integral of the difference between esophageal pressure and the recoil pressure of the chest wall, as described previously [189, 190].  $\text{PTPes}_{\text{insp}}$  was partitioned in resistive, elastic, and intrinsic PEEP components. A calculated theoretical value was used for the recoil pressure of the chest wall, as described previously [191]. Effort of the expiratory muscles was quantified by calculating the gastric pressure–time product ( $\text{PTPga}_{\text{exp}}$ ) during expiration.  $\text{PTPga}_{\text{exp}}$  was calculated as the time integral of the rise in gastric pressure during expiration, as described previously [153, 177]. Total pressure–time product for the respiratory muscles was calculated as  $\text{PTPes}_{\text{insp}} + \text{PTPga}_{\text{exp}}$ .

Dynamic compliance ( $C_{\text{dyn}}$ ) and airway resistance of the lung and airways ( $R_{\text{aw}}$ ) were calculated as described previously [192]. In short,  $C_{\text{dyn}}$  was measured as the ratio of the VT to the change in transpulmonary pressure (difference in pressure between the esophagus and the mouthpiece) between instants of zero air flow. For calculation of  $R_{\text{aw}}$ , points were selected during the inspiratory phase and expiratory phase when lung volumes were identical and flow rates were about maximal. The ratio of the change in transpulmonary pressure between these points to the corresponding change in flow between these points represents an “average” flow resistance for inspiration and expiration.

## Statistical analysis

Statistical analysis was performed using IBM SPSS Statistics version 22 (IBM Corp., USA), and the data were visualized using GraphPad Prism version 5 (GraphPad Software, Inc., USA). In response to peer review, we adapted the statistical analysis of our data by replacing a linear mixed model design with a two-way repeated measures ANOVA. Assumption of normality was tested using the Shapiro–Wilk normality test. Note that because of the limited sample size per group, this test may lack power to detect deviation from normality. First, to analyze the effects of removing ventilator assist, a paired Student's *t* test (pressure support ventilation vs. first minute of the spontaneous breathing trial) or its nonparametric equivalent, the Wilcoxon signed-rank test, was performed for the different variables per group (failure and success). Second, to analyze the effect of time and group on the different variables during the spontaneous breathing trial, a two-way repeated measures ANOVA with time as within-subjects factor (seven time points from minute one to the last minute)

and group as between-subjects factor (success or failure) was performed. Third, to analyze respiratory muscle activity during the expiratory phase a two-way repeated measures ANOVA was performed with time as within-subjects factor (peak and quartile 1 to quartile) and group as between-subjects factor (success or failure). A fourth-order robust polynomial fit was calculated to visualize the trend of respiratory muscle activity during the expiratory phase. Mauchly's test of sphericity was used to test the homogeneity of variance for the mixed ANOVAs. Where Mauchly's test of sphericity was significant ( $P \leq 0.05$ ), Greenhouse–Geisser corrections were applied. In the presence of a significant interaction or between-subject factor, *post hoc* pairwise comparisons between groups at each time point were performed by paired Student's *t* tests with Bonferroni correction. The correlation between the peak expiratory flow and  $\Delta P_{gaexp}$  for the average values per time point during the spontaneous breathing trial was calculated using a Pearson correlation for both weaning groups. The resulting Pearson correlation coefficients were transformed by performing the Fisher's *r* to *z* transformation and subsequently compared by determining the observed *z* test statistic. For all tests, a two-tailed  $P \leq 0.05$  was considered significant. The data are described as means  $\pm$  SD.

## RESULTS

Nine patients met the criteria for weaning failure, five patients failed the spontaneous breathing trial, and four were reintubated within 48 h after extubation. Eleven patients completed the 60-min spontaneous breathing trial and remained extubated for at least 48 h. Patient characteristics and ventilator settings at study inclusion are presented in **Table 1**. Diaphragm electrical activity and transdiaphragmatic pressure signals of one patient in the weaning-success group were excluded from analysis due to dislocation of the catheter during the spontaneous breathing trial. From another patient in the failure group, diaphragm electrical activity was excluded from analysis due to electrode artefacts detected during offline signal analysis.



Table 1. Patient Characteristics

Patient No. and Diagnosis	Age (yr)	BMI (kg/m <sup>2</sup> )	Sex	Days on Ventilator	PSV Level (cm H <sub>2</sub> O)	NAVA Level (cm H <sub>2</sub> O/μV)	PEEP Level (cm H <sub>2</sub> O)	FiO <sub>2</sub>	Pao <sub>2</sub> /Fio <sub>2</sub> (mmHg)	Time to Failure (min)
<b>Failure group (n = 9)</b>										
1 Cardiac arrest	88	24	F	24	-	2.3	6	0.40	268	60 <sup>*</sup>
2 Pneumonia	64	22	F	49	10		6	0.30	328	52
3 Postoperative, CABG	72	27	F	83	10		8	0.40	194	60 <sup>*</sup>
4 Multitrauma	45	28	M	4	10		5	0.30	318	24
5 Exacerbation COPD	58	25	M	14	8		10	0.30	405	60 <sup>*</sup>
6 Postoperative, CABG	67	29	F	8	0		8	0.40	214	16
7 Postoperative, AAA	63	27	M	7	4		8	0.40	199	60 <sup>*</sup>
8 Postoperative, papillary muscle rupture	80	24	M	8	0		8	0.45	132	13
9 Cardiogenic shock	76	23	M	21	-	0.4	10	0.30	228	23
<b>Success group (n = 11)</b>										
1 Tracheal stenosis, COPD	69	25	M	7	14		3	0.45	190	
2 Postoperative, aortoenteric fistula, COPD	71	26	M	8	5		6	0.40	†	
3 Sepsis	58	26	F	7	0		6	0.35	330	
4 Postoperative, CABG	73	29	M	14	10		10	-	†	
5 Cardiac arrest	76	29	F	17	6		6	0.45	248	
6 Postoperative, AAA	82	28	M	5	9		5	0.45	258	
7 Sepsis	73	29	M	24	8		6	0.25	306	
8 Multitrauma	46	25	M	9	0		5	0.30	†	
9 Sepsis	63	24	F	7	0		8	0.30	†	
10 Pneumonia	60	21	M	12	6		6	0.35	291	
11 Postoperative, CABG	78	30	M	3	4		10	0.40	358	

\*Reintubation within 48h. †Patient without arterial line.

AAA = abdominal aortic aneurysm; BMI = body mass index; CABG = coronary artery bypass graft; COPD = chronic obstructive pulmonary disease; F = female; Fio<sub>2</sub> = fractional inspired oxygen tension; M = male; NAVA = neurally adjusted ventilatory assist; PEEP = positive end-expiratory pressure; PSV = pressure support ventilation.

**Table 2.** Variables of Ventilation, Respiratory Timing, and Mechanics during PSV and the SBT for the Failure Group and Success Group

	Group	PSV	SBT Start	SBT End	Main Effect		Interaction (Time × Group)
					P Value		
					Time	Group	
$V_T$ (ml)	F	535 ± 153*	384 ± 183	401 ± 214	0.901	0.830	0.670
	S	486 ± 233*	414 ± 205	413 ± 171			
Peak inspiratory flow (ml/s)	F	766 ± 232*	647 ± 213	801 ± 356	0.017	0.399	0.055
	S	714 ± 246*	637 ± 270	650 ± 257			
Peak expiratory flow (ml/s)	F	-618 ± 132	-556 ± 151	-651 ± 244	0.079	0.362	0.417
	S	-586 ± 193*	-525 ± 216	-547 ± 194			
Frequency (breaths/min)	F	22.1 ± 8.8*	26.9 ± 8.2	30.2 ± 8.4	0.128	0.743	0.171
	S	24.9 ± 8.2*	27.6 ± 9.1	28.0 ± 9.4			
Minute ventilation (l/min)	F	11.3 ± 4.0	10.0 ± 4.5	11.6 ± 6.4	0.247	0.985	0.385
	S	11.5 ± 4.8	11.1 ± 5.2	11.1 ± 4.6			
Inspiratory time (s)	F	1.01 ± 0.33*	0.87 ± 0.26	0.72 ± 0.20	0.024	0.126	0.033
	S	0.95 ± 0.22	0.96 ± 0.28	0.96 ± 0.32			
Expiratory time (s)	F	2.20 ± 1.16*	1.70 ± 0.87	1.52 ± 0.60	0.414	0.747	0.375
	S	1.76 ± 0.81*	1.48 ± 0.64	1.53 ± 0.16			
Inspiratory time/breath cycle time	F	0.29 ± 0.12	0.35 ± 0.08	0.33 ± 0.06	0.202	0.048	0.466
	S	0.37 ± 0.06*	0.41 ± 0.07	0.40 ± 0.06			
Frequency/ $V_T$ (breaths · min <sup>-1</sup> · l <sup>-1</sup> )	F	46 ± 28*	83 ± 44	98 ± 55	0.182	0.437	0.057
	S	61 ± 29*	78 ± 34	78 ± 33			
PEEPi (cm H <sub>2</sub> O)	F	2.7 ± 2.7*	4.9 ± 3.6	5.3 ± 4.5	0.621	0.160	0.649
	S	2.0 ± 1.5	2.8 ± 2.6	3.4 ± 3.0			
$C_{dyn}$ (ml/cm H <sub>2</sub> O)	F	39.5 ± 19.4*	31.9 ± 16.8	29.4 ± 24.2	0.464	0.529	0.695
	S	35.1 ± 12.6	40.8 ± 28.6	35.9 ± 23.5			
$R_{aw}$ (cm H <sub>2</sub> O · l <sup>-1</sup> · s <sup>-1</sup> )	F	9.1 ± 7.4*	16.6 ± 8.6	17.2 ± 8.3	0.833	0.682	0.501
	S	7.3 ± 3.6*	14.4 ± 7.9	15.9 ± 10.3			

Note that only data at start and end of the SBT are shown and not the time intervals in between. The P values in table reflect results during the SBT (mixed ANOVA).

\* $P \leq 0.05$  PSV versus SBT start.

$C_{dyn}$  = dynamic compliance; F = weaning-failure group; PEEPi = intrinsic positive end-expiratory pressure; PSV = pressure support ventilation;  $R_{aw}$  = airway resistance; S = weaning-success group; SBT = spontaneous breathing trial;  $V_T$  = tidal volume.

### Ventilation, respiratory timing, and lung mechanics

Variables of ventilation, respiratory time, and lung mechanics are listed in **Table 2**. Immediately after the transition from pressure support ventilation to spontaneous breathing trial,  $V_T$  decreased in both groups but thereafter remained stable for the rest of the spontaneous breathing trial. In both groups, respiratory frequency and the ratio between respiratory frequency and  $V_T$  (*i.e.*, an index of rapid shallow breathing) increased after the transition to the spontaneous breathing trial. Only in the weaning-failure group, inspiratory time significantly decreased, and rapid shallow breathing index increased (borderline significant) during the spontaneous breathing trial.  $V_E$  did not change significantly during the spontaneous breathing trial and was not different between groups.

### Respiratory muscle activity during expiration

In **Figure 2 (A–F)**, activity of the diaphragm ( $\Delta EAdi_{exp}$  and  $\Delta Pdi_{exp}$ ) during the expiration (divided into four equally sized quartiles) together with peak activity during inspiration is shown during pressure support ventilation and during the first and last minute of the spontaneous breathing trial. Changes in expiratory gastric pressure are shown in **Figure 2 (G–I)**, together with peak activity of gastric pressure during expiration. At the end of the spontaneous breathing trial, expiratory gastric pressure increased in the failure group compared to the success group. A significant correlation was found between peak expiratory flow and  $\Delta Pga_{exp}$  during the spontaneous breathing trial in the weaning-failure group ( $R^2 = 0.90$ ,  $P = 0.001$ ) but not in the weaning-success group ( $R^2 = 0.10$ ,  $P = 0.486$ ). The correlation coefficients were significantly different ( $P = 0.039$ ).

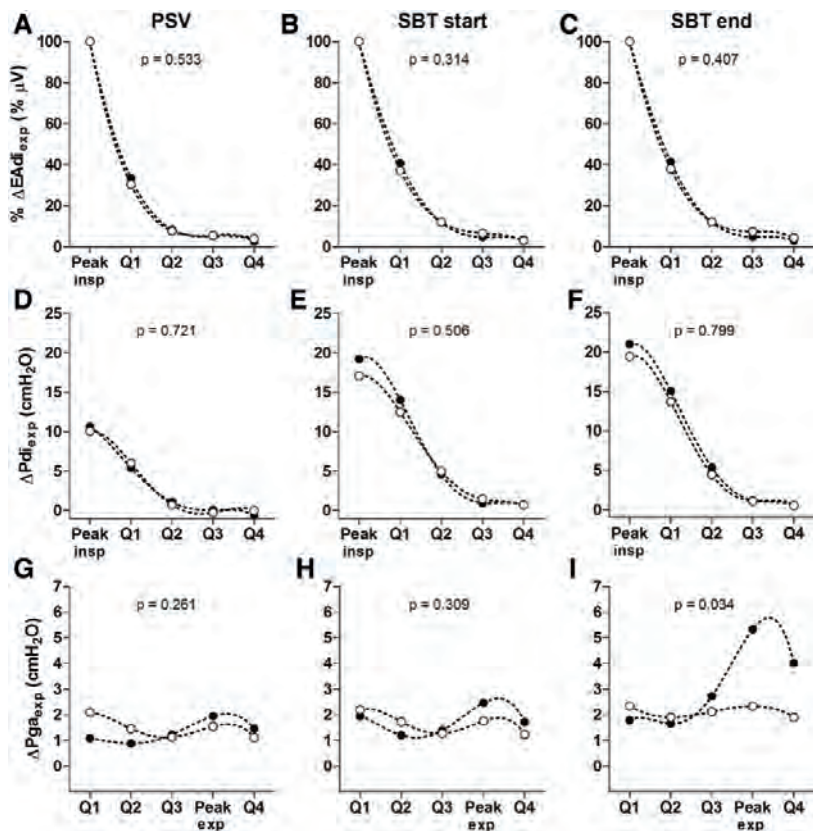


**Figure 2.** Diaphragm electrical activity (EAdi), transdiaphragmatic pressure (Pdi), and gastric pressure (Pga) during expiration. Mean expiratory diaphragm electrical activity ( $\Delta EAdi_{exp}$ ) values were normalized to the individual EAdi peak during inspiration (insp). Expiratory (exp) peak values of Pga were plotted between quartile (Q) 3 and Q4, the most common position of the peak during expiration (see Figure 1). There is no expiratory activity of the diaphragm in Q4 during pressure support ventilation (PSV) or during the spontaneous breathing trial (SBT). There is a significant increase in expiratory gastric pressure ( $\Delta Pga_{exp}$ ) at the end of the SBT in the failure group compared to the success group. The circles in the figure represent the calculated mean values per quartile and the peak values (white circles indicate success, black circles indicate failure), whereas the dashed curves show the fourth order polynomial fit. SD ranged between 1.9 and 11.7%, between 0.6 and 8.8 cmH<sub>2</sub>O and between 0.4 and 3.3 cm H<sub>2</sub>O for %  $\Delta EAdi_{exp}$ ,  $\Delta Pdi_{exp}$ , and  $\Delta Pga_{exp}$ , respectively. The reported P values in each panel represent the interaction term (time  $\times$  group) of the two-way repeated measures ANOVA.

### Respiratory muscle activity during inspiration

**Figure 3** shows respiratory muscle activity during inspiration under pressure support and during the spontaneous breathing trial. Removal of ventilator assist caused immediate increases in  $\Delta Pdi_{insp}$ ,  $\Delta Pes_{insp}$  and  $\Delta EAdi_{insp}$  in both groups, whereas  $NMedi_{insp}$  did not change in the first minute after the removal of inspiratory support.

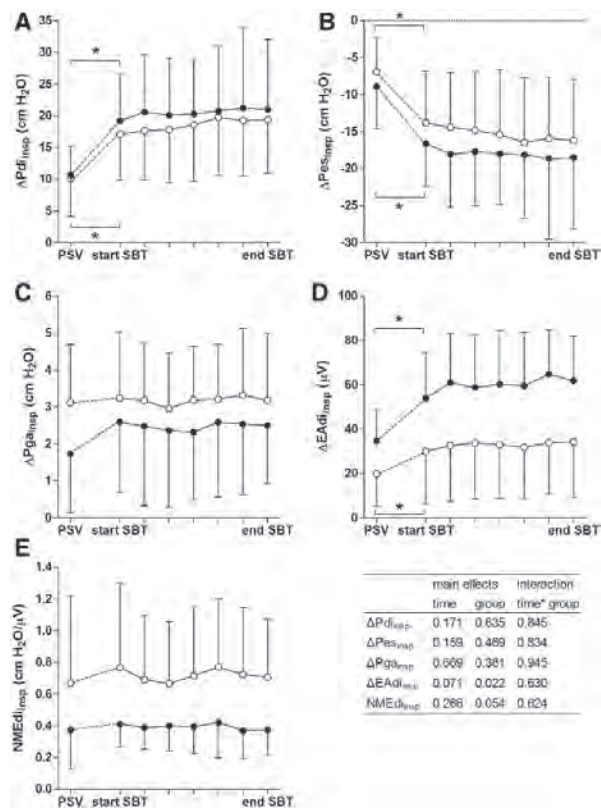


**Figure 3.** Changes in transdiaphragmatic pressure ( $\Delta Pdi_{insp}$ ), esophageal pressure ( $\Delta Pes_{insp}$ ), gastric pressure ( $\Delta Pga_{insp}$ ), diaphragm electrical activity ( $\Delta EAdi_{insp}$ ), and neuromechanical efficiency ( $NMEdi_{insp}$ ) during inspiration for pressure support ventilation (PSV) and during the spontaneous breathing trial (SBT) in the weaning-success (white circles) and weaning-failure (black circles) groups. After removal of ventilator assist  $\Delta Pdi_{insp}$ ,  $\Delta Pes_{insp}$  and  $\Delta EAdi_{insp}$  increased in both groups. During the SBT, data were analyzed at seven points in time: the first minute (start SBT) and last minute (end SBT) and five epochs of at least 1 min taken at equal time intervals in between (ticks in between). A P value table is inserted with the results of the repeated measures ANOVA for each variable during the SBT. \*P < 0.05 PSV versus start SBT.

During the course of the spontaneous breathing trial, no significant interactions were found between time and group for  $\Delta Pdi_{insp}$ ,  $\Delta Pes_{insp}$ ,  $\Delta EAdi_{insp}$ , and  $NMEdi_{insp}$ . However,  $\Delta EAdi_{insp}$  was significantly higher in the failure group compared to the success group during the entire spontaneous breathing trial. Consequently,  $NMEdi_{insp}$  was lower in the weaning-failure group compared to the success group (**Figure 3E**). In the failure group, intrinsic PEEP increased after removal of ventilator assist, but during the spontaneous breathing trial, there were no differences between both groups (**Table 2**).

# Pressure–time product of the respiratory muscles

**Figure 4** shows the pressure–time products of the expiratory muscle and inspiratory muscles during pressure support ventilation and the first and last minute of the spontaneous breathing trial. The transition from pressure support ventilation to spontaneous breathing did not affect  $PTPg_{exp}$  but increased in  $PTP_{es_{insp}}$  in both groups. During the spontaneous breathing trial, there were no differences in  $PTP_{es_{insp}}$  between weaning-failure and weaning-success patients. In addition, there were no differences between the intrinsic PEEP and the elastic and resistive components of  $PTP_{es_{insp}}$  between groups. The apparent increase in  $PTPg_{exp}$  in the failure group did not reach statistical significance ( $P = 0.099$ ).

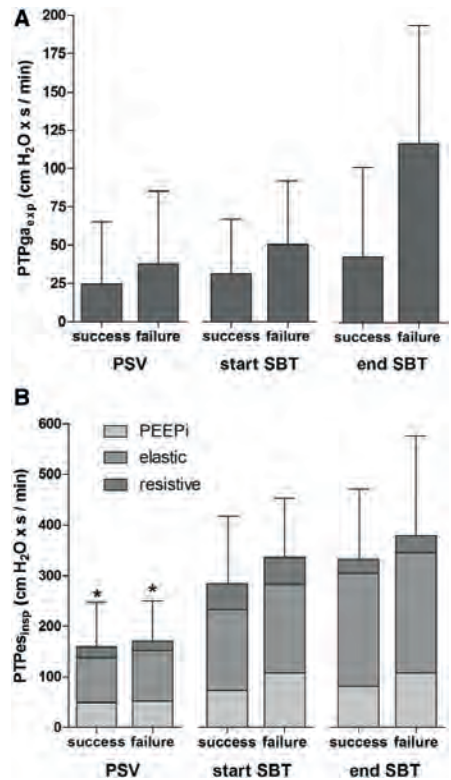


**Figure 4.** Expiratory muscle pressure–time product (A) and inspiratory muscle pressure–time product (B) for pressure support ventilation (PSV) and during the spontaneous breathing trial (SBT) in the weaning-success and weaning-failure groups. After removal of ventilator assist, esophageal pressure–time product during inspiration ( $PTP_{es_{insp}}$ ) increased in both groups. During the SBT, there were no effects of time and group on  $PTP_{es}$ . The apparent increase in gastric pressure–time product during expiration ( $PTPg_{exp}$ ) did not reach statistical significance for the interaction term of the mixed ANOVA ( $P = 0.099$ ). Note that only data at start and end of the SBT are shown and not the time intervals in between. \* $P < 0.05$  PSV versus start SBT. PEEPi = intrinsic positive end-expiratory pressure.

However, the contribution of the expiratory muscles to the total pressure–time product significantly increased from  $13 \pm 9\%$  at the start of the spontaneous breathing trial to  $24 \pm 10\%$  at the end of the spontaneous breathing trial in the weaning-failure group but did not change in the weaning-success group (**Figure 5**).

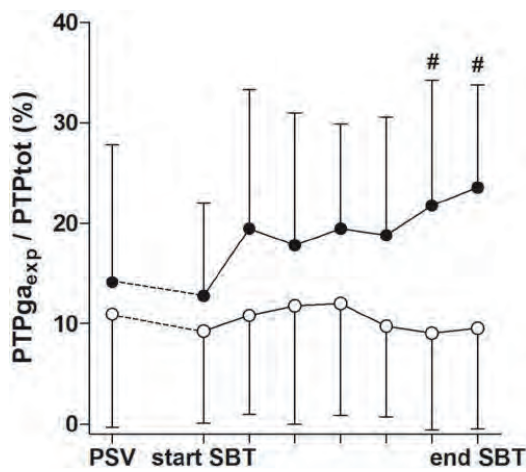


**Figure 5.** The contribution of the expiratory muscles to total respiratory muscle effort for pressure support ventilation (PSV) and during the spontaneous breathing trial (SBT) in the weaning-success (white circle) and weaning-failure (black circle) groups. During the SBT, there was a significant interaction between the time and group ( $P = 0.049$ ) on the ratio between the expiratory gastric pressure–time product and the total respiratory pressure–time product ( $PTP_{ga\_exp} / PTP_{tot}$ ). # $P \leq 0.05$  pairwise *post hoc* comparison between success and failure group.

**Arterial blood gas measurements and hemodynamics**

In **Table 3**, the blood gas values and hemodynamic variables are presented. There were significant effects of time and group on  $PaCO_2$ , such that  $PaCO_2$  increased over time during the spontaneous breathing trial and was higher in the failure group. However, the interaction between the effects of time and group were not significant, indicating that the increase in  $PaCO_2$  was not different between both groups.

**Table 3.** Blood Gas Values and Hemodynamic Variables before and after the SBT for the Failure Group and the Success Group

	Group	PSV <sup>*</sup>	SBT End	P Value		
				Main Effect		Interaction (Time × Group)
				Time	Group	
Pao <sub>2</sub> (mmHg)	F	91 ± 26	101 ± 18	0.225	0.127	0.595
	S	102 ± 21	99 ± 26			
Paco <sub>2</sub> (mmHg)	F	46 ± 11	50 ± 14	0.014	0.045	0.128
	S	38 ± 4	40 ± 5			
pH	F	7.42 ± 0.07	7.39 ± 0.08	0.015	0.261	0.427
	S	7.45 ± 0.04	7.44 ± 0.04			
MAP (mmHg)	F	88 ± 20	92 ± 23	0.621	0.707	0.157
	S	96 ± 25	94 ± 21			
Heart rate	F	87 ± 17	91 ± 21	0.194	0.312	0.425
	S	81 ± 11	82 ± 9			

<sup>\*</sup>Blood gas values were drawn just before start of the SBT.

F = weaning failure; MAP = mean arterial pressure; PSV = pressure support ventilation; S = weaning success; SBT = spontaneous breathing trial.

# DISCUSSION

The present study provides new insights in the recruitment and effort of the respiratory muscles during expiration in a heterogeneous group of patients weaning from mechanical ventilation. First, we found that in weaning-failure patients, expiratory muscles recruitment is as high as 24% of the total respiratory muscle effort at the end of the trial. Second, we found no difference in tonic activity of the diaphragm during expiration between weaning-failure patients and weaning-success patients. Finally, neuromechanical efficiency of the diaphragm is lower in weaning-failure patients compared to weaning-success patients, both during pressure support ventilation and during a spontaneous breathing trial.

## Respiratory muscle effort during expiration

The pressure–time product has been used to quantify breathing effort [189, 190]. Experimental studies have demonstrated that changes in inspiratory PTPes are correlated with changes in diaphragmatic energy expenditure [193, 194]. In the present study, we found an increase in PTPes during inspiration with the transition from mechanical ventilation to unassisted breathing, with no differences between the success group and the failure group. At first sight, this seems surprising, but under conditions of increased loading and/or impaired diaphragm function, the expiratory muscles could be recruited [141]. Indeed, in the present study, expiratory muscle activity, as indicated by an expiratory rise in gastric pressure, was found in the weaning-failure group during the spontaneous breathing trial. This expiratory rise in gastric pressure is consistent with previous findings in patients weaning from mechanical ventilation with COPD [67, 176]. Expiratory muscle recruitment



may increase the energy expenditure of respiration. In exercising healthy subjects, expiratory pressure generation is a significant contributor to the perception of dyspnea [195]. Therefore, muscle effort during expiration should be taken into account when calculating respiratory muscle effort. To this end, we calculated the expiratory pressure–time product from the gastric pressure curve. In the weaning-failure group, the contribution of the expiratory muscles to total respiratory muscle effort progressively increased during the spontaneous breathing trial, whereas it remained stable in successfully extubated patients. Whether the increase in expiratory muscle effort resulted from activation of the abdominal muscles, expiratory rib cage muscles, or a combination of the two is unknown; the relative contribution of each muscle group during expiration cannot be derived from the expiratory rise in gastric pressure [67].

Pellegrini et al. [118] have recently demonstrated that in lung-injured pigs, decreasing extrinsic PEEP increases diaphragm activity during expiration. Diaphragmatic contraction during expiration will affect  $\Delta P_{ga_{exp}}$  and  $PTP_{ga_{exp}}$  in patients weaning from mechanical ventilation. In the current study, there was negligible low tonic diaphragmatic activity in the last quartile of the expiratory phase during the spontaneous breathing trial. However, in the first expiratory quartile, diaphragm activity was approximately 40% of its peak value. In our opinion, it is debatable whether the electrical activity of the diaphragm in the first expiratory quartile should be defined as persistent activity of the diaphragm in expiration [118, 178] or should be regarded as the termination of the inspiratory activity. Regardless, in our study there was no difference in activity of the diaphragm (diaphragm electrical activity and transdiaphragmatic pressure) between weaning-failure patients and weaning-success patients for all expiratory quartiles during the spontaneous breathing trial. Therefore, it is reasonable to assume that cyclic expiratory changes in gastric pressure at the end of the spontaneous breathing trial in weaning-failure patients are the result of expiratory muscle activity. In addition, the rise in gastric pressure was correlated with peak expiratory flow in the weaning-failure group, consistent with increased expiratory muscle activity.

It has been reasoned that an important goal of expiratory muscle recruitment is to assist the inspiratory muscles by decreasing end-expiratory lung volume [141, 196]. A decrease in end-expiratory lung volume places the diaphragm at a more optimal position of the length-tension curve. However, intrinsic PEEP (corrected for the expiratory rise in gastric pressure) in the current study, a surrogate of end-expiratory lung volume, was not lower in the failure group compared to the success group. On the contrary, intrinsic PEEP tended to be higher in the failure group. In addition,

we found no improvements in  $NMEdi_{insp}$  in the failure group as a result of increased expiratory muscle recruitment. In line with these findings, it has been demonstrated that expiratory muscle recruitment does not increase  $NMEdi_{insp}$  in COPD patients [196]. Thus, it is questionable whether expiratory muscle recruitment assists the inspiratory muscles in weaning-failure patients. Whether expiratory muscle recruitment aids weaning patients should be addressed in future studies.

### Neuromechanical efficiency of the diaphragm during inspiration

As expected, removal of ventilator assist increased  $\Delta Pdi_{insp}$  and  $\Delta EAdi_{insp}$  in both groups.  $NMEdi_{insp}$  was lower in weaning-failure patients compared to the success group. The neuromechanical efficiency of the diaphragm in weaning-failure patients and weaning-success patients in our study were approximately 30 and 50% of the values we reported for healthy subjects, respectively [187]. To the best of our knowledge, our study is the first to continuously measure  $NMEdi_{insp}$  during a T-tube trial using diaphragm electrical activity and transdiaphragmatic pressure. Previously,  $NMEdi_{insp}$  has been calculated intermittently during a 30-min weaning trial as the decrease in airway pressure divided by  $\Delta EAdi_{insp}$  during an inspiratory occlusion [23]. In the latter study, the weaning trial was performed with 5 cmH<sub>2</sub>O of continuous positive airway pressure. The addition of 5 cmH<sub>2</sub>O of continuous positive airway pressure decreases the work of breathing by as much as 40% in ventilated patients [190]. Nevertheless, the reduced ability of the diaphragm to convert neural respiratory drive into pressure in weaning-failure patients is a consistent finding among studies [23, 174].

Numerous studies have demonstrated that diaphragm weakness develops in critically ill patients [4, 5, 13, 52, 171, 172]. Reduced pressure-generating capacity of the diaphragm may result from structural modifications but also from the development of muscle fatigue, altered force-velocity relation, or altered force-length relation of the muscle. These factors may play a role in the development of weakness during a spontaneous breathing trial. However, previously it was demonstrated that a 1-h spontaneous breathing trial did not cause long-lasting fatigue of the diaphragm [102]. Increased end-expiratory lung volume may place the diaphragm at a less favorable position on a length-tension curve. An increase in lung volume from functional residual capacity to total lung capacity reduces transdiaphragmatic pressure by 60% for a given  $\Delta EAdi_{insp}$  [74]. Although we did not directly measure end-expiratory lung volume, corrected intrinsic PEEP and lung mechanics were not significantly different between groups during weaning, suggesting no major differences in lung volume. Accordingly, reduced neuromechanical efficiency in the failure group may largely

be explained by structural modifications, such as diaphragm atrophy, but we cannot completely rule out impaired respiratory mechanics.

In contrast to a previous study by Jubran and Tobin [189], we did not find a difference in  $PTP_{\text{insp}}$  between weaning-success and weaning-failure patients. This difference may be explained by patient selection and weaning failure criteria. In Jubran and Tobin's study, only patients with COPD were included. This provides an explanation for the fact that the higher  $PTP_{\text{insp}}$  resulted from higher resistance and intrinsic PEEP. Furthermore, we defined weaning failure as failing the spontaneous breathing trial or reintubation within 48 h after extubation, whereas in their study, weaning failure was defined as failing the spontaneous breathing trial.

In the present study, increased respiratory muscle effort (including expiratory muscle effort) and reduced neuromechanical efficiency of the diaphragm appear to play a role in failure to wean from mechanical ventilation. However, it is important to note that cardiac dysfunction, cognitive dysfunction, and metabolic disorders are recognized causes for weaning failure as well [169, 170] and may have contributed to weaning failure in the current study.

### Limitations

In the present study, raw EAdi signals were recorded and processed according to the methods of Sinderby et al [61-63]. Today, many studies record electrical activity of the diaphragm not in its raw format but as a processed signal via the SERVO-i (Maquet Critical Care) ventilator. Differences between algorithms to process EAdi can lead to differences in absolute values of  $\Delta EAdi_{\text{insp}}$ . Therefore, absolute values of  $\Delta EAdi_{\text{insp}}$  (and  $NMEdi_{\text{insp}}$ ) obtained in our study cannot be directly compared to values obtained with recordings from the SERVO-i (Maquet Critical Care) ventilator.

We did not record electrical activity of the abdominal wall muscles. However, we are confident that  $\Delta Pga_{\text{exp}}$  reflects expiratory muscle recruitment in our study. First, we excluded the possibility of expiratory diaphragmatic activity contributing to  $\Delta Pga_{\text{exp}}$ . Second, we found a strong correlation between peak expiratory flow and  $\Delta Pga_{\text{exp}}$  in weaning-failure patients. Third, a strong correlation has previously been demonstrated between  $\Delta Pga_{\text{exp}}$  and electrical activity of the abdominal wall muscles [147].

In conclusion, the expiratory muscles significantly contribute to respiratory muscle effort in a mixed group of weaning-failure patients. Therefore, the expiratory pressure–time product should be measured when estimating energy expenditure of the respiratory muscles during weaning from mechanical ventilation. We did

not find evidence of increased expiratory tonic diaphragmatic contraction during weaning failure. In addition, our findings confirm that impaired pressure-generating capacity of the diaphragm, regardless of its origin, plays a role in failure to wean from mechanical ventilation.

## ACKNOWLEDGMENTS

The authors thank Wiebe Pestman, Ph.D. (Department of Biostatistics, Radboud University Medical Center, Nijmegen, The Netherlands), for his statistical advice and review of the manuscript.

### Research Support

This study was investigator-initiated and financed by institutional resources (Department of Critical Care Medicine, Radboud University Medical Center, Nijmegen, The Netherlands).

## REFERENCES

See page 166.



**PART II:**  
**Monitoring diaphragm function in**  
**acutely ventilated patients**

## Chapter 5

# Estimation of the diaphragm neuromuscular efficiency index in mechanically ventilated critically ill patients

---

**Diana Jansen**, Annemijn H. Jonkman, Lisanne Roesthuis, Suvarna Gadgil, Johannes G. van der Hoeven, Gert-Jan J. Scheffer, Armand Girbes, Jonne Doorduyn, Christer S. Sinderby and Leo M. A. Heunks

*Critical Care* (2018) 22:238    <https://doi.org/10.1186/s13054-018-2172-0>



## ABSTRACT

### Background

Diaphragm dysfunction develops frequently in ventilated intensive care unit (ICU) patients. Both disuse atrophy (ventilator over-assist) and high respiratory muscle effort (ventilator under-assist) seem to be involved. A strong rationale exists to monitor diaphragm effort and titrate support to maintain respiratory muscle activity within physiological limits. Diaphragm electromyography is used to quantify breathing effort and has been correlated with transdiaphragmatic pressure and esophageal pressure. The neuromuscular efficiency index (NME) can be used to estimate inspiratory effort, however its repeatability has not been investigated yet. Our goal is to evaluate NME repeatability during an end-expiratory occlusion (NMEoccl) and its use to estimate the pressure generated by the inspiratory muscles (Pmus).

### Methods

This is a prospective cohort study, performed in a medical-surgical ICU. A total of 31 adult patients were included, all ventilated in neurally adjusted ventilator assist (NAVA) mode with an electrical activity of the diaphragm (EAdi) catheter in situ. At four time points within 72 h five repeated end-expiratory occlusion maneuvers were performed. NMEoccl was calculated by  $\Delta P_{aw} / \Delta E_{Adi}$  and was used to estimate Pmus. The repeatability coefficient (RC) was calculated to investigate the NMEoccl variability.

### Results

A total number of 459 maneuvers were obtained. At time  $T = 0$  mean NMEoccl was  $1.22 \pm 0.86 \text{ cmH}_2\text{O}/\mu\text{V}$  with a RC of 82.6%. This implies that when NMEoccl is  $1.22 \text{ cmH}_2\text{O}/\mu\text{V}$ , it is expected with a probability of 95% that the subsequent measured NMEoccl will be between  $2.22$  and  $0.22 \text{ cmH}_2\text{O}/\mu\text{V}$ . Additional EAdi waveform analysis to correct for non-physiological appearing waveforms, did not improve NMEoccl variability. Selecting three out of five occlusions with the lowest variability reduced the RC to 29.8%.

### Conclusions

Repeated measurements of NMEoccl exhibit high variability, limiting the ability of a single NMEoccl maneuver to estimate neuromuscular efficiency and therefore the pressure generated by the inspiratory muscles based on EAdi.

**Keywords:** Diaphragm dysfunction, Neuromuscular efficiency index, Mechanical ventilation, Partially supported mode, Diaphragm electromyography, Monitoring

## BACKGROUND

Diaphragm dysfunction frequently develops in mechanically ventilated intensive care unit (ICU) patients and is associated with adverse clinical outcomes including prolonged mechanical ventilation and mortality [3, 5, 13, 41, 172, 197, 198]. It appears that non-physiological diaphragm activity plays an important role [42], in which both disuse atrophy resulting from ventilator over-assist [4, 5, 12] and high respiratory muscle effort resulting from ventilator under-assist [44, 45, 199] have been associated with diaphragm dysfunction in ICU patients. Therefore, there is a strong physiological rationale for monitoring diaphragm effort [17, 18, 91] and titrating support to maintain respiratory muscle activity within physiological limits [33].

Variations in esophageal pressure (Pes) during breathing have been used for decades to quantify breathing effort. Recently, two state-of-the-art papers reviewed the technical and clinical aspects of esophageal pressure (Pes) monitoring in ICU patients [20, 200]. Limitations of this technique include strict control of balloon inflation volume and complexity of signal interpretation, in particular when expiratory muscles are recruited.

Diaphragm electromyography (EMG) is an alternative technique used to quantify breathing effort in ICU patients [17]. Strong correlation has been reported between the electrical activity of the diaphragm (EAdi) and transdiaphragmatic pressure (Pdi) or Pes [21, 22]. The neuromechanical efficiency (NMEoccl), defined by delta airway pressure ( $\Delta P_{aw}$ ) divided by  $\Delta E_{Adi}$  measured during an end-expiratory occlusion, has been used to estimate the inspiratory effort breath by breath [22, 23]. This ratio describes how much pressure can be generated for each microvolt of EAdi signal, in other words how efficient the diaphragm is in generating pressure for a certain amount of electrical activity. This is of potential interest for monitoring diaphragm function (over time) and helps to titrate ventilatory support in order to minimize diaphragm dysfunction resulting from ventilator over-assist and under-assist [33]. Today, this index has only been evaluated in studies including limited numbers of patients [22, 23, 25, 26] and the repeatability, an essential characteristic for a diagnostic tool, has not been investigated at all. Therefore, the aim of our study was to evaluate the NMEoccl repeatability in mechanically ventilated ICU patients and its use to estimate the maximum inspiratory pressure generated by the inspiratory muscles (Pmus).

## METHODS

### Study design and population

This prospective cohort study was performed in an academic ICU. Adult patients, with a dedicated EAdi catheter (Maquet critical care, Solna Sweden) in situ and mechanically ventilated in neurally adjusted ventilator assist (NAVA) mode were eligible for inclusion. The institutional ethical committee approved the study protocol and informed consent was waived due to the non-invasive nature of the study and negligible risks.

### Study protocol

The EAdi catheter was positioned according to the manufacturer's instructions using a dedicated software tool on the Servo-i ventilator. The catheter position was verified before data acquisition. When patients exhibited a stable breathing pattern (i.e. no coughing, hiccups or disproportional differences in respiratory rate), measurements to assess respiratory muscle function were performed: (1) an end-expiratory occlusion maneuver (obtained by activating the expiratory hold button on the ventilator for one inspiratory effort) for measurement of NMEoccl and (2) a "zero assist breath" in which inspiratory support was decreased to zero for one single breath to calculate patient-ventilator breath contribution (PVBC) [24, 201]. Both maneuvers were repeated five times with at least a one-minute interval. The number of breaths between maneuvers was variable to prevent anticipation by the patient. Measurements were recorded and stored for offline analysis at time  $T = 0$  and after 12 h ( $T = 12$ ), 24 h ( $T = 24$ ) and 72 h ( $T = 72$ ).

### Data acquisition

EAdi, flow and Paw waveforms were acquired from the Servo-i ventilator via a RS232 serial port connected to a laptop with dedicated software (Servo Tracker version 4.1, Maquet, Solna, Sweden). Maximum inspiratory pressure (MIP) measurements were performed with a manovacuumeter (Micro Respiratory Pressure Meter, Carefusion, Yorba Linda, CA, USA) connected to the endotracheal tube [202].

### Data analysis

A software routine developed for MatLab (version R2016b, MathWorks Inc., Natick, MA, USA) was used for offline analysis. NMEoccl was calculated in three different ways (**Figure 1**): (1) by dividing  $\Delta P_{aw}$  by  $\Delta E_{adi}$  [22], in which  $\Delta P_{aw}$  is the difference in pressure between the lowest Paw during end-expiratory occlusion and the preceding end-expiratory pressure level, (2) by dividing the area under the curve (AUC) of Paw and EAdi, and (3) by dividing Paw and EAdi at fixed points (steps of 3  $\mu V$ ) on the EAdi waveform.

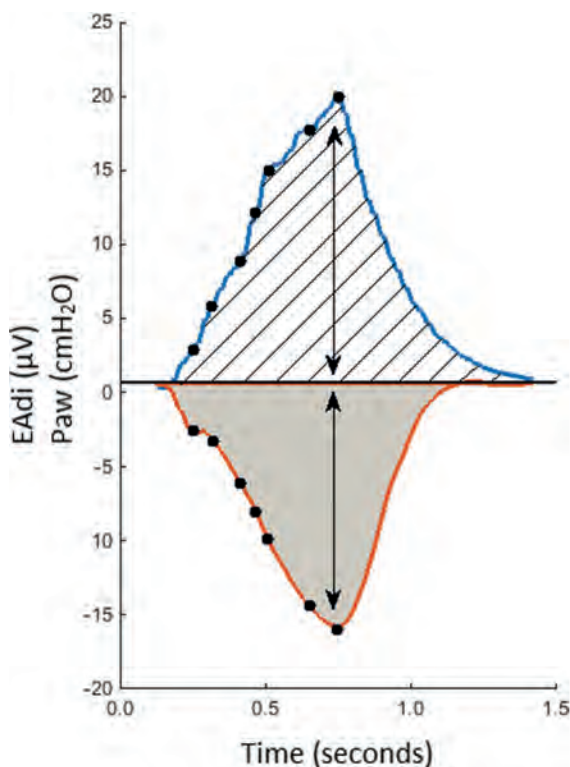


**Figure 1.** Example of a single neuromechanical efficiency index during an end-expiratory occlusion (NMEoccl) maneuver. The blue line represents the electrical activity of the diaphragm (EAdi) signal expressed in microvolts. The orange line represents the airway pressure (Paw) expressed in centimeters of water. As described above, the NMEoccl was calculated in three different ways, with the calculation based on (1) delta peak values of electrical activity of the diaphragm (EAdi) and Paw, shown as arrows; (2) area under the curve (AUC) of the EAdi and Paw signal, shown by diagonal lines and gray area, respectively; (3) using fixed points (steps of 3  $\mu\text{V}$ ) on the EAdi curve (during inspiration) and corresponding Paw, shown as black dots.

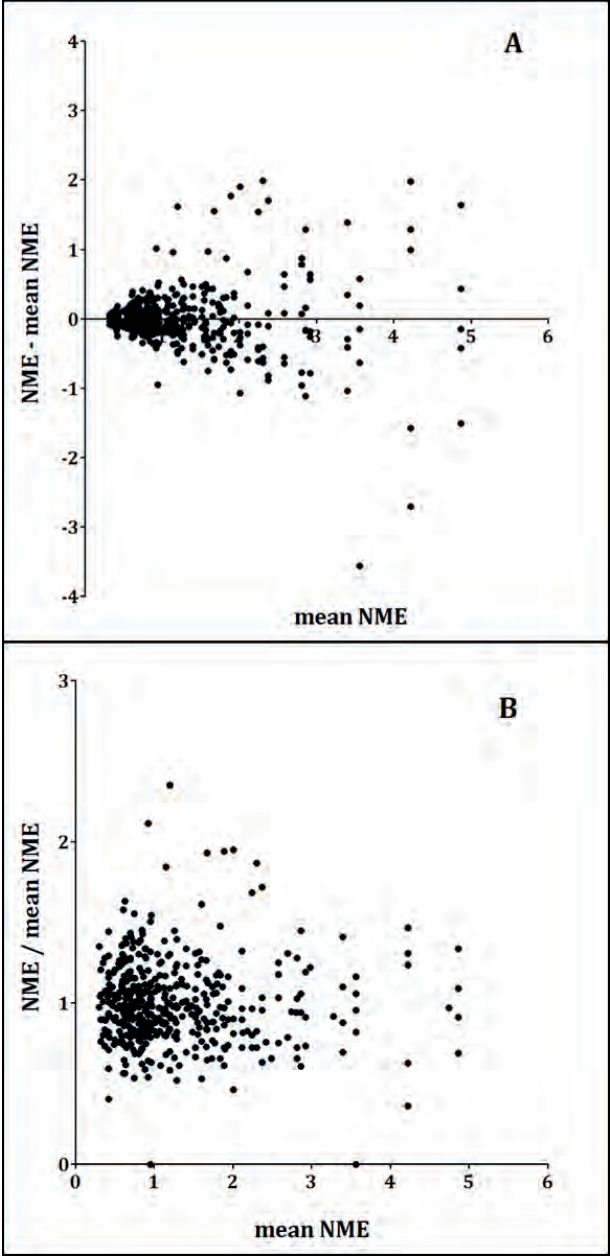
The inspiratory time ( $T_i$ ) was defined as the period between the onset of EAdi and 70% peak of EAdi. To investigate the effect of an occlusion on the inspiratory time, we compared  $T_i$  during occlusion with the  $T_i$  of three preceding unloaded breaths. To estimate  $P_{\text{mus}}$  under clinical conditions, the mean EAdi of five tidal breaths (before the end-expiratory occlusion) was multiplied by  $\text{NMEoccl}/1.5$  [22]. The correction of 1.5 compensates for the fact that in the presence of flow, the diaphragm generates less pressure for the same EAdi than during an occlusion [22]. The tension-time index (TTI) was calculated as  $P_{\text{mus}}/\text{MIP}$  multiplied by the ratio of  $T_i$  to total respiratory cycle time ( $T_{\text{tot}}$ ) [203].

### Statistical analysis

Statistical analysis was performed with GraphPad PRISM (version 5.03 for Mac/Windows, Software Inc. San Diego, CA, USA). Data were analyzed as median  $\pm$  interquartile range (IQR), except as stated otherwise. Statistical significance was indicated by a p value  $<0.05$ . The repeatability coefficient (RC) represents the absolute value by which two repeated measurements in one subject will differ in 95% of cases. The formula developed by Bland and Altman was used to calculate RC:  $1.96 \times \sqrt{2} \times \text{Within-subject standard deviation (SD)}$  [204]. One-way analysis of variance (ANOVA) was used to obtain the within-subject SD with the subject as dependent factor and the repeated NMEoccl measurements as independent factors. Since the NMEoccl variability increased as the magnitude of NMEoccl increased, the ratio of a single NMEoccl measurement to the mean NMEoccl of five repeated measurements was used (see **Additional Figure 1**) [204].

The correlation coefficient with repeated observation was used to investigate the within-subject correlation between Paw and EAdi [205, 206] (IBM SPSS Statistics version 22).

In addition, to obtain the within-subject NMEoccl variation, per patient for each time point a coefficient of variation (CoV) was calculated by the ratio of the within-subject SD to the mean. The median CoV was used to divide the study population into two groups with CoV higher or lower than median. The paired t test was used to test for differences in clinical parameters (that might affect NMEoccl variability) between both groups. The Pearson correlation coefficient was calculated to test correlation between  $T_i$  and NMEoccl, and between  $TTI$  and  $P_{mus}$ . One-way ANOVA was used to investigate the changes in NMEoccl and inspiratory muscle pressure over time.



**Additional Figure 1.** Since the variability of NMEoccl increased as the magnitude of the NMEoccl increased, the ratio of a single NMEoccl value to the mean NMEoccl of five repeated measurements was used to calculate the variability of NMEoccl [204]. In **panel A** the difference in NME is expressed against mean NME. In **panel B** the ratio of NME is expresses against mean NME.

## RESULTS

**Table 1** shows the main characteristics of the study population. A total 459 occlusions were performed (see Additional Figure 2, not included in this thesis). In 19 patients, the measurements could not be obtained at all four time points due to various reasons: extubation ( $n = 7$ ), agitation ( $n = 2$ ), low EAdi ( $n = 3$ ), return to controlled mode ( $n = 2$ ), death ( $n = 1$ ) and others ( $n = 4$ ).

**Table 1. Main characteristics of the study population**

Characteristics	N=31
Age (years), median [IQR]	69 [55.5-72]
Sex, male/female	22/9
BMI ( $\text{kg}/\text{m}^2$ ), median [IQR]	24.7 [21.6-26]
Comorbidity, n= (%)	
Cardiac diseases	9 (29%)
Diabetes	6 (19%)
COPD	4 (13%)
Reason of admission, n= (%)	
Pneumonia	13 (42%)
Postoperative	8 (26%)
Trauma	7 (23%)
Others	3 (10%)
ARDS at admission, n= (%)	9 (29%)
Sepsis during admission, n= (%)	6 (19%)
Duration of MV on T=0 (days), median [IQR]	10 [8.5-18.5]
Partially supported mode before T=0	9 [4-14]
Controlled mode before T=0	1 [0-3.5]
Total days of MV (days), median [IQR]	24 [14.5-29.5]
NAVA level, median [IQR]	0.7 [0.5-1.2]
Tidal volume (ml), median [IQR]	450 [381-554]
Respiratory rate (per minute), median [IQR]	25 [18-30]
PEEP ( $\text{cmH}_2\text{O}$ ), median [IQR]	8 [6-10]

### NMEoccl variability

A representative NMEoccl maneuver is shown in **Figure 1**. At  $T = 0$ , 149 maneuvers were obtained in 31 patients, 6 maneuvers were lost due to technical issues. Mean  $\Delta\text{Paw}$  was  $14.1 \pm 7.9 \text{ cmH}_2\text{O}$  and mean  $\Delta\text{EAdi}$   $14.8 \pm 9.9 \mu\text{V}$ . Mean NMEoccl was  $1.22 \pm 0.86 \text{ cmH}_2\text{O}/\mu\text{V}$  (ranging from 0.41 to  $3.56 \text{ cmH}_2\text{O}/\mu\text{V}$ ), with a RC of 82.6%. This implies that when NMEoccl is  $1.0 \text{ cmH}_2\text{O}/\mu\text{V}$ , it is expected with a probability of 95% that the subsequent measured NMEoccl will be between 0.17 and  $1.83 \text{ cmH}_2\text{O}/\mu\text{V}$ . When the EAdi of this patient during normal breathing is  $10 \mu\text{V}$ , the estimated pressure generated by the inspiratory muscles would be somewhere between  $1.1 \text{ cmH}_2\text{O}$  and  $12.2 \text{ cmH}_2\text{O}$  (calculated as  $\text{EAdi} * \text{NMEoccl}/1.5$ , see “Methods”). In addition, the RC of NMEoccl calculated by the AUC and at fixed points on the EAdi

curve (**Figure 2**) remained high: 87.7% for AUC and 85.5–175.9% at fixed points. The RC of the separate components of NMEoccl was 95.7% for EAdi and 73.9% for Paw. **Figure 2** shows there was moderate correlation between  $\Delta$ EAdi and  $\Delta$ Paw in the individual patient (mean  $r = 0.52$ ,  $p < 0.0005$ ; ranging from  $r = -0.90$  to  $r = 1.0$ ).

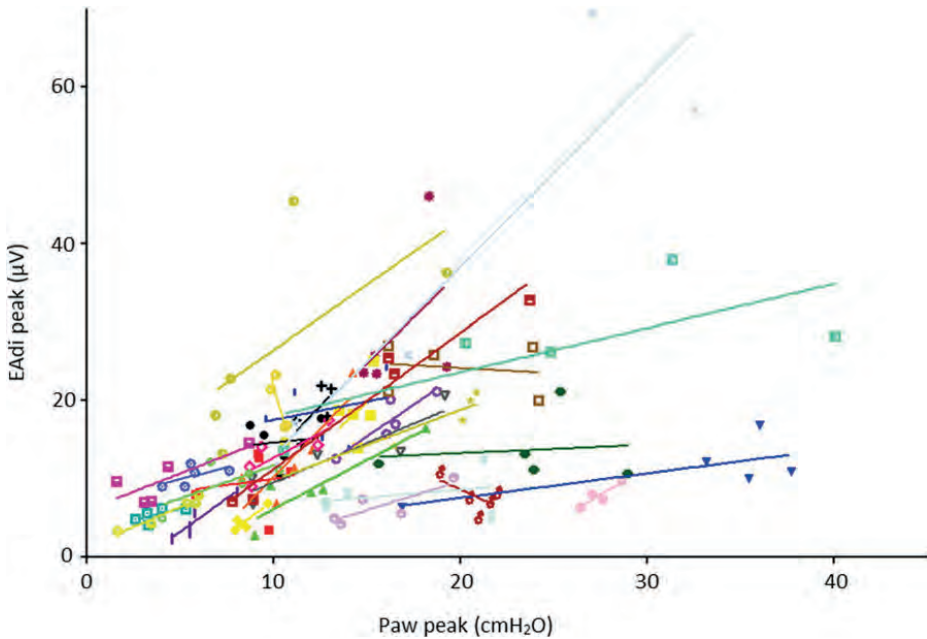


**Figure 2.** Overview of the correlation of airway pressure (Paw) peak and electrical activity of the diaphragm (EAdi) peak of all maneuvers at time  $T = 0$ . Each color represents an individual patient with five repeated measurements (dots) and the corresponding slope (line).

Upon visual inspection it appeared that some of the EAdi tracings exhibit a rather non-physiological shape: a plateau during inspiration (while an increase would be expected) or at maximum inspiration, or a delayed increase in EAdi relative to the decrease in Paw (**Figure 3**). It was reasoned that non-physiological-appearing EAdi waveforms contribute to the high NMEoccl variability.



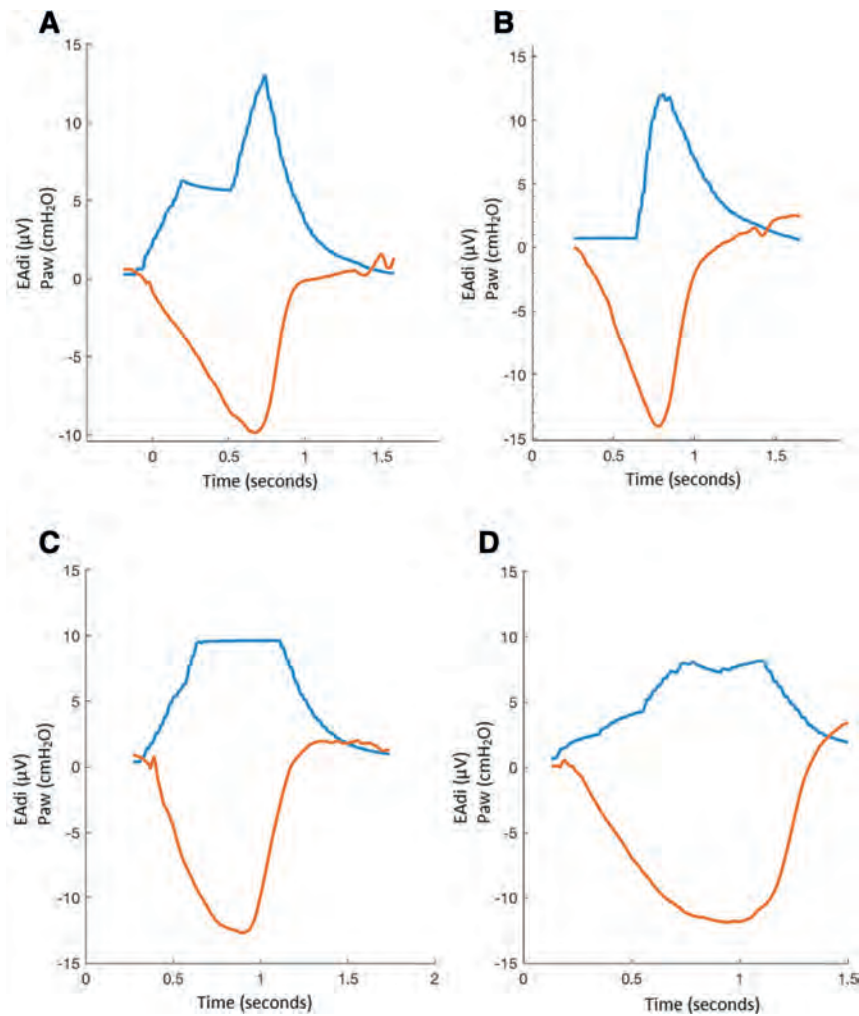


**Figure 3.** Four examples of electrical activity of the diaphragm (EAdi) waveform irregularities during an end-expiratory occlusion. The blue line represents the EAdi signal expressed in microvolts. The orange line represent the airway pressure (Paw) expressed in centimeters of water. **A:** Slope < 0 during the ascending part of the EAdi waveform. **B:** Delay in start of EAdi peak. **C:** EAdi peak cut off. **D:** Split EAdi peak.

**Additional file 2 (not included in this thesis)** shows every occlusion maneuver obtained in this study. Different mathematical approaches were used in order to try to objectively detect and exclude non-physiological EAdi waveforms (**See additional file 3, not included in this thesis**). Despite these mathematical approaches the NMEoccl repeatability remained high with a RC of 63.4%.

Finally, we pragmatically selected three out of five occlusions with the lowest variability and averaged the three values to obtain a single NMEoccl for each individual patient. This approach reduces the influence of erroneous values, irrespective of the origin, and will result in a more reproducible NMEoccl value. As a result, the RC improved to 29.8%. This approach was used for subsequent analysis.

#### Correlation of NMEoccl variability with clinical parameters and inspiratory time

The median CoV NMEoccl at T = 0 was 23.1% (IQR 18.7–29.9%). After dividing the study population into two groups with CoV higher or lower than median, respectively, no significant differences in clinical parameters were found (see **Additional Figure 4**). Median Ti during occlusion was 0.51 s (IQR 0.35–0.65 s) and of the preceding breaths 0.65 s (IQR 0.48–0.84 s). On average, in 48% of the measurements within a patient, Ti of the occluded breath was longer compared to Ti of the preceding breaths. Only moderate negative correlation was found between Ti and NMEoccl ( $r = -0.219$ ).

**Additional File 4. Correlation of clinical parameters and NMEoccl variability at T=0.**

Clinical parameters	All (N=31)	CoV above median (N=15)	CoV below median (N=16)	P-value
RASS, median [IQR]	-1 [0/-2]	-1 [0/-1.5]	-2 [-0.5/-3]	0.086
Sedatives, n= (%)	8 (25.8%)	4 (26.7%)	4 (25%)	0.919
Opioids, n= (%)	13 (41.9%)	6 (40%)	7 (43.8%)	0.839
Use of steroids, n= (%)	8 (26%)	5 (33%)	3 (19%)	0.374
RR (per minute), median [IQR]	25 [17-30]	20 [16-28]	26 [19-31]	0.151
VT (ml), median [IQR]	450 [395-438]	450 [415-490]	420 [389-545]	0.521
NAVA level, median [IQR]	0.8 [0.5-1.3]	0.8 [0.6-1.4]	0.7 [0.2-1]	0.056
EAdi (μV), median [IQR]	13.0 [7.5- 20.7]	12.2 [7.3-19.1]	13.0 [9.0-19.1]	0.546
Low Eadi (<5μV), n= (%)	2 (6.5%)	2 (13.3%)	0 (0%)	0.164
Duration of MV on T=0 (days), median [IQR]	10 [8.5-18.5]	9 [4.5-19]	11.5 [9-17]	0.292
HR (beats/min), median [IQR]	84 [75-95]	80 [72-88]	88 [79-95]	0.258
Atrial fibrillation, n= (%)	1 (3,2%)	0 (0%)	1 (6,3%)	0.333
Temperature, median [IQR]	37.7 [37-38.2]	37.4 [36.9-37.8]	37.8 [37.2-38.3]	0.118
COPD, n= (%)	4 (12.9%)	2 (13.3%)	2 (12.5%)	0.947
Neuromuscular disease, n= (%)	4 (12.9%)	3 (20%)	1 (6.3%)	0.278

**Additional Figure 4.** Correlation of clinical parameters and NMEoccl variability at T = 0. First, the coefficient of variation (CoV) was calculated for each patient. The median CoV for NMEoccl at T = 0 was 23.1% (IQR 18.7–29.9%). The study population was divided in two groups, with the CoV higher or lower than the median, respectively. CoV = coefficient of variation; COPD = chronic obstructive pulmonary disease; EAdi = electrical activity of the diaphragm; HR = heart rate; IQR = interquartile range; NAVA = neutrally adjusted ventilatory assist; RASS = Richmond agitation sedation scale; RR = respiratory rate; VT = tidal volume.

### Changes in NMEoccl over time

Twelve patients completed the 72 h study period. In these patients, NMEoccl at T = 0 was 0.8 cmH<sub>2</sub>O/μV (IQR 0.7–1.1 cmH<sub>2</sub>O/μV) and did not change over time (p = 0.75); 0.7 cmH<sub>2</sub>O/μV (IQR 0.4–0.9 cmH<sub>2</sub>O/μV), 0.8 cmH<sub>2</sub>O/μV (IQR 0.6–1.1 cmH<sub>2</sub>O/μV), 0.9 cmH<sub>2</sub>O/μV (IQR 0.6–1.3 cmH<sub>2</sub>O/μV) for T = 12, T = 24 and T = 72, respectively.

### Diaphragm muscle effort

The mean EAdi of five unloaded breaths before the end-expiratory occlusion were used to calculate Pmus. At T = 0, median Pmus was 9.4 cmH<sub>2</sub>O (IQR 6.0–12.8cmH<sub>2</sub>O) and did not change over time (p = 0.58); 10.4cmH<sub>2</sub>O (IQR 5.4–15.4 cmH<sub>2</sub>O), 10.7 cmH<sub>2</sub>O (IQR 4.8–13.1 cmH<sub>2</sub>O) and 8.2 cmH<sub>2</sub>O (IQR 6.0–15.9cmH<sub>2</sub>O) for T = 12, T = 24 and T = 72, respectively. The median Pmus varied widely among patients, ranging from 1.8 to 36.0 cmH<sub>2</sub>O. Based on previous literature [22, 25], we defined a physiological Pmus between 5 and 10 cmH<sub>2</sub>O. At T = 0, 6 patients (19.4%) had a mean Pmus < 5cmH<sub>2</sub>O and 12 patients (38.7%) > 10cmH<sub>2</sub>O, indicating ventilator over-assist or under-assist, respectively. MIP was obtained in 15 patients in the week before or after the NME measurements, which allowed us to calculate TTI. Median MIP was 29 cmH<sub>2</sub>O (IQR 24–38 cmH<sub>2</sub>O) and median TTI was 0.12 (IQR 0.08–0.17). **Figure 4** shows the relationship between TTI and Pmus.

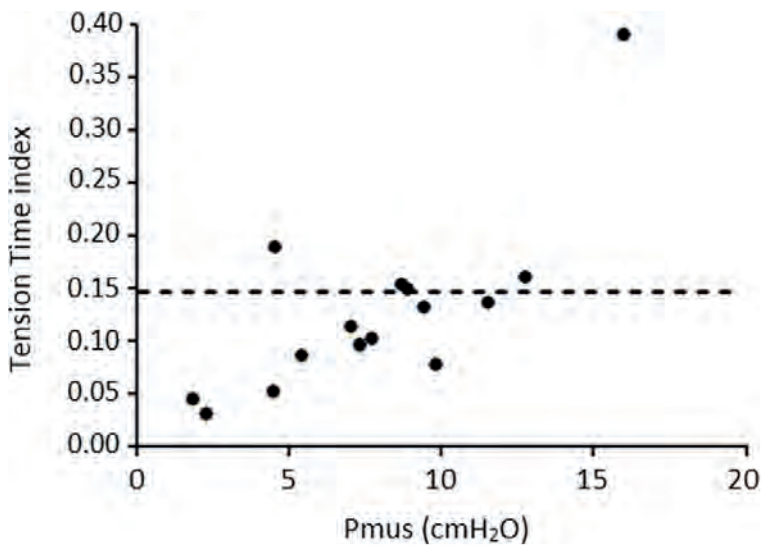


**Figure 4.** Overview of correlation between the tension-time index and inspiratory pressure (Pmus) in 15 patients in whom maximum inspiratory pressure was measured (dots). The dotted line represents the cut off for diaphragm fatigue [207].

## DISCUSSION

The main findings of the present study can be summarized as follows: (1) repeated measurements of NMEoccl within an individual patient exhibited unacceptably high variation, indicating that a single NMEoccl cannot be used to estimate pressure generated by the inspiratory muscles; (2) no correlation was found between NMEoccl variability and clinical parameters; (3) extensive waveform analyses did not improve the repeatability of NMEoccl; (4) NMEoccl and Pmus remain stable over time in a heterogeneous group of patients and (5) both low and high diaphragm effort are common in this cohort of patients on partially supported mode.

### NMEoccl variability

Variability of both components of NMEoccl (Paw and EAdi) is expected given the variability in inspiratory drive, even during occlusions. However, NMEoccl itself is independent from respiratory drive and should therefore be more stable from breath to breath.

Beck and colleagues reported a linear relationship between EAdi and Pdi in healthy subjects, at least up to 75% of maximum force [208]. Their subsequent study also demonstrated a linear relationship between EAdi and Pdi in patients with acute respiratory failure [21]. Bellani et al. showed that NMEoccl derived from airway pressure closely reflects NME during normal breathing (NMEdyn) derived from Pes and concluded that calculation of NMEoccl allows a clinically valuable estimate of inspiratory effort [22]. In this latter study, two end-expiratory occlusions were obtained in each patient, but repeatability was not reported. Furthermore, they report that despite changes in level of support, NMEoccl remained rather stable within individual patients, as supported by the linear relationship between Pmus and EAdi ( $r^2 = 0.78$ ) [22]. This is in apparent contrast with our findings, as we found only moderate correlation between Pmus and EAdi (**Figure 2**). However, differences in data analysis should be acknowledged. Bellani used the Pearson correlation coefficient to test the correlation between Paw and EAdi, in which all measurements from different patients were analyzed together as if they were from a single patient. However, the variability of between-subject measurements is different compared to the variability of the within-subject measurements [209]. Therefore, calculating the correlation coefficient of repeated observations, as in the current study, seems more appropriate [205, 206]. Indeed, Figure 2 demonstrates that the slope of Paw and EAdi in the individual patient is highly variable. This is consistent with the results of Bellani, exhibiting high interindividual variability [22].

The high NMEoccl repeatability reported in the current study precludes its application in clinical practice. Based on visual inspection of the EAdi waveforms, we proposed that suboptimal filtering and replacement of cardiac electric activity by the ventilator software are important. Several techniques for waveform analyses were applied, but did not improve repeatability, suggesting that in addition to suboptimal filtering other factors might be involved. Beck et al. showed that an increase in volume from functional reserve capacity (FRC) to total lung capacity (TLC) reduces Pdi by 60% for a given EAdi [74]. Similarly, muscle weakness may affect NMEoccl, but both are unlikely to explain the high variability in our study, given that all measurements were obtained in a time window of 5–10 min.

As none of the techniques for waveform analyses resulted improved NMEoccl repeatability, a more pragmatic approach was explored that is also feasible in clinical practice. In thermodilution cardiac output measurements, three repeated measurements are averaged, provided that these values are within 10% of their average. If not, a total of five measurements are performed in which the lowest and highest value are eliminated [210]. In our study, this strategy reduced the influence of erroneous NMEoccl values, irrespective of the cause, and will result in a more reproducible value of NMEoccl.

### **NMEoccl as monitoring tool**

Theoretically, the NMEoccl could be helpful to titrate ventilator support in patients on partially supported modes. NMEoccl is calculated by dividing  $\Delta P_{aw}$  by  $\Delta E_{adi}$  during an end-expiratory occlusion. During an occlusion  $\Delta P_{aw}$  equals  $\Delta P_{mus}$  and therefore NMEoccl can be obtained without direct measurement of  $P_{mus}$  (requiring an esophageal balloon). Rearranging this formula to  $P_{mus} = NMEoccl * E_{adi}$  allows calculation of  $P_{mus}$  breath by breath, after dividing this value by 1.5 to correct for differences in NME obtained under static and dynamic conditions [22]. Interestingly, NMEoccl may be used to evaluate respiratory muscle function over time. A decrease in NMEoccl indicates that the respiratory muscles are less efficient in converting electrical activity into pressure. Possible causes for variability in NMEoccl require further studies, but may include intrinsic positive end-expiratory pressure (PEEP) and impaired function of the contractile proteins.

In our study population there were no significant changes in NMEoccl over time ( $p = 0.75$ ), which corresponds to the results of Bellani et al. [25]. However, it should be noted that during our study period the ventilatory settings were not fixed, which might explain why NMEoccl did not change over time.

In our study  $P_{mus}$  varied among patients but remained relatively stable in individual patients over time. In some patients estimated inspiratory effort was  $> 20 \text{ cmH}_2\text{O}$ . An important question is whether a relatively high inspiratory pressure generated by the respiratory muscles may result in the development of contractile fatigue. A  $TTI \geq 0.15$  puts the diaphragm at risk of development of fatigue [207]. In our study, all patients except for two, with a  $P_{mus} < 12 \text{ cmH}_2\text{O}$ , had a  $TTI < 0.15$ . This might suggest that titration of ventilatory support to a pressure  $< 12 \text{ cmH}_2\text{O}$  could limit the risk of fatigue development. However, this has to be studied before it can be applied in clinical practice.

### Strengths and limitations

The strengths of our study are the high number of occlusions analyzed and the fact that at each time point five repeated occlusions were obtained. This allows thorough analysis of the repeatability of NMEoccl and provides methods to improve its variability under clinical conditions. In addition, several waveform analysis techniques were performed to evaluate the high NMEoccl variability; however, this did not improve the RC for NMEoccl. It was suggested that suboptimal filtering might be important. Software engineers should further improve ventilator software for EAdi signal filtering.

Several limitations should be acknowledged. First, patients in our study did not have an esophageal balloon in situ and therefore we could not validate our measurements against the gold standard. However, previous studies have shown excellent correlation between  $\Delta P_{aw}$  and  $\Delta P_{es}$  during an occlusion maneuver [211–213]. Second, our study was conducted in a single center and in a selected group of ICU patients. The generalizability of the findings needs to be assessed.

## CONCLUSION

End-expiratory occlusion allows measurement of static change in EAdi and Paw for calculation of NMEoccl. This maneuver is simple to conduct and safe in ICU patients ventilated in partially supported mode. However, the present study demonstrates that a single maneuver cannot be used to calculate NMEoccl, given the unacceptably high variability. Further studies should be conducted to improve software for EAdi analysis for this specific purpose. For now, selecting three out of five occlusions with the lowest variability seems to be the best method to estimate inspiratory muscle effort from EAdi.

## ACKNOWLEDGEMENTS

For technical help: Norman Comtois, St. Michael's Hospital, University of Toronto, ON, Canada.

### **Ethics approval and consent to participate**

Institutional ethical committee (CMO Region Arnhem - Nijmegen) approved the study protocol (case number 2015–1799, file code kYMYB) and informed consent was waived due to the non-invasive nature of the study and negligible risks.

# REFERENCES

See page 166.





## Chapter 6

# Monitoring patient-ventilator breath contribution in critically ill patients during neurally-adjusted ventilatory assist: reliability and improved algorithms

---

Annemijn H. Jonkman, **Diana Jansen**, Suvarna Gadgil, Christiaan Keijzer, Armand R.J. Girbes, Gert-Jan Scheffer, Johannes G. van der Hoeven, Pieter Roel Tuinman, Angélique M.E. Spoelstra-de Man, Christer S. Sinderby and Leo M.A. Heunks

*Journal of Applied Physiology* 2019   DOI: 10.1152/japplphysiol.00071.2019

## ABSTRACT

The patient-ventilator breath contribution (PVBC) index estimates the relative contribution of the patient to total tidal volume ( $V_{\text{tinsp}}$ ) during mechanical ventilation in neurally-adjusted ventilator assist (NAVA) mode and has been used to titrate ventilator support. The reliability of this index in ventilated patients is unknown and was investigated in this study. PVBC was calculated by comparing tidal volume ( $V_{\text{tinsp}}$ ) and diaphragm electrical activity (EAdi) during assisted breaths ( $V_{\text{tinsp}}/\text{EAdi}$ )<sub>assist</sub> and unassisted breaths ( $V_{\text{tinsp}}/\text{EAdi}$ )<sub>no-assist</sub>.  $V_{\text{tinsp}}$  was normalized to peak EAdi ( $\text{EAdi}_{\text{peak}}$ ) using either A) one assisted breath, B) five consecutive assisted breaths, or C) five assisted breaths with matching EAdi preceding the unassisted breath ( $^{\text{N1}}\text{PVBC}^2$ ,  $^{\text{X5}}\text{PVBC}^2$ , and  $^{\text{X5}}\text{PVBC}^2\text{EAdi-matching}$ ). In addition, PVBC was calculated by comparing only  $V_{\text{tinsp}}$  for breaths with matching EAdi ( $\text{PVBC}\beta^3$ ). Test-retest reliability of the different PVBC calculation methods was evaluated with the intraclass correlation coefficient (ICC) using five repeated PVBC maneuvers performed with a 1-min interval. In total, 125 PVBC maneuvers were analyzed in 25 patients. ICC [95% CI] values were 0.46 [0.23-0.66], 0.51 [0.33-0.70] and 0.42 [0.14-0.69] for  $^{\text{N1}}\text{PVBC}^2$ ,  $^{\text{X5}}\text{PVBC}^2$ , and  $^{\text{X5}}\text{PVBC}^2\text{EAdi-matching}$ , respectively. Complex waveform analyses showed that insufficient EAdi filtering by the ventilator software affect reliability of PVBC calculation. With our new EAdi matching techniques reliability improved ( $\text{PVBC}\beta^3$  ICC: 0.78 [0.60-0.90]). We conclude that current techniques to calculate PVBC exhibit low reliability and that our newly developed criteria and estimation of PVBC – using  $V_{\text{tinsp}}$  of assisted breaths and unassisted breaths with matching EAdi – improves reliability. This may help to implement PVBC in clinical practice.

### New & Noteworthy

The patient-ventilator breath contribution (PVBC) index estimates the relative contribution of the patient to tidal volume generated by the patient and the mechanical ventilator during mechanical ventilation in neurally-adjusted ventilator assist (NAVA) mode. It could be used to titrate ventilator support and such to limit development of diaphragm dysfunction in ICU patients. Currently available methods for bedside assessment of PVBC are unreliable. Our newly developed criteria and estimation of PVBC largely improved reliability and helps to quantify patient contribution to total inspiratory effort.

**Keywords:** Diaphragm dysfunction; Diaphragm electromyography; Mechanical ventilation; Monitoring; Patient-Ventilator Breath Contribution index

## INTRODUCTION

Mechanically ventilated intensive care unit (ICU) patients are prone to develop diaphragm weakness, which is associated with difficult weaning, prolonged duration of mechanical ventilation and ICU mortality [3, 5, 12, 13, 41, 171, 172, 197]. Potential mechanisms include the development of diaphragm muscle atrophy as a result of ventilator over-assist, and diaphragmatic injury as a consequence of ventilator under-assist [4, 5, 12, 42, 44, 199]. Especially in partially supported modes of ventilation, where the work of breathing is shared between the patient and ventilator, there appears a strong rationale to monitor diaphragm effort and to titrate the level of ventilator assist to allow patients' breathing effort within physiological range [17, 18, 33, 91]. It should be noted that monitoring patient breathing effort is unreliable using standard ventilator waveforms such as airway pressure or flow [16]. Esophageal pressure (Pes) monitoring is considered the state-of-the-art technique to monitor mechanical breathing effort in ventilated patients, but this technique is invasive and interpretation of waveforms may be complex [19, 20]. Diaphragm electromyography (EMG) is used to quantify neural breathing effort [17, 22], but the calculation of muscle pressure from EMG amplitude should be done with caution as high within-patient variability was recently described [68].

The neuroventilatory efficiency (NVE) index defines the ability to generate tidal volumes ( $V_{tinsp}$ ) per microvolt of diaphragm electrical activity (EAdi) [23, 214]. The patient-ventilator breath contribution (PVBC) index estimates the relative contribution of the patient to the total  $V_{tinsp}$  generated by the patient and the ventilator together. As this index requires a strong correlation between the change in  $V_{tinsp}$  and the change in EAdi (i.e. proportionality) it has only been studied in neurally-adjusted ventilatory assist (NAVA) mode [24, 201]. The PVBC index is obtained by comparing a breath without ventilator assistance (patient effort only) to assisted breaths (patient effort + ventilator effort) and can be calculated using different approaches: either by normalizing  $V_{tinsp}$  to EAdi, or by comparing  $V_{tinsp}$  for breaths with similar EAdi [24, 201]. A PVBC value of 1.0 indicates that  $V_{tinsp}$  is fully generated by the patient, whereas a PVBC value of 0.0 suggests that  $V_{tinsp}$  is completely generated by the ventilator.

Validation of PVBC has been tested by using the patient's contribution to total transpulmonary pressure as gold standard in both animals and humans [24, 201]. Accordingly, the PVBC index may be useful to titrate ventilator support and such to limit consequences of ventilator over-assist or under-assist. However, the reliability of PVBC measurements at the bedside has not been evaluated yet. Therefore, the aim of the current study was to investigate the test-retest reliability of the PVBC index in a

heterogeneous cohort of ICU patients ventilated in NAVA mode. Test-retest reliability was assessed for the different approaches to calculate PVBC. We hypothesized that reliability of PVBC improves when comparing  $V_{tinsp}$  for breaths with similar EAdi. In addition, methods were developed to further improve the applicability of the PVBC index as a bedside monitoring tool for quantifying the patient's contribution versus that of the ventilator during NAVA.

## METHODS

### Study Design and Population

This prospective cohort study was conducted at the ICU of the Radboudumc in Nijmegen. Data are part of a larger study evaluating reliability of diaphragm monitoring techniques in mechanically ventilated patients [68]. Adult patients with an EAdi catheter in situ and ventilated in NAVA mode (Servo-i; MAQUET Critical Care, Solna, Sweden) were eligible for inclusion.

### Ethics Approval and Consent to Participate

The institutional ethical committee (CMO Region Arnhem–Nijmegen) approved the study protocol (case no. 2015-1799). Informed consent was waived because of the noninvasive nature of the study and negligible risks.

### Study Protocol

Before data acquisition the EAdi catheter position was verified with dedicated software available on the ventilator. When patients exhibited a stable breathing pattern (i.e., no coughing, hiccups) inspiratory support (NAVA level) was abruptly decreased to zero to obtain the first single unassisted breath for analysis. This “zero-assist maneuver” was repeated five times with an  $\pm 1$ -min interval. The number of breaths between maneuvers was variable, to prevent the patient's anticipation.

### Data Acquisition

Ventilator flow, airway pressure (Paw), and EAdi waveforms were sampled at 100 Hz and obtained via the RS232 serial port connected to a laptop with dedicated software (Servo Tracker version 4.1). Data were stored for off-line analysis in a software routine developed in Microsoft Visual Basic (Microsoft, 2010) and MATLAB (R2017a; MathWorks).

## Off-Line Signal Processing

Neural inspiratory time (EAdi-TI) was defined as the period from increasing EAdi > 0.5  $\mu\text{V}$  above baseline until EAdi decreased to 70% of its peak (i.e., cycling-off criterion in NAVA). VT<sub>insp</sub> was calculated as the time integral of inspiratory ventilator flow. Events should meet the following criteria to be considered a patient effort and to be included in further analyses: VT<sub>insp</sub>  $\geq$  50 ml, EAdi<sub>peak</sub>  $\geq$  2  $\mu\text{V}$ , EAdi-TI > 400 ms.

## PVBC Calculation Methods

PVBC was calculated as the ratio of VT<sub>insp</sub>/EAdi during unassisted breaths to that during assisted breaths [(VT<sub>insp</sub>/EAdi)<sub>no-assist</sub>/(VT<sub>insp</sub>/EAdi<sub>peak</sub>)<sub>assist</sub>]. PVBC indexes were squared because previous studies demonstrated improved agreement with relative breathing effort estimated from Pes measurements [24]. If PVBC<sup>2</sup> values exceeded 1.0, which is possible mathematically but not conceptually, PVBC<sup>2</sup> was considered 1.0.

### Single and averaged breaths

(VT<sub>insp</sub>/EAdi<sub>peak</sub>)<sub>assist</sub> was calculated in two ways (**Figure 1**), by using 1) VT<sub>insp</sub> and EAdi<sub>peak</sub> of one breath ("N1") preceding the unassisted breath (<sup>N1</sup>PVBC<sup>2</sup>) or 2) mean VT<sub>insp</sub> and EAdi<sub>peak</sub> of five consecutive breaths ("X5") preceding the unassisted breath (<sup>X5</sup>PVBC<sup>2</sup>) [24].

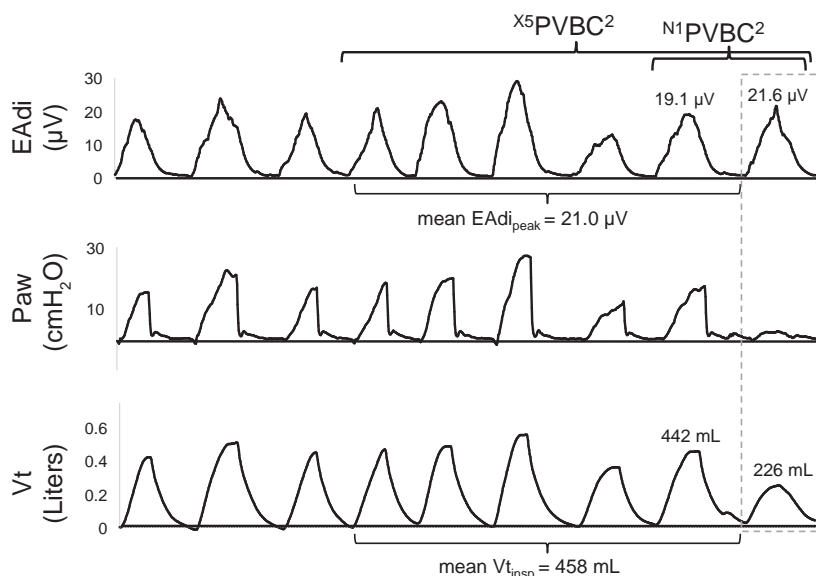


**Figure 1.** A representative patient-ventilator breath contribution (PVBC) maneuver and calculation methods for <sup>N1</sup>PVBC<sup>2</sup> and <sup>X5</sup>PVBC<sup>2</sup>. The gray dashed box represents waveforms of the unassisted breath [i.e., airway pressure (Paw) is close to 0]. PVBC was calculated using peak electrical activity of the diaphragm (EAdi<sub>peak</sub>) and inspiratory tidal volume (VT<sub>insp</sub>) of 1 breath before the unassisted breath (<sup>N1</sup>PVBC<sup>2</sup>) and based on the mean EAdi<sub>peak</sub> and VT<sub>insp</sub> of 5 breaths before the unassisted breath (<sup>X5</sup>PVBC<sup>2</sup>). For each patient 5 of these maneuvers were obtained per time point.

### *Matching EAdi*

Because initial results demonstrated poor reliability of  $N^1PVBC^2$  and  $^{x5}PVBC^2$ , new analysis techniques were developed to match EAdi between the assisted breaths and the unassisted breath. To this end, five assisted breaths were selected for analysis only if they showed EAdi waveforms similar to the unassisted breath ( $^{x5}PVBC^2$ , EAdi-matching). Breaths could be selected any time in the 1-min interval before the unassisted breath. Matching was defined as similarity in the inspiratory increase of EAdi. This was tested mathematically by performing linear fitting to each EAdiassist-EAdino-assist curve. The determination coefficient ( $R^2$ ), regression slope, and trend line intersection with the y-axis were computed (**Figure 2**). Assisted and unassisted breaths were considered a match when all of the following criteria were met: 1)  $R^2 \geq 0.85$ , 2) regression slope between 0.75 and 1.33, and 3) trend line intersection between  $-1.5 \mu V$  and  $1.5 \mu V$ . The averaged VT<sub>insp</sub> of five matched assisted breaths before the unassisted breath was used for VT<sub>insp,assist</sub>. Matching EAdi of the assisted breaths and unassisted breath may eliminate the need for normalization of VT<sub>insp</sub> to EAdi<sub>peak</sub>. PVBC<sup>2</sup> could then be simply calculated as  $(VT_{insp,no-assist}/VT_{insp,assist})^2$ , using the averaged VT<sub>insp</sub> of five matched assisted breaths ( $PVBC\beta^2$ ).

### *Additional techniques derived from $^{x5}PVBC^2$*

As EAdi matching is not yet available in routine clinical practice, additional techniques that can be used at the bedside were developed post hoc as modifications of  $^{x5}PVBC^2$ . First, we pragmatically selected three from five  $^{x5}PVBC^2$  maneuvers with lowest variability, provided that these values were within 20% of their median. Selection was done by calculating the standard deviation (SD) of all possible combinations of three of five  $^{x5}PVBC^2$  maneuvers for each patient. The combination with lowest SD was subsequently included in the statistical analysis if the variability of the three repeated  $^{x5}PVBC^2$  measurements was  $<20\%$ . This method is referred to as  $^{x5}PVBC^2_{3/5}$ . Second, for reasons clarified in DISCUSSION, we aimed to exclude the influence of non-physiological EAdi waveforms and calculated  $^{x5}PVBC^2$  based on only VT<sub>insp</sub> of the five assisted breaths before the unassisted breath ( $^{x5}PVBC^2_{VT}$ , no EAdi signal used). For clarity, **Table 1** explains the different techniques used to calculate PVBC.

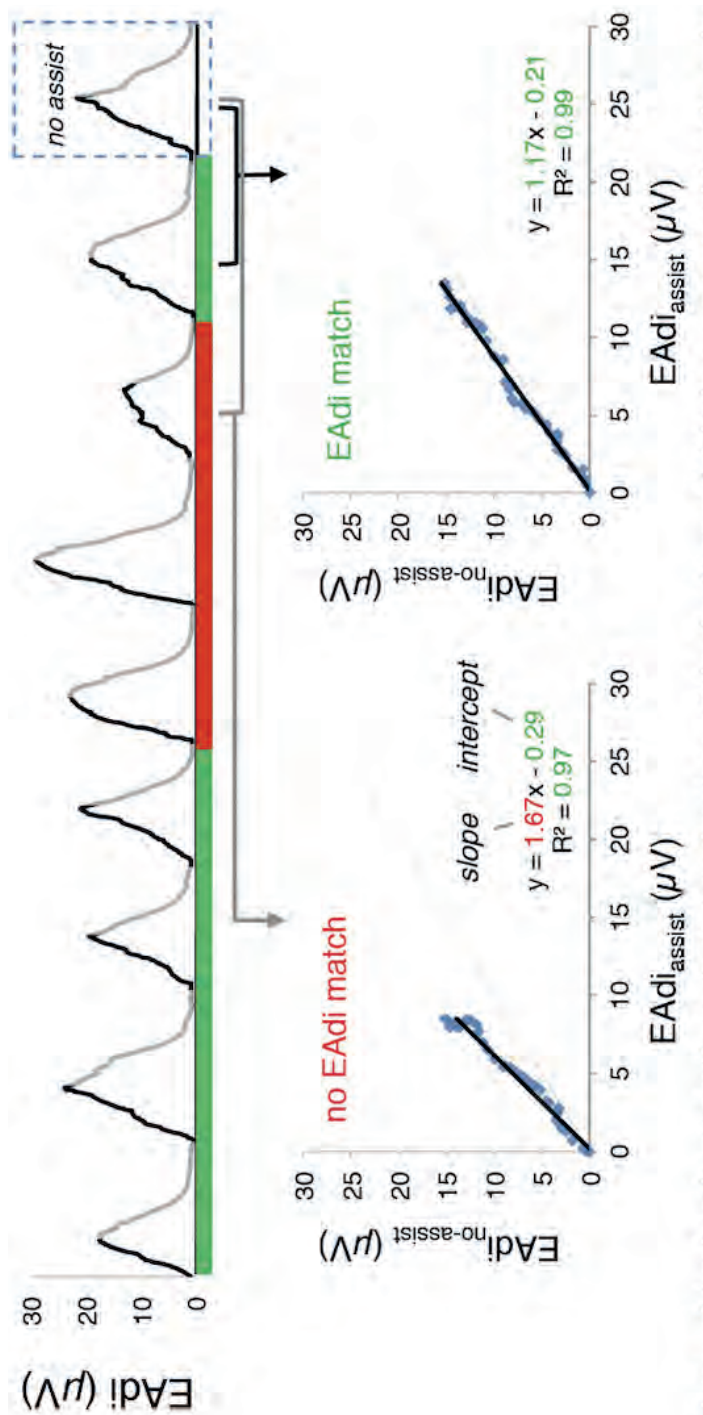


**Figure 2.** Matching algorithm explained to detect similarity in electrical activity of the diaphragm (EAdi) between assisted breaths and unassisted breaths, using the same patient-ventilator breath contribution (PVBC) maneuver as explained in Figure 1. Similarity in EAdi between each assisted breath and the unassisted breath was evaluated by performing linear regression fitting for the  $EAdi_{no-assist} - EAdi_{assist}$  curve. To correct for differences in EAdi inspiratory time between the assisted breath and the unassisted breath, similarity was evaluated from start EAdi of both breaths until the time point where either  $EAdi_{assist}$  or  $EAdi_{no-assist}$  reached its peak or plateau, whichever occurred first. The red bar below the EAdi of the assisted breaths indicates that there was no match with the unassisted EAdi. In this example, the slope parameter of the linear fit was too high (in red). The green bar below the EAdi of the assisted breaths indicates a proper match with the unassisted breath [slope, intercept, and determination coefficient ( $R^2$ ) parameters are within predefined range; see METHODS]. Mean  $EAdi_{peak}$  and mean inspiratory tidal volume values of the 5 matching breaths were subsequently used in the calculation of  $x \cdot PVBC_{EAdi-matching}^2$  and  $PVBC^2$ .



Table 1. Explanation of different methods used to calculate PVBC index

PVBC	Patient-ventilator breath contribution: $(V_{T_{\text{insp}}}/EAdi_{\text{peak}})_{\text{no-assist}}/(V_{T_{\text{insp}}}/EAdi_{\text{peak}})_{\text{assist}}$
$N_1PVBC^2$	Squared PVBC based on $V_{T_{\text{insp}}}$ and $EAdi_{\text{peak}}$ of 1st ("N1") assisted breath before the unassisted breath
$x5PVBC^2$	Squared PVBC based on the mean $V_{T_{\text{insp}}}$ and mean $EAdi_{\text{peak}}$ of 5 consecutive ("X5") assisted breaths before the unassisted breath
$x5PVBC^2_{EAdi\text{-}matching}$	Squared PVBC using the mean $V_{T_{\text{insp}}}$ and mean $EAdi_{\text{peak}}$ of 5 matching assisted breaths in the 1-min interval preceding the unassisted breath; for EAdi-matching criteria, see METHODS
$PVBC\beta^2$	Squared PVBC using only the mean $V_{T_{\text{insp}}}$ of 5 matching assisted breaths in the 1-min interval preceding the unassisted breath
$x5PVBC^2_{3/5}$	$[(V_{T_{\text{insp, no-assist}}}/V_{T_{\text{insp, assist}}})^2]$ $x5PVBC^2$ using 3 of 5 PVBC maneuvers with lowest variability, provided that these values are within 20% of their average
$x5PVBC^2_{VT}$	$x5PVBC^2$ calculated based on mean $V_{T_{\text{insp}}}$ of 5 assisted breaths just before the unassisted breath; no EAdi matching applied

$V_{T_{\text{insp}}}$ , inspiratory tidal volume;  $EAdi_{\text{peak}}$ , peak electrical activity of diaphragm.

## Statistical Analysis

Statistical analyses were performed with SPSS (IBM SPSS Statistics, version 22) and Prism (GraphPad Software, version 7.04). Data were analyzed as median [interquartile range (IQR)], except as otherwise stated. Statistical significance is indicated by a  $P$  value  $< 0.05$ .

Test-retest reliability of PVBC was evaluated with the intraclass correlation coefficient (ICC), which is the ratio of between-subject variance to total variance (i.e., sum of between-subject and within-subject variance) [215, 216]. Hence, high ICC indicates high similarity between measurements taken from the same subject. ICC values and their 95% confidence intervals (CIs) were calculated based on an absolute-agreement, two-way random-effects model with random factors for subject and for measurement index. Single-measurement ICC values were of primary interest, to evaluate whether a single PVBC measurement can be reliably used as a bedside monitoring tool. As an exception, for  $^{x5}PVBC^{2/3/5}$  only the average-measurement ICC was of interest, as this calculation method is in itself based on the average of repeated PVBC maneuvers. ICC values were interpreted as follows:  $<0.5$ : poor reliability,  $0.5-0.75$ : moderate reliability,  $0.75-0.9$ : good reliability, and  $>0.9$ : excellent reliability [217]. To test for differences in ICC between the various PVBC calculation methods we calculated the 84% CI; no overlap in these CIs was considered corresponding to  $P < 0.05$  [218].

ICC of  $^{x5}PVBC_{EAdi-matching}^2$  and  $PVBC\beta^2$  was evaluated in patients with sufficient EAdi matching for at least three of the five unassisted breaths. Since ICC models cannot handle missing data, only the first three successful measurements were included. Second, the coefficient of variation (CoV) of repeated PVBC measurements for all individual patients was calculated as the ratio of within-subject SD to the mean, in order to evaluate dispersion of the repeated PVBC measurements. The median of these individual CoVs was used as the overall within-subject CoV for a given PVBC calculation method. This median CoV of  $PVBC\beta^2$  was used to divide the study population into two groups with CoV higher or lower than median. Paired  $t$ -tests and  $\chi^2$ -tests were performed to test for differences in clinical parameters between groups.

## RESULTS

The main characteristics of the study population ( $n = 25$ ) are shown in **Table 2**. A total of 125 PVBC maneuvers were analyzed. Reliability parameters of all PVBC calculation methods are presented in **Table 3**.

Table 2. *Main characteristics of study population*

Characteristics	
Age, yr (median [IQR])	69 [56–72]
Sex, male/female	19/6
BMI, kg/m <sup>2</sup> (median [IQR])	24.7 [21.8–26]
Comorbidity, <i>n</i> (%)	
Cardiac diseases	14 (56%)
COPD	4 (16%)
Reason for admission, <i>n</i> (%)	
Pneumonia	10 (40%)
Postoperative	7 (28%)
Trauma	8 (32%)
ARDS at admission, <i>n</i> (%)	7 (28%)
Sepsis during admission, <i>n</i> (%)	3 (12%)
Duration of MV at measurement time point, days (median [IQR])	10 [7–16]
Partially supported mode	8 [4–12]
Controlled mode	1 [0–2.8]
Duration of MV on partially supported mode, after measurement time point,* days (median [IQR])	13 [5–19]
Ventilation characteristics at measurement time point (median [IQR])	
NAVA level	0.7 [0.5–1.1]
EAdi peak, $\mu\text{V}$	11.3 [7.8–18.1]
Tidal volume, ml	441 [352–472]
Respiratory rate, min <sup>-1</sup>	23 [18–30]
PEEP, cmH <sub>2</sub> O	8 [6–10]
PF ratio	259 [220–311]
Use of opioids/sedatives, <i>n</i> (%)	17 (68%)
Within-hospital 30-day mortality, <i>n</i> (%)	6 (32%)

Values are for *n* = 25 patients. ARDS, acute respiratory distress syndrome; COPD, chronic obstructive pulmonary disease; EAdi, electrical activity of diaphragm; IQR, interquartile range; MV, mechanical ventilation; NAVA, neurally adjusted ventilatory assist; PEEP, positive end-expiratory pressure, PF, arterial partial pressure of oxygen to inspired oxygen fraction. \**n* = 21. Four patients were lost to follow-up; these patients were transferred to another hospital.

Table 3. Reliability of PVBC index as assessed with different calculation methods

PVBC	CoV, % (median [IQR])	Single-Measurement ICC [95% CI]	Average-Measurement ICC [95% CI]	Single-Measurement ICC Significantly Different from PVBC $\beta^2$ ?
$N^1$ PVBC $^2$	31.3 [20.0–39.3]	0.46 [0.23–0.66]	0.81 [0.66–0.91]	$P < 0.05$ , lower ICC
$x^5$ PVBC $^2$	27.2 [19.3–36.0]	0.51 [0.33–0.70]	0.84 [0.71–0.92]	$P < 0.05$ , lower ICC
$x^5$ PVBC $^2_{\text{EAdi-matching}}$	20.4 [15.6–24.0]	0.42§ [0.14–0.69]	0.68 [0.33–0.87]	$P < 0.05$ , lower ICC
PVBC $\beta^2$	12.1 [6.9–19.1]	0.78§ [0.60–0.90]	0.92 [0.82–0.97]	Not applicable
$x^5$ PVBC $^2_{\text{Vt}}$	21.4 [15.3–29.2]	0.39 [0.22–0.60]	0.77 [0.58–0.88]	$P < 0.05$ , lower ICC
$x^5$ PVBC $^2_{3/5}$	5.9 [1.4–7.4]	Not applicable	0.99† [0.98–0.99]	$P < 0.05$ , higher ICC

Methods used to calculate patient-ventilator breath contribution (PVBC) index are explained in Table 1. CI, confidence interval; CoV, coefficient of variation; EAdi, electrical activity of diaphragm; ICC, intraclass correlation coefficient; IQR, interquartile range; Vt, inspiratory tidal volume. \*No overlap in the 84% CIs between PVBC methods indicates significant difference ( $P < 0.05$ ) (25). †Matching EAdi was not sufficient for all 5 repeated measurements in each patient. ICC values are therefore based on the first 3 successful attempts of  $x^5$ PVBC $^2_{\text{EAdi-matching}}$  and PVBC $\beta^2$ , which was obtained in 19 patients. ‡ICC values are based on 21 patients. Four patients were excluded from the  $x^5$ PVBC $^2_{3/5}$  data set because in these patients the 3 of 5 measurements with lowest variability still had a CoV  $> 20\%$ .

## Single and Average Breaths

$^{N1}PVBC^2$  indicated poor reliability: ICC 0.46 [0.23–0.66] and median CoV 31.3% (**Table 3**). The latter suggests that if the mean of five  $^{N1}PVBC^2$  measurements was 0.6, the five repeated measurements would likely vary between 0.23 and 0.97 (95% interval range; i.e.,  $^{N1}PVBC^2 \pm 1.96 \times 0.1$  CoV), which is a clinically unacceptably wide range. One should also note that because of the nature of PVBC this interval range is bounded by 0 and 1.

**Figure 1** shows physiological variability in EAdipeak and thus in Paw and VTinsp (i.e., proportionality of NAVA) of the assisted breaths before the unassisted breath. Median CoV of EAdipeak of the five assisted breaths before the unassisted breath was 20.9% [15.3–24.6%]. Given the poor reliability of  $^{N1}PVBC^2$ , it was reasoned that averaging five assisted breaths before the unassisted breath limits the variability of the repeated PVBC measurements. As shown in Table 3, reliability of  $^{X5}PVBC^2$  did not improve compared with  $^{N1}PVBC^2$ .

## Matching EAdi

Upon visual inspection, some EAdi waveforms exhibited a rather non-physiological shape, i.e., a plateau or decrease during inspiration (while an increase would be expected) or at maximum inspiration (see **Figure 3**).

For reasons clarified in DISCUSSION, these “non-physiological EAdi waveforms” may contribute to the poor reliability of  $^{N1}PVBC^2$  and  $^{X5}PVBC^2$ , and we hypothesized that EAdi matching to select assisted and unassisted breaths with similar respiratory drive would improve reliability. Where  $^{X5}PVBC^2$ EAdi-matching did not improve reliability (**Table 3**), calculating PVBC based on only tidal volumes of these EAdi-matched breaths ( $PVBC\beta^2$ ) exhibited good reliability: ICC 0.78 [0.60–0.90] and median CoV 12.1%.

After the study population was divided into two groups with CoV of  $PVBC\beta^2$  either lower or higher than median (14.2%), statistically significant differences were only found in mean unassisted VTinsp ( $372 \pm 100$  ml vs.  $278 \pm 72$  ml,  $P = 0.048$ ) and CoV of unassisted VTinsp ( $5.9 \pm 7.9\%$  vs.  $14.4 \pm 5.5\%$ ,  $P = 0.023$ ). No differences in clinical characteristics were found between the two groups.

## Additional Techniques Derived from $^{X5}PVBC^2$

Because EAdi matching precludes direct clinical implementation of PVBC, additional techniques that can be used at the bedside were developed. Reliability results of  $^{X5}PVBC^{23/5}$  and  $^{X5}PVBC^2VT$  calculation methods are provided in **Table 3**.

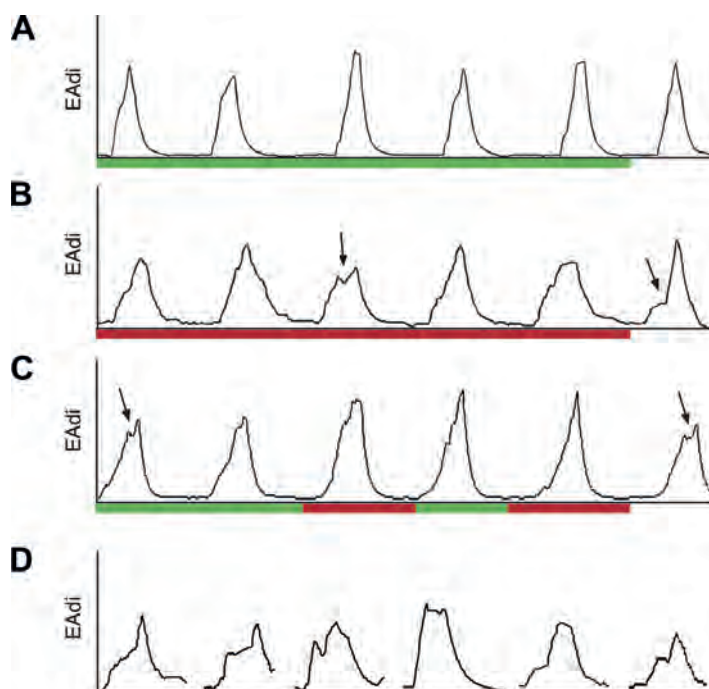


**Figure 3.** Examples of diaphragm electrical activity (EAdi) waveforms and insufficient filtering. Tracings **A**, **B**, and **C** were obtained from 3 different patients. In each of these tracings the last breath represents an unassisted breath. Green bar, effective matching (for criteria see METHODS) of assisted EAdi with unassisted EAdi. Red bar, no adequate matching between assisted EAdi and unassisted EAdi. **A:** proper EAdi filtering: all assisted breaths are matching the unassisted EAdi. **B:** filtering error in the unassisted EAdi (arrow, last EAdi), resulting in an abrupt change in slope during the inspiration. In addition, the third assisted EAdi shows a non-physiological EAdi waveform (i.e., split peak, see arrow). Because of this filtering error in the unassisted EAdi, none of the assisted EAdi is matching with the unassisted EAdi. **C:** minor filtering error in the unassisted EAdi (i.e., split peak, see arrow). Therefore, matching between the assisted and unassisted EAdi was only sufficient for those assisted breaths that show a similar EAdi waveform. **D:** random examples of various non-physiological EAdi waveforms observed; data from different patients.

## DISCUSSION

The aim of the present study was to investigate the test-retest reliability of the PVBC index in clinical practice. The main finding is that currently available bedside methods to assess the PVBC index in ICU patients are unreliable. However, we present a new algorithm for EAdi matching between assisted breaths and unassisted breaths, which increases the reliability of PVBC and thus its clinical value. Calculation of PVBC with our EAdi-matching technique may be useful to monitor the relative contribution of the patient to total tidal volume during mechanical ventilation in NAVA mode.

### Validity of PVBC

Because NAVA is a proportional ventilator mode,  $VT_{\text{insp,assist}}$  reflects the patient's inspiratory effort (EAdi) plus the proportional ventilator effort ( $\Delta P_{\text{aw}}$ ). Where  $VT_{\text{insp,no-assist}}$  is generated by the patient's effort solely, the  $VT_{\text{insp,no-assist}}$ -to- $VT_{\text{insp,assist}}$  ratio should reflect the contribution of the patient versus that of the ventilator. In an animal study, Grasselli et al. [201] normalized  $VT_{\text{insp}}$  to  $EAdi_{\text{peak}}$ , to account for physiological variability in neural respiratory drive between consecutive breaths. They validated the PVBC index against the relative contribution of  $\Delta P_{\text{es}}$  to dynamic transpulmonary pressure ( $\Delta P_{\text{L,dyn}}$ ). As  $\Delta P_{\text{es}}$  estimates the patient's inspiratory effort and  $\Delta P_{\text{L,dyn}}$  reflects total breathing effort (patient + ventilator), the ratio of  $\Delta P_{\text{es}}$  to  $\Delta P_{\text{L,dyn}}$  is considered the gold standard for PVBC assessment. There was a near-perfect 1:1 linear relationship between  $PVBC^2$  and  $\Delta P_{\text{es}}/\Delta P_{\text{L,dyn}}$ , which was confirmed in patients with acute respiratory failure [24]. Therefore, in the present study we did not validate PVBC to  $\Delta P_{\text{es}}/\Delta P_{\text{L,dyn}}$  measurements. Instead, we focused on the test-retest reliability of the PVBC index and developed techniques to improve its reliability.

### Reliability of PVBC

Because of normalization of  $VT_{\text{insp}}$  to  $EAdi_{\text{peak}}$ , PVBC should be stable from breath to breath within a short time interval. Unexpectedly, we found a poor reliability of  $^{N1}PVBC^2$ . It was reasoned that the variability in  $VT_{\text{insp}}$  and  $EAdi_{\text{peak}}$  of the assisted breaths might have contributed to this low reliability. Averaging five assisted breaths just before the unassisted breath ( $^{x5}PVBC^2$ ) only slightly improved reliability. This suggests that the within-subject variability is due to an erroneous measurement, as it is highly unlikely that this within-subject variability is related to altered neuro-ventilatory coupling in the short time period of measurements (5 min). In light of the present findings, we propose that suboptimal acquisition and/or filtering of the EAdi signal plays an important role. Artifacts originating from, e.g., cardiac electrical activity, cross talk from other muscles, and esophageal peristalsis affect EAdi signal



quality and are replaced by filtering algorithms within the ventilator software. Suboptimal filtering results in non-physiological EAdi waveforms and thereby introduces measurement errors (see **Figure 3**). Inadequate filtering of the EAdi signal affects the VT<sub>insp</sub> delivered by the ventilator, as in NAVA mode inspiratory support is determined by this filtered EAdi signal [219]. In contrast, during an unassisted breath the generated tidal volume is the result of the patient's true respiratory drive, irrespective of EAdi filtering (there is no ventilator assist). Thus a filtering artifact present in the unassisted EAdi results in a VT<sub>insp,no-assist-to-EAdipeak,no-assist</sub> ratio that is not necessarily representative for that tidal volume (i.e., overestimated as inadequate filtering results in an EAdi<sub>peak</sub> lower than true EAdi<sub>peak</sub>). With our technique for EAdi matching, only breaths with similar EAdi waveforms are included in the PVBC calculation. This means that the inspiratory effort for the assisted and unassisted breaths of that patient are comparable and that the measurement error related to non-physiological EAdi signals is reduced. With our criteria for detecting EAdi similarity (linear regression fit parameters:  $R^2 \geq 0.85$ , regression slope between 0.75 and 1.33 and trend line intersection between -1.5  $\mu\text{V}$  and 1.5  $\mu\text{V}$ ), we indeed demonstrated improved reliability of PVBC $\beta^2$  (**Table 3**). This also confirms that EAdi is the factor determining the poor reliability of other techniques to calculate PVBC. As PVBC $\beta^2$  has already been validated against the gold standard ( $\Delta\text{Pes}/\Delta\text{PL,dyn}$ ) [24], our data indicate that a single PVBC $\beta^2$  measurement as obtained with our newly developed EAdi-matching criteria can be reliably used to assess the true contribution of the patient versus that of the ventilator.

The concept of EAdi matching has been used previously to improve the relationship between PVBC and  $\Delta\text{Pes}/\Delta\text{PL,dyn}$  [24]. However, important differences in EAdi matching from our study should be acknowledged. First, Liu et al. [24] applied EAdi matching solely based on EAdi<sub>peak</sub> ratio of assisted and unassisted breaths, where a ratio between 0.8 and 1.3 was defined as a match. In contrast, our matching criteria were based on the inspiratory increase in EAdi. It was reasoned that this is more appropriate for limiting the influence of non-physiological EAdi waveforms. For instance, if cardiac artifact replacements are present in the inspiratory EAdi increase, the EAdi<sub>peak</sub> ratio might be within the 0.8–1.3 range while the peak value itself underestimates true EAdi<sub>peak</sub>. With our matching criteria, such breaths would be excluded. Second, in their study only the five assisted breaths preceding the unassisted breath were tested for similarity, whereas in our study breaths were selected in the 1-min interval before the unassisted breath.

As our matching algorithm precludes direct bedside implementation of the PVBC index, we aimed to optimize the  $^{x5}\text{PVBC}^2$  method by 1) pragmatically selecting



three out of five PVBC maneuvers with the lowest standard error ( $^{x5}PVBC^{23/5}$ ) and 2) calculating  $^{x5}PVBC^2$  based on tidal volumes only ( $^{x5}PVBC^{2VT}$ ). The first strategy is comparable to measurements of thermodilution cardiac output and to our proposed estimation of neuromuscular efficiency, where three repeated measurements were averaged, provided that these values are within 15% of their median [68, 210].  $^{x5}PVBC^{23/5}$  showed excellent reliability (ICC 0.99 [0.98–0.99]), whereas  $^{x5}PVBC^{2VT}$  showed good reliability (ICC 0.77 [0.58–0.88]) only for average measurements.

Although both methods are more time-consuming because five unassisted maneuvers should be performed, no EAdi matching is required. It should, however, be noted that both methods are only statistical techniques to reduce measurement error, whereas with our EAdi matching technique reliability is improved by reducing the influence of non-physiological EAdi waveforms. Therefore, it was reasoned that it was inappropriate to test agreement of  $PVBC\beta^2$  with  $^{x5}PVBC^{23/5}$  and  $^{x5}PVBC^{2VT}$  in order to provide further conclusions about the validity of both methods. In contrast, the validity of  $^{x5}PVBC^{23/5}$  and  $^{x5}PVBC^{2VT}$  should be further investigated by comparing these methods to  $\Delta Pes/\Delta PL_{dyn}$ .

In the meantime, software engineers should further improve ventilator software for EAdi filtering and implement a matching algorithm such as that developed in the present study, so that  $PVBC\beta^2$  becomes available at the bedside as a sophisticated and reliable monitoring method for the relative contribution of the patient to total inspiratory volume during NAVA.

## Clinical Implications of PVBC

PVBC is potentially helpful in quantifying the patient's contribution to total tidal volume (patient + ventilator) for patients ventilated in NAVA mode. This could help the clinician in adjusting ventilator assist without the need for Pes measurements. This is of clinical importance, given the adverse effects related to ventilator under-assist and ventilator over-assist [3, 33]. However, to limit the detrimental effects of mechanical ventilation on the diaphragm, the PVBC index should always be interpreted in the light of absolute ventilator assist (inspiratory airway pressure) and patient effort (EAdi). For example, a high PVBC value may be found in patients with very high respiratory drive and in patients with low drive ready to be weaned. In the former, there is insufficient inspiratory assist by the ventilator (low inspiratory airway pressure) and high EAdi. In the latter, EAdi will be low, reflecting low patient effort, but the high PVBC indicates that the majority of effort is still generated by the patient, so most likely this patient is ready to be weaned from the ventilator. Accordingly, PVBC holds promise for future clinical application, but technical aspects

should be improved as demonstrated in the present report and clinicians should be aware of the rather complex interpretation of the PVBC value.

### Strengths and Limitations

The strengths of our study are the high number of PVBC maneuvers performed within a short time period. This allows extensive waveform analysis such that different methods for PVBC calculation could be evaluated. In addition, an EAdi-matching technique was developed to detect similarity in EAdi between assisted and unassisted breaths.

Some limitations should be addressed. First, we did not validate PVBC to Pes measurements, as this has been done previously [24, 201]. Second, six patients were excluded from the analysis of  $^{x5}PVBC^2EAdi$ -matching and  $PVBC\beta^2$  because predefined matching criteria were not met. This could have been anticipated by applying less stringent matching criteria; however, this subsequently increases the possibility of introducing measurement error. On the other hand, reasons for matching failure were identified and substantiate the need for improved EAdi signal processing, such that PVBC measurements could become available in all patients ventilated in NAVA mode. Finally, although the PVBC index is a promising monitoring technique that has been validated in experimental studies [24, 201], it was not the aim of the present study to provide clinical guidance regarding the interpretation of the PVBC index during the course of mechanical ventilation. Instead, we focused on the reliability of this index and found that improvement of current bedside techniques for PVBC calculation is required before this index can be reliably used for titrating ventilator support. This highlights the importance of reliability studies for new monitoring indexes before implementation in clinical practice. Future clinical studies should focus on the diagnostic implications of PVBC during the course of mechanical ventilation and in weaning trials. Then, guidelines should be developed on how PVBC can be used as part of a diaphragm-protective ventilation strategy.

In conclusion, this study shows that the methods currently available to assess the PVBC at the bedside are unreliable. Our newly developed criteria and estimation of PVBC (selecting only matching EAdi between assisted and unassisted breaths) increased reliability. When an EAdi-matching algorithm is implemented in the ventilator software, the PVBC index is continuously available at the bedside as a tool that helps the clinician in assessing the contribution of the patient versus that of the ventilator during NAVA. Future studies need to focus on the diagnostic implications of PVBC during the course of mechanical ventilation and in weaning trials.

## **ACKNOWLEDGMENT**

We thank Norman Comtois, St. Michael's Hospital, University of Toronto, ON, Canada for technical help and Dr. Peter M. van de Ven, Department of Epidemiology and Biostatistics, Amsterdam University Medical Centers, location VU University Medical Centre, Amsterdam, The Netherlands for statistical advice.

## REFERENCES

See page 166.

**PART III:**  
**Novel pharmacological interventions  
to modulate diaphragm function**

## Chapter 7

# Acetylcholine receptor antagonists in acute respiratory distress syndrome: much more than muscle relaxants

---

**Diana Jansen,** Heder de Vries and Leo M. A. Heunks

*Critical Care* 2018 DOI: 10.1186/s13054-018-1979-z

## ABSTRACT

Acetylcholine receptor antagonists have been shown to improve outcome in patients with severe acute respiratory distress syndrome. However, it is incompletely understood how these agents improve outcome. In the current editorial, we discuss the mechanisms of action of acetylcholine receptor antagonists beyond neuromuscular blockade.

**Keywords:** Neuromuscular blockers, Acute respiratory distress syndrome, Direct anti-inflammatory effect, Acetylcholine, Acetylcholine receptors, Lung injury markers, Respiratory muscles, Low tidal volume ventilation, Partial neuromuscular blockade

### Main text

Non-depolarizing neuromuscular blockers (NMBs), such as rocuronium and cisatracurium, are frequently used in patients with acute respiratory distress syndrome (ARDS). The Lung-Safe study reported that NMBs were used in 6.8% of mild ARDS and up to 37.8% of severe ARDS patients [220]. Three clinical studies on the use of NMB in ARDS have been conducted by Papazian and colleagues [221-223]. In their largest multicenter randomized controlled trial (ACURASYS study) it was demonstrated that continuous cisatracurium for 48 h reduced 90-day mortality (primary outcome) and improved oxygenation, in particular in patients with  $\text{PaO}_2/\text{FiO}_2$  ratio  $\leq 120$  mmHg [223]. Today, it is incompletely understood how NMBs improve outcome. Possible mechanisms include reduction of oxygen consumption, decrease in cardiac output and pulmonary blood flow, and direct anti-inflammatory effects of NMBs, but the most intuitive mechanism is by abolishing patient breathing effort and thereby limiting the risk of both alveolar collapse and over-distention [224, 225]. However, it is remarkable that no significant differences were found between groups in tidal volume, PEEP, plateau pressure, and minute ventilation [223]. This suggests that other factors, not directly related to respiratory mechanics, may play a role in the beneficial effects of NMBs.

### Acetylcholine receptors

NMBs exert their action through interaction with the acetylcholine receptor (AChR) in the neuromuscular junction. Two major types of AChRs have been characterized: the metabotropic muscarinic receptors (mAChRs) and the ionotropic nicotinic receptors (nAChRs); both are activated by ACh [226]. The nAChR, a ligand-gated ion channel, is primarily found in the neuromuscular junction where binding with acetylcholine results in inflow of sodium and calcium and outflow of potassium, depolarizing the motor endplate and creating a potential that triggers muscle

contraction [227, 228]. In addition, nAChRs are expressed by other tissues and cells, including brain, autonomic ganglia, macrophages, endothelial cells, and epithelial cells [226], explaining their involvement in physiological processes such as addiction, inflammation, and metabolic tonus. The mAChR is a G-protein-coupled receptor comprising five subtypes (M1–5) [226, 229] which are also widely expressed throughout the body. **Table 1** shows an overview of the most important types of AChRs with their locations and main function.

**Table 1** Types of AChR with their locations and main function

Type	Location of expression	Function
nAChR		
Muscle-type	Neuromuscular junction	Muscle contraction, mainly by increased Na <sup>+</sup> and K <sup>+</sup> permeability
Neuronal-type	Autonomic ganglia	Activation of autonomic nervous system (sympathetic and parasympathetic), mainly by increased Na <sup>+</sup> and K <sup>+</sup> permeability
	Hippocampus / cortex	Cognition, modulate the induction of synaptic plasticity, effect on learning and memory formation, i.e., can improve neurovascular coupling
	Midbrain	Reward center and initiation of the nicotine addiction process
	Neuro-endocrine neurons in the hypothalamus	Facilitate the Ca <sup>2+</sup> -dependent release of vasopressin and oxytocin
	Others	Improvement of neurovascular coupling (in neurodegenerative disease and ischemia)
mAChR		
M1	Autonomic ganglia	Mediates slow EPSP in postganglionic nerve
	Exocrine glands	Stimulates secretion
	Central nervous system	Activates slow after-depolarizing potentials in neurons
M2	Heart	Reduce of heart rate, contractile forces of the atrium and conduction velocity in AV node
	Central nervous system	Activates slow after-depolarizing potentials in neurons
M3	Smooth muscles	Vasoconstriction, vasodilatation, bronchoconstriction
	Endocrine and exocrine glands	Stimulate secretion
	Central nervous system	Activates slow after-depolarizing potentials in neurons
	Eye	Lacrimation, miosis and accommodation by contraction of the sphincter papillae and ciliary body
M4	Central nervous system	Activates slow after-depolarizing potentials in neurons
M5	Not well known	-

*EPSP* excitatory postsynaptic potential



## NMBs and inflammation

Given the expression of AChRs in different cells throughout the body, it is likely that NMBs exert effects other than neuromuscular blockade. It has been demonstrated in a rat lung injury model that non-depolarizing NMBs (cisatracurium and pancuronium) protect against the development of ventilator-induced lung injury (VILI) through a direct, dose-dependent anti-inflammatory effect mediated by the nAChR $\alpha$ 1 expressed on epithelial, endothelial, and CD14+ cells [230]. In patients with early ARDS (N = 36), continuous administration of cisatracurium for 48h attenuated pulmonary inflammation (interleukin (IL)-8) and systemic inflammation (IL-6, IL-8) compared to placebo [222]. Recently, new data published in Critical Care by Sottile and colleagues [231] support the anti-inflammatory role of NMBs in patients with ARDS. The authors investigated in a secondary analysis of the ARMA trial [232] the effect of NMBs on surfactant protein-D (SP-D) and von Willebrand factor (VWF), biomarkers specific for epithelial and endothelial lung injury, respectively, in addition to markers of systemic inflammation (IL-8). In the overall cohort (N = 446), the use of NMB was significantly associated with an increase in SP-D, but no effect on VWF or IL-8. Interestingly, after adjusting for multiple confounders the use of NMBs was associated with a significant decrease in SP-D, VWF, and IL-8, but only in patients with a PaO<sub>2</sub>/FiO<sub>2</sub> ratio  $\leq$  120 and ventilated with low tidal volumes. In patients with higher PaO<sub>2</sub>/FiO<sub>2</sub> ratios, or high tidal volumes, NMBs did not affect SP-D, VWF, or IL-8. These data provide evidence that NMBs attenuate endothelial and epithelial injury in selected ARDS patients.

## Clinical impact on respiratory muscles and further research

Clinicians may become somewhat confused by the recent literature regarding the role of disuse in the development of critical illness-associated respiratory muscle weakness. On the one hand, excellent data by Goligher et al. [3] demonstrated that in ventilated ICU patients low diaphragm effort is associated with decreased thickness of the diaphragm muscle. In addition, the development of decreased thickness is associated with adverse outcome, including delayed ventilator weaning. On the other hand, the ACURASYS trial [223] demonstrated that 48h of NMB (resulting in full diaphragm muscle inactivity) improved outcome, including more ventilator-free days (and no development of muscle weakness) compared to placebo. An intriguing explanation is that the beneficial effects of NMBs are at least partly independent of respiratory muscle pump inactivation, but more the result of modulation of inflammation and injury [222, 230, 231] or even unexplored mechanisms. Of note, we have recently demonstrated in a proof of concept study that partial neuromuscular blockade (low dose rocuronium) controls the mechanical effects of high respiratory drive, resulting in pressures consistent with both lung-protective ventilation and diaphragm-protective ventilation [33, 34]. So we might “ménager la chèvre et le chou”.

In conclusion, non-depolarizing NMBs have been used for decades in critical care, but we still do not fully understand their effects beyond muscle paralysis. New mechanisms of action may help us to identify patients that benefit the most from the use of NMBs and help us to select appropriate doses.

# REFERENCES

See page 166.





## Chapter 8

# Neuromuscular blockers modulate inflammatory response and reactive oxygen production by peripheral blood mononuclear cells of healthy volunteers

---

**Diana Jansen**, Jelle Gerretsen, Matthijs Kox, Lucas T. van Eijk, Leo M.A. Heunks

*Submitted*

## ABSTRACT

### Background

There is discussion in the literature regarding the beneficial effects of neuromuscular blocking agents (NMBAs) on the outcome in acute respiratory distress syndrome. Some data suggest that NMBA may protect against the development of ventilator-induced lung injury by decreasing lung stress, but possibly also by attenuating the inflammatory response. In the current study, we investigated the effects of NMBAs on cytokine and reactive oxygen species production by primary human leukocytes in more detail.

### Methods

The *ex vivo* cytokine production capacity of peripheral blood mononuclear cells of 12 healthy volunteers was investigated by stimulation with E.coli-derived lipopolysaccharide in the absence and presence of different concentrations of rocuronium, cisatracurium and succinylcholine. In addition, whole blood obtained from the 6 healthy volunteers was stimulated with opsonized zymosan in the presence and absence of these NMBAs to assess the generation of reactive oxygen species.

### Results

Rocuronium, cisatracurium and succinylcholine all significantly reduced lipopolysaccharide-induced production of interleukin-6, tumor necrosis factor and interleukin-10, as well as zymosan-induced generation of reactive oxygen species in a non-dose dependent manner. Cell viability was not affected by any of the NMBAs.

### Conclusion

NMBAs attenuate production of pro- and anti-inflammatory cytokines, as well as reactive oxygen species generation by activated primary human leukocytes. These data may help to understand the effects of NMBA on outcome in selected patients with acute respiratory distress syndrome.

## BACKGROUND

In patients with acute respiratory distress syndrome (ARDS) neuromuscular blockers (NMBA) may be used to facilitate lung-protective mechanical ventilation, as mitigating patients' breathing efforts can reduce stress applied to the lung. It was demonstrated that 48-hour treatment with the NMBA atracurium conferred a survival benefit compared with placebo for patients with severe early ARDS ( $\text{PaO}_2/\text{FiO}_2$  ratio  $\leq 120$ ) [223]. However, this possible protective effect of NMBA in severe ARDS patients was not found in the ROSE trial. The trial was stopped at the second interim analysis for futility because no significant difference in 90-day mortality was found between patients who received continuous cisatracurium infusion and those who were treated with the usual-care approach [233].

NMBAs exert their action through interaction with the nicotinic acetylcholine receptor (nAChR) subunit  $\alpha$ -2, primarily located in the neuromuscular junction, but AChRs are also expressed by other tissues and cells, including the brain, macrophages, autonomic ganglia, endothelial cells, and epithelial cells [234]. The effect of NMBAs on striated muscle function are well known, but the impact of NMBAs on other cells is less well understood [226]. Interestingly, in patients with early ARDS, continuous administration of cisatracurium for 48h attenuated pulmonary inflammation (interleukin(IL)-8) and systemic inflammation (IL-6, IL-8) compared to placebo-treated patients [222]. Furthermore, in a rat lung injury model, non-depolarizing NMBAs protected against the development of ventilator-induced lung injury (VILI), likely through attenuation of the inflammatory response [230]. These data suggest that one of the mechanisms by which NMBAs attenuate lung injury is mitigation of the inflammatory response, but evidence of direct immunomodulatory effects of NMBAs is lacking. In the current study, we investigated the effects of NMBAs on cytokine production and reactive oxygen generation by primary human leukocytes.

## METHODS

### Study design, population and ethics

In this experimental study, blood was obtained from a total of 12 healthy volunteers (11 male / 1 female) to investigate the modulatory effects of NMBAs on cytokine production and reactive oxygen species (ROS) generation. The study was conducted in the research unit of the Intensive Care of the Radboud University Medical Center, Nijmegen, the Netherlands, after written informed consent was obtained from each



healthy volunteer. The study was approved by the local ethics committee (CMO Arnhem-Nijmegen, registration no. CMO2299 2010/104).

### Cytokine production

Twenty mL ethylenediamine tetraacetic acid (EDTA)-anticoagulated blood was obtained from 12 healthy volunteers to assess the effects of rocuronium, cisatracurium and succinylcholine on lipopolysaccharide(LPS)-induced cytokine production in peripheral blood mononuclear cells (PBMCs). PBMCs were isolated by density gradient centrifugation using Ficoll-Paque PLUS (GE Healthcare, Illinois, USA) and Sepmate tubes (STEMCELL Technologies, Vancouver, Canada). After washing of the cells with phosphate-buffered saline (PBS), PBMCs ( $5 \times 10^5$ ) were dissolved in RPMI 1640 Dutch modification medium (Invitrogen) supplemented with 10  $\mu\text{g/mL}$  gentamicin, 10 mM Glutamax and 10 mM pyruvate (RPMI+++), and incubated ( $37^\circ\text{C}$ , 5%  $\text{CO}_2$ ) in duplicate in round-bottom 96-well plates with the different NMBA (rocuronium: 0.0005, 0.005, 0.05, 0.5, 5, 50  $\mu\text{g/mL}$ ; cisatracurium: 0.0001, 0.001, 0.01, 0.1, 1, 10  $\mu\text{g/mL}$ ; succinylcholine 0.001, 0.01, 0.1, 1, 10, 100  $\mu\text{g/mL}$ ) or RPMI+++ (control) for 30 minutes. The NMBA concentrations used include clinically relevant as well as higher and lower concentrations. Subsequently, LPS (10 ng/mL, *E. coli*-derived, serotype O55:B5, Sigma Aldrich) or RPMI+++ (control) was added. Twenty-four hours later, cultures were centrifuged (8 min, 1400 RPM, room temperature) and supernatants were stored at  $-80^\circ\text{C}$  until analysis of concentrations of pro-inflammatory (tumor necrosis factor (TNF) and IL-6) and anti-inflammatory (IL-10) cytokines using enzyme-linked immunosorbent assays (ELISA, R&D systems Inc., Minneapolis, USA).

### Cell viability

Cell viability of stimulated PBMCs was checked after incubation by measuring lactate dehydrogenase (LDH) in supernatants using a Cytotox96 non-radioactive assay (Promega, Wisconsin, USA), according to instructions of the manufacturer.

### ROS generation

To test the effects of three different concentrations of rocuronium, cisatracurium and succinylcholine on ROS generation, an additional 4 mL lithium-heparin anticoagulated blood was collected from 6 (all male) of the 12 healthy volunteers. PBMCs were isolated and prepared as described above, and incubated for 30 minutes ( $37^\circ\text{C}$ , 5%  $\text{CO}_2$ ) in duplicate in round-bottom 96-well plates with the different NMBA (rocuronium: 0.5, 5, 50  $\mu\text{g/mL}$ ; cisatracurium: 0.1, 1, 10  $\mu\text{g/mL}$ ; succinylcholine 1, 10, 100  $\mu\text{g/mL}$ ) or HBSS (control). Then luminol (0.83 mM, Z4250, Sigma-Aldrich) and opsonized zymosan (3 mg/mL, Z4250, Sigma-Aldrich) w added. Hereafter,

chemiluminescence was measured every 142 s at 37°C during 1 hour on a 96-well plate reader (Biotek, Vermont, USA) to determine ROS production.

### **Statistical analysis**

Statistical analysis was performed using GraphPad Prism version 5 (GraphPad Software, Inc., San Diego, USA). Data are presented as median and interquartile range. The Wilcoxon signed-rank test was used to detect the effect of the different NMBAs on cytokine production, ROS generation and cell viability. For all tests, a two-tailed P value  $\leq 0.05$  was considered statistically significant.

## **RESULTS**

### **Effects of NMBAs on LPS-induced cytokine production**

LPS stimulation induced a marked production of pro-inflammatory cytokines IL-6 and TNF as well as the anti-inflammatory cytokine IL-10 by PBMCs (Figure 1). Rocuronium, cisatracurium and succinylcholine all attenuated LPS-induced cytokine production (**Figure 1**), with no apparent differences between NMBAs or dose-dependency.

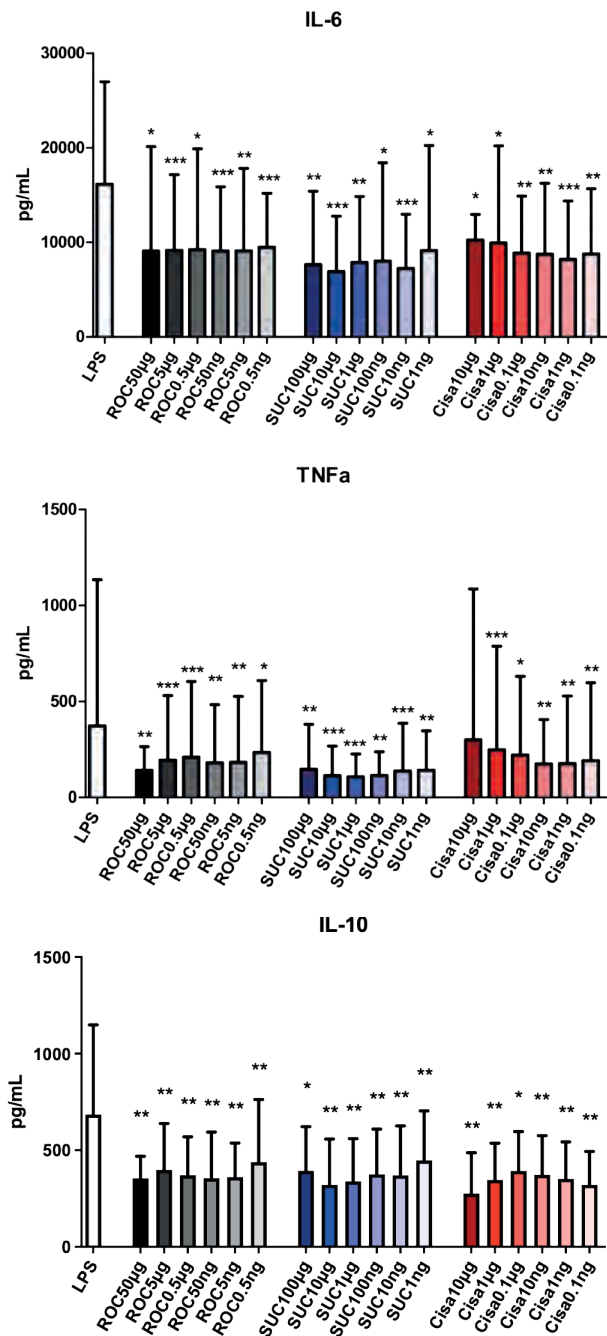


**Figure 1.** Effect of rocuronium (0.0005, 0.005, 0.05, 0.5, 5, 50 µg/mL), succinylcholine (0.001, 0.01, 0.1, 1, 10, 100 µg/mL) and cisatracurium (0.0001, 0.001, 0.01, 0.1, 1, 10 µg/mL) on the LPS-induced cytokine response of the pro-inflammatory cytokines IL-6 and TNF-alfa and the anti-inflammatory cytokine IL-10. P value: \* < 0.05, \*\* < 0.01, \*\*\* < 0.001.

### Effects of NMBAs on cell viability

To rule out cell death as a possible explanation for the attenuated cytokine response caused by NMBAs, we investigated viability of the LPS-stimulated PBMCs in the absence and presence of different NMBAs. As shown in **Figure 2**, neither LPS nor any of the NMBAs in combination with LPS affected cell viability.

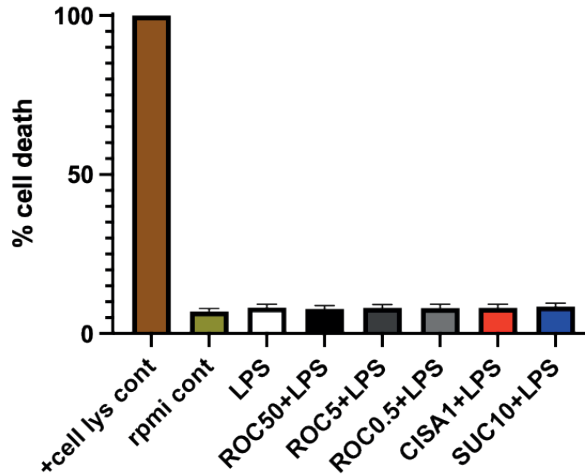


**Figure 2.** Viability of the LPS-stimulated peripheral blood mononuclear cells itself and after administration of rocuronium (0.5, 5, 50  $\mu\text{g}/\text{mL}$ ), succinylcholine (10  $\mu\text{g}/\text{mL}$ ) and cisatracurium (1  $\mu\text{g}/\text{mL}$ ). P value: \*\*<0.01.

### Effect of NMBAs on ROS production

Zymosan profoundly induced ROS production in whole blood cultures (**Figure 3**). Zymosan-induced ROS production was dose-dependently attenuated by rocuronium, succinylcholine and cisatracurium (**Figure 3**).

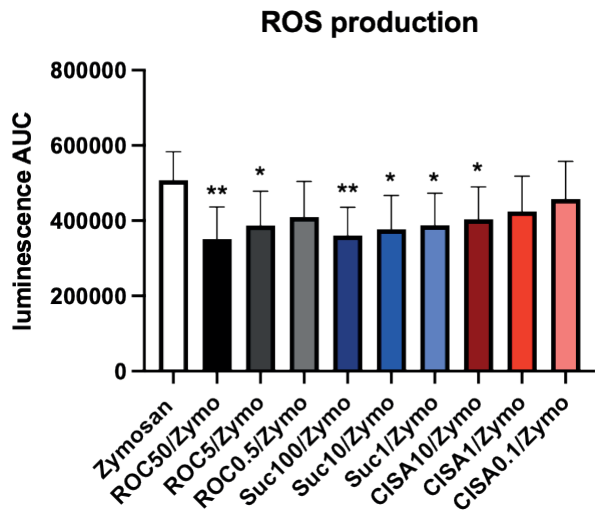


**Figure 3.** Effect of rocuronium (0.5, 5, 50  $\mu\text{g/mL}$ ), succinylcholine (1, 10, 100  $\mu\text{g/mL}$ ) and cisatracurium (0.1, 1, 10  $\mu\text{g/mL}$ ) on the ROS production. P value: \* $<0.05$ , \*\* $<0.01$ , \*\*\* $<0.001$ .

## DISCUSSION

The current study investigates the effects of NMBAs on cytokine production and reactive oxygen generation by primary human leukocytes. We demonstrate that NMBAs both decreased the production of pro- and anti-inflammatory cytokines and ROS in activated inflammatory cells of healthy volunteers.

Although a lower production of pro-inflammatory cytokines was previously found in the lungs and blood of ARDS patients receiving NMBAs [222], the mechanism by which inflammation is attenuated has not been completely clarified to date. An indirect effect has been suggested, where reduction of ventilator-induced lung injury by NMBAs subsequently leads to less inflammation. However, we show that NMBAs also directly attenuate the inflammatory response in primary human leukocytes. Our study is in line with other studies that report an anti-inflammatory effect of NMBAs [230, 231]. The broad expression of nAChR receptors on a variety of cells including epithelial cells, endothelial cells and leucocytes adds to the biological plausibility of this finding. Interestingly, in the lungs, nAChR $\alpha$ 1 serves as an alternative receptor for urokinase on neutrophils, leading to the release of inflammatory cytokines such as IL-1 $\alpha$ , TNF and macrophage inflammatory protein-2 [235]. Blocking this effect would therefore result in an anti-inflammatory profile. Indeed the intrinsic anti-inflammatory effect of cisatracurium was shown in a lung injury model in rats [230].

In addition, challenging several human cell types (including CD14+ leucocytes) with various stimuli (LPS, bronchoalveolar lavage fluid or plasma for ARDS patients) showed an abolished inflammatory response in the presence of cisatracurium and pancuronium, the effect being blocked after silencing the nAChR $\alpha$ 1 receptor. Of note, these authors reported a dose dependent effect of NMBAs on IL-6 production, whereas in our study the inhibitory effect was independent from the NMBA concentrations used. The reason for this apparent discrepancy remains unclear, but cell death due to experimental conditions was excluded.

Although nAChR $\alpha$ 1 and 2 are the most studied subtype in relation to the effects of muscle relaxants, NMBAs' actions are not confined to this subtype. On the contrary, all NMBAs have been shown to inhibit multiple muscle and neuronal nAChR subtypes including the  $\alpha$ 7nAChR [236]. This receptor subtype is of particular interest in relation to inflammation, as it is the effector receptor in the cholinergic anti-inflammatory pathway, in which inflammation is attenuated by stimulation or activation of the vagus nerve [237]. As such, NMBAs might theoretically block this pathway and contribute to a more pronounced (systemic) inflammatory response. However, the fact that NMBAs have a direct anti-inflammatory effect as shown by us and others, taken together with clinical observation of attenuated inflammation in ARDS patients after administration of NMBAs indicates that the potential blockade of the cholinergic anti-inflammatory pathway by NMBAs is probably of minor clinical importance.

The LPS-induced production of the anti-inflammatory cytokine IL-10 was also decreased after NMBA exposure. This may be explained from the fact that IL-10 is produced in response to pro-inflammatory cytokines as a compensatory mechanism. Along these lines, less pro-inflammatory cytokine production therefore also leads to a blunted IL-10 response, although a direct effect of NMBAs on IL-10 production cannot be excluded.

NMBAs also blunted ROS generation in whole blood cultures. This is an important finding as ROS enhance the inflammatory response, but also have a direct harmful effect on organ cells (most notably endothelial cells). They therefore contribute to endothelial failure by enhancing inflammation and decreasing vascular tone [238]. Jeong et al. investigated the effect of NMBAs on vascular endothelial function following ROS-induced injury [239]. They demonstrated a dose-dependent effect of NMBAs on the preservation of ACh-induced relaxation, which implies that NMBA could act as ROS scavengers. In our study, we demonstrated that all NMBAs decrease ROS production in a dose-dependent manner. Because in our experimental set-up, NMBAs were present throughout the ROS-production assay, scavenging of ROS by

NMBAs indeed may offer an explanation of how NMBAs are able to reduce ROS, although we have not examined the mechanism of action in detail. In any case, our findings confirm that NMBAs could play a role in the prevention of ROS-induced endothelial damage.

Our study is limited by the relatively small group of healthy volunteers included in the study and therefore the results cannot not be readily extrapolated to ICU patients. In general, (cells from) critically ill patients on the ICU frequently exhibit aberrant immunological phenotypes, with some suffering from an exaggerated inflammatory response leading tot shock and organ failure, while others have a particularly suppressed immune status, making them vulnerable to opportunistic infections. In addition, the use of NMBAs can have adverse effects such as ICU-acquired weakness. Therefore modulating the inflammatory response in ICU patients using NMBAs may in concept be a attractive idea, but should be used with caution. The results from our study mainly contribute to our understanding of the potential mechanism by which NMBAs exert their beneficial role in early ARDS.

## CONCLUSION

In conclusion, we demonstrate that NMBAs mitigate the LPS-induced inflammatory response and ROS production in primary human leukocytes of healthy volunteers. These data may help to understand the effects of NMBA in ventilated critically ill patients, beyond muscle paralysis.

## REFERENCES

See page 166.



**PART IV:**  
**Summary and future perspective**

## Chapter 9

### Summary

---

In the last decade, it has become clear that mechanical ventilation itself is an important contributing factor in the development of respiratory muscle dysfunction, which is associated with adverse outcomes, prolonged ICU admission and increased mortality. Ventilator-induced respiratory muscle dysfunction is caused by excessive unloading or unnoticed loading of the respiratory muscles. To date, most studies focused mainly on the effect of different ventilatory modes and levels of assist at the main inspiratory muscle, the diaphragm. In this thesis, we examined the effect of other frequently used ventilatory settings and the impact of the expiratory muscles on the pathophysiology of diaphragm dysfunction. In addition, several monitoring tools and preventive strategies were investigated.

The first part of this thesis refers to other contributing factors in the development of ventilator-induced diaphragm dysfunction. For example, positive end-expiratory pressure (PEEP) is a ventilator setting routinely used in daily practice. It aims to increase end-expiratory lung volume (EELV), improve lung homogeneity and thereby may improve oxygenation and respiratory mechanics. From animal studies it is known that PEEP, due to an increase in EELV, shortens the diaphragm muscle in the zone of apposition, which leads to muscle fiber remodeling, characterized by the loss of sarcomeres in series (termed longitudinal atrophy). This is considered an adaptive response in order to restore the optimal length for force generation. Whether PEEP-induced longitudinal fiber atrophy develops in the human diaphragm is unknown. Therefore, we studied in **Chapter 2** the acute effects of positive end-expiratory pressure on both the geometry and function of the human diaphragm. Nineteen healthy volunteers were non-invasively ventilated with PEEP of 2, 5, 10 and 15 cmH<sub>2</sub>O. We found that when PEEP was increased from 2 to 15 cmH<sub>2</sub>O, the diaphragm moves caudally, the zones of apposition shortens and the diaphragm thickens up to 36.4%. As a result, the neuromechanical efficiency (NME) reduced by 48%, which means that the diaphragm becomes less efficient (by 48%) in generating force. These findings demonstrate that also in humans, the application of PEEP results in conditions associated with the development of longitudinal atrophy of the diaphragm.

It is striking that the role of the expiratory muscles in the pathophysiology of ventilator-induced respiratory muscle dysfunction is largely neglected. In **Chapter 3** we thus reviewed the current knowledge on the (patho)physiology of expiratory muscle function in Intensive Care Unit patients. The expiratory muscles include of the lateral abdominal wall muscles and some of the rib cage muscles. During tidal breathing they exhibit tonic activity to counteract gravitational forces and maintain the diaphragm at optimal length for pressure generation. When the respiratory load

increases (i.e. as during exercise, low respiratory system compliance, sepsis or due to intrinsic PEEP) or the inspiratory muscle capacity decreases (i.e. due to muscle weakness) the expiratory muscles become active in the expiratory phase. This may have beneficial effects, including reduction in EELV, reduction in transpulmonary pressure and improvement of the inspiratory muscle capacity. However, just like the inspiratory muscles, the expiratory muscle function can become weak. Several techniques are provided to assess expiratory muscle function in the critically ill patient, including gastric pressure and ultrasound, but their clinical implications still need to be established.

Thus, the expiratory muscles may play a significant role in patients with respiratory failure or muscle weakness. This was also shown in **Chapter 4**, in which we analyze the inspiratory and expiratory muscle function and respiratory mechanics during a spontaneous breathing trial in a heterogenous group of critically ill patients. We found that patients who failed weaning from mechanical ventilation increased their expiratory muscle effort at the end of the spontaneous breathing trial, accounting for 24% of the total respiratory muscle effort, whereas it remained stable in successfully extubated patients. In addition, the neuromechanical efficiency index was lower in the weaning-failure patients. This suggests that the impaired force-generating capacity of the diaphragm also plays an important role in failed weaning from mechanical ventilation.

Despite the increasing availability of respiratory monitoring tools, assessment of respiratory muscle effort is still not part of routine clinical care. For implementation in daily practice it is necessary to provide indices that can be easily determined at the bedside. Therefore, in the second part of this thesis we evaluated the reliability of two indices that can be measured by the use of a dedicated nasogastric tube. In **Chapter 5** we investigate the repeatability of the neuromechanical efficiency index (NME), defined by delta airway pressure ( $\Delta P_{aw}$ ) divided by delta electrical activity of the diaphragm ( $\Delta E_{Adi}$ ) measured during an end-expiratory occlusion in thirty-one ventilated ICU patients. We demonstrated that repeated NME maneuvers within an individual patient exhibited unacceptably high variation, up to 82.6%. This indicates that a single NME maneuver cannot be used to estimate the pressure generated by the diaphragm. Additional EAdi waveform analysis to correct for non-physiological appearing waveforms did not decrease variability. But selecting three out of five occlusions with the lowest variability reduced the variation to 29.8%. In addition to the NME index, the patient-ventilator breath contribution (PVBC) index can be used to estimate the inspiratory muscle effort. This index measures the relative contribution of the patient to the total tidal volume generated during mechanical

ventilation, based on the ratio of EAdi and Paw during assisted and unassisted breaths. The results from **Chapter 6** show that the method currently available to assess PVBC at bedside is unreliable. Only when our new algorithm for matching EAdi between assisted and unassisted breaths was used, the reliability of this index increased and might be useful for daily practice. However, this algorithm is quite complex and could only be helpful for a clinician when it gets implemented in the ventilator software.

In the third part of this thesis, we discuss strategies in order to prevent the development of diaphragm dysfunction. As the underlying cause of diaphragm dysfunction is multifactorial, it is difficult to find one solution that can prevent or restore diaphragm dysfunction. One of our corner stones lies in the effort to reduce excessive respiratory muscle activity, for example by the administration of partial neuromuscular blockade. **Chapter 7** provides an overview of the mechanism of action of the neuromuscular blocking agent (NMBA) itself, which goes beyond neuromuscular blockade. NMBAs exert their neuromuscular effect through interaction with the acetylcholine receptor (AChR) in the neuromuscular junction. However, AChRs are also expressed by other tissues and cells and thus it is likely that NMBAs exert effects other than neuromuscular blockade alone. Several studies have demonstrated that non-depolarizing NMBAs might protect against the development of ventilator-induced lung injury through a direct, dose-dependent anti-inflammatory effect. Most of these studies were performed with cisatracurium although other neuromuscular blockers, including rocuronium and succinylcholine are more frequently used. In the last chapter of this thesis, **Chapter 8** we demonstrated the immunomodulatory effects of these three NMBAs using PBMC's of healthy subjects. We found that NMBA decreased both the production of pro- and anti-inflammatory cytokines, as well as the production of reactive oxygen species by activated inflammatory cells. These data provide an alternative explanation for the observed beneficial effects of NMBA in ventilated (critically ill) patients.





## Chapter 10

### Discussion and future perspectives

---



## DISCUSSION AND FUTURE PERSPECTIVE

Diaphragm dysfunction frequently develops in ventilated critically ill patients and is associated with increased morbidity and mortality. In this thesis we provide new information about the pathophysiology of diaphragm dysfunction, discuss indices to monitor diaphragm function and get in more detail on one of the preventive strategies.

### Physiological insights in inspiratory and expiratory muscle function

From previous studies is known that in ventilated patients both diaphragm injury (ventilator under-assist) [33, 44, 45] and diaphragm atrophy (ventilator over-assist) [4, 171] may lead to a reduced contractility of the diaphragm [6, 12, 13]. Besides the mode of ventilation and the level of inspiratory assist, also positive end-expiratory pressure (PEEP) influences diaphragm geometry and function. From animal studies is known that PEEP (due to an increase in end-expiratory lung volume) shortens the diaphragm muscle in the zone of apposition, which leads to muscle fiber remodeling, characterized by the loss of sarcomeres in series, termed longitudinal atrophy [7]. The results in **Chapter 2** confirmed that PEEP shortens the diaphragm muscle in humans, which resulted in impaired force-generation. Thus, it appears that, in addition to experimental models, in humans, conditions required to develop longitudinal atrophy, are present. Further studies should focus on whether and when muscle fiber remodeling occurs in the human diaphragm, as this (mal)adaptation to PEEP may precede weaning failure when PEEP is released during a spontaneous breathing trial. The diaphragm then becomes 'overstretched' and less efficient in force generation (**Figure 1**). This provides an entirely novel mechanism for ventilator weaning failure in ICU patients.

Most of previous studies on the impact of mechanical ventilation on the development of diaphragm dysfunction focused on its effect at the inspiratory muscles. In **Chapter 3** we provide an overview of the importance of the expiratory muscles, the other part of the respiratory pump. They play a role in the development of effective cough (facilitate airway clearance) [109], counteract gravitational forces and maintain the diaphragm at optimal length for pressure generation during normal tidal breathing [97-99]. Active recruitment of the expiratory muscles has been demonstrated in COPD patients with acute respiratory failure [176], but is also seen frequently in ventilated critically ill patients in the presence of an imbalance between inspiratory muscle load and capacity. It enhances inspiratory muscle capacity in two ways: the increase in abdominal pressure lengthens the diaphragm into the optimal length for tension generation [104, 105] and stores elastic energy which facilitates

the next inspiration [106, 107]. However, this increase in abdominal pressure may also have undesirable effects, as it may lead to cyclic alveolar collapse and airway closure in ARDS patients [113-116] (which can be reduced by the administration of neuromuscular blockers [117, 118]) and could generate intrinsic PEEP as a result of expiratory flow limitation. In addition, the energy used by the expiratory muscles progressively increases during a spontaneous breathing trial in patients that failed weaning from mechanical ventilation, as demonstrated in **Chapter 4**. Along with a reduced NME, this challenges the concept that expiratory muscle activation improves diaphragm contractile efficiency, although this requires further evaluation. Nevertheless, recruitment of the expiratory muscles during a weaning trial appears to be a strong marker of weaning failure. Therefore assessing expiratory muscle function in addition to inspiratory function may be of value in the weaning of critically ill patients.

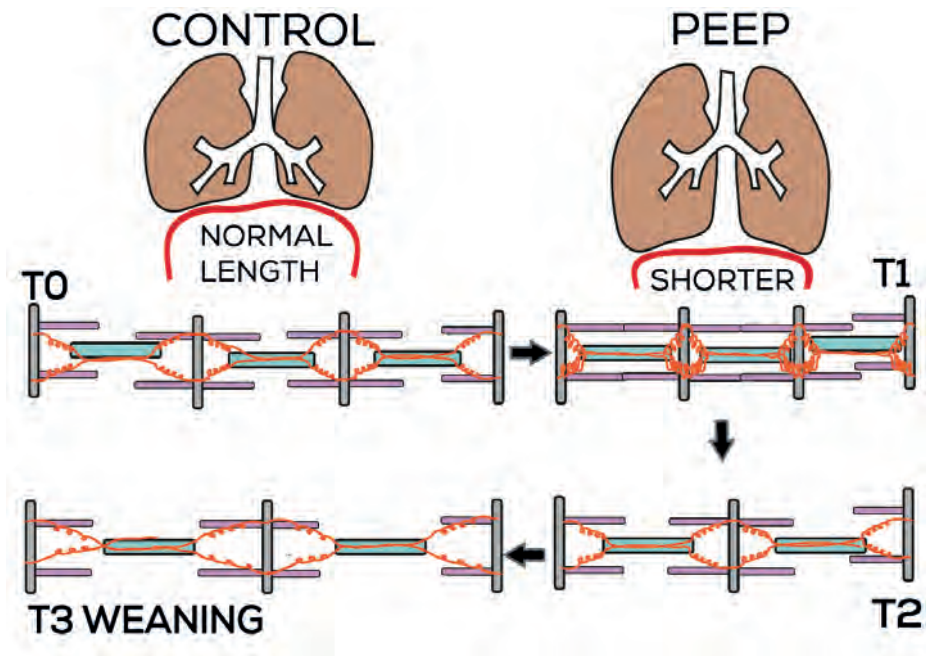


**Figure 1.** Schematic illustration of the development of longitudinal atrophy in diaphragm fibers during mechanical ventilation with positive end-expiratory pressure (PEEP). T0: Normal muscle length at end-expiration, without PEEP. For simplicity, only three sarcomeres are drawn. T1: The acute effect of PEEP on sarcomere length, resulting in a shorter muscle, more overlap in the thin and thick filaments and therefore less efficient in the generation of tension. T2: Long-term PEEP causes sarcomere absorption to restore sarcomere length and consequently restore its tension generation back to normal. T3: During weaning and normalization of end-expiratory pressure, the diaphragm fibers are stretched to lengths beyond optimal sarcomere length. The schematic illustration shows a length at which thick-thin filament overlap is absent and no force can be generated by the muscle fiber.

## Monitoring diaphragm function in the acutely ventilated patients

Based on previous knowledge of the pathophysiology of ventilator-induced diaphragm dysfunction, it appears reasonable to conclude that prevention of both disuse and high breathing effort is important. Several monitoring tools are feasible in critically ill patients, including monitoring of esophageal pressure (Pes), diaphragm electromyography (EMG), and ultrasound [17, 18]. In addition, recently a novel non-invasive method ( $\Delta P_{occ}$ ) has become available that can measure both excessive inspiratory effort and dynamic lung stress [28].

The assessment of the transdiaphragmatic pressure (Pdi) is the state of the art technique for monitoring diaphragm effort. It requires simultaneous measurement of Pes and gastric pressure (Pga) as surrogates for the pleural and abdominal pressure, respectively. However, this technique is quite invasive and interpretation of waveforms may be complex [19, 20]. Diaphragm EMG, acquired by using a dedicated nasogastric feeding tube with nine electrodes positioned at the level of the diaphragm, is an alternative technique used to quantify breathing effort in ICU patients [17], with a strong correlation with Pes and Pdi [21, 22]. We used the diaphragm EMG to estimate the respiratory effort based on two indices previously described in the literature: 1) NME, defined by  $\Delta P_{aw} / \Delta E_{adi}$  [22, 23, 25, 26], and 2) PVBC, which provides an estimation of the fraction of breathing effort that is generated by the patient [24]. However, the results of **Chapter 5** and **6** show that both indices demonstrate high variability, making them unreliable as bedside monitoring tool. Only when complex algorithms were applied the variability improved. However, this algorithm could only be helpful for a clinician when it gets implemented in the ventilator software. A less invasive method to assess diaphragm function is measuring diaphragm thickening fraction by ultrasound. It was demonstrated that in ventilated ICU patients both an increase (high effort) and decrease (low effort) in diaphragm thickness was related to a decrease in maximal thickening fraction, i.e. diaphragm function [3, 12]. However, in only 10% of the mechanically ventilated patients, the diaphragm thickening fraction was related to a change in transdiaphragmatic pressure [240]. Therefore, this ultrasound index seems to be not useful as a surrogate of diaphragm function.

Last years, parameters as the driving pressure en P0.1 become popular since these are simple, quick en non-invasive, but none of them provide information about both the inspiratory drive and total dynamic lung stress [27, 241, 242]. However, recently it became clear that with the measurement of delta airway occlusion ( $\Delta P_{occl}$ ) from three randomly applied end-expiratory occlusion maneuvers both excessive inspiratory effort (Pmus) and dynamic lung stress (delta transpulmonary pressure)

can be detected [28]. And it seems that irrespective of depth of sedation or mode of ventilation, both frequently exceed safe thresholds in clinical care. Of note, the number of patients in this study was relatively small (N=16), which can possibly limit the generalizability of the validation. Despite the known clinical relevance and increased number in monitoring tools, assessment of important respiratory mechanics is still challenging but of great importance for future investigation.

### **Novel pharmacological interventions to modulate diaphragm function**

Most of the ventilated ICU patients develop diaphragm dysfunction while they are in the ICU. Importantly 53% exhibited diaphragm dysfunction already at ICU admission, suggesting that other factors play a role besides mechanical ventilation [14]. Since the underlying cause of diaphragm dysfunction is multifactorial, it is difficult to find one solution that can prevent or restore diaphragm dysfunction. It is beyond the scope of this thesis to discuss all possible options for prevention, thus in this part we will focus on inflammation and diaphragm dysfunction. Histological analysis of the diaphragm [6, 9, 10] demonstrates an increase in inflammatory cells in both rats and human on mechanical ventilation. In addition, studies in mechanically ventilated ICU patients that had an infection showed a decrease in *in vivo* diaphragmatic contractile force [13, 15]. This supports a role for inflammatory mediators in the development of diaphragm atrophy or injury. It has been shown in a rat lung injury model that non-depolarizing NMBAs may protect against the development of ventilator-induced lung injury (VILI) through a direct, dose-dependent anti-inflammatory effect [230]. But also in patients with severe ARDS (PaO<sub>2</sub>/FiO<sub>2</sub> ratio ≤ 120) it seems that NMBAs can decrease the systemic and pulmonary inflammatory response [222, 231]. The mechanism behind this anti-inflammatory response is not yet clarified, but a explanation may be that NMBAs also bind (and exert their effect) to nicotinic acetylcholine receptors present in various tissues and cells outside the neuromuscular junction, as described in **Chapter 7**. However, most of the previous studies were performed with cisatracurium while in our country rocuronium and succinylcholine are more frequently used. Therefore, the immunomodulatory effects of both rocuronium, cisatracurium and succinylcholine in healthy subjects were investigated in **Chapter 8**. We demonstrated that these NMBAs decreased the production of both pro- and anti-inflammatory cytokines, probably depending on which of the nAChR subtypes the NBMA action was mainly exerted. Taken together with the fact that ICU patients have different immunological phenotypes (and even may 'switch' during their ICU stay) makes that modulating the inflammatory response using NMBAs in concept is an attractive idea, but should be used with caution.

# REFERENCES

See page 166.





## Chapter 11

### Nederlandse samenvatting

---



In de laatste decennia is het duidelijk geworden dat mechanische beademing op zichzelf een belangrijke factor is in de ontwikkeling van disfunctie van de ademhalingsspieren, geassocieerd met nadelige uitkomsten, verlengde opname duur op de Intensive Care en verhoogde mortaliteit. Beademing-geïnduceerde disfunctie van de ademhalingsspieren, waarvan het middenrif de meest belangrijkste is, wordt veroorzaakt door teveel of te weinig ondersteuning. Tot op heden focuste de meeste studies zich vooral op het effect van de verschillende beademingsmodi en mate van ondersteuning door de beademing. In deze thesis zullen we het effect van andere vaak gebruikte beademingsinstellingen bespreken, en de impact van de expiratoire spieren op de pathofysiologie van disfunctie van de ademhalingsspieren. Daarnaast hebben we diverse manieren van monitoring onderzocht en gekeken naar preventieve mogelijkheden.

In het eerste deel van deze thesis hebben we gekeken naar andere bijdragende factoren voor de ontwikkeling van beademing-geïnduceerde disfunctie van de ademhalingsspieren. Zo is positieve eind-expiratoire druk (PEEP) een beademingsinstelling die dagelijks wordt toegepast. Het vergroot het eind-expiratoire long volume (EELV), verbetert de long homogeniteit en kan daardoor zowel de oxygenatie als bepaalde respiratoire mechanica optimaliseren. Uit dierstudies is bekend dat PEEP, door een toename van EELV, de middenrif spier kan verkorten in het gebied waar de spier aanhecht aan de thoraxwand ('zone of apposition'), wat kan leiden tot spiervezel remodeling gekarakteriseerd door het verlies van sarcomeren in serie (= longitudinale atrofie). Dit wordt gezien als een adaptatieve reactie om zo de optimale lengte van de spier, die nodig is voor het ontwikkelen van kracht, te herstellen. Of deze PEEP-geïnduceerde longitudinale spiervezel atrofie ook optreedt in het middenrif van de mens is vooralsnog onbekend. Daarom hebben we in **Hoofdstuk 2** de acute effecten van PEEP op zowel de geometrie als de functie van het middenrif onderzocht. Negentien gezonde vrijwilligers werden non-invasie beademd met PEEP van 2, 5, 10 en 15cmH<sub>2</sub>O. We ontdekten dat wanneer we de PEEP ophoogde van 2 naar 15cmH<sub>2</sub>O, dat het middenrif zich naar caudaal verplaatste en de zones of apposition zich verkortte en het middenrif dikker werd met 36,4%. Als gevolg hiervan daalde de neuromusculaire efficiëntie (NME) met 48%, wat betekent dat het middenrif (48%) minder efficiënt werd in het genereren van kracht. Deze bevindingen bevestigen dat ook in het menselijk middenrif het geven van PEEP leidt tot condities die geassocieerd zijn met het ontwikkelen van longitudinale atrofie van het middenrif.

Het is opvallend dat de rol van de expiratoire spieren in de pathofysiologie van beademings-gerelateerde disfunctie van de ademhalingsspieren grotendeels

negeert wordt. In **Hoofdstuk 3** hebben we de huidige kennis van de (patho)fysiologie van de expiratoire spierfunctie in Intensive Care Unit patients beoordeeld. De expiratoire spieren bevatten de laterale spieren van de buikwand en sommige van de tussenrib spieren. Tijdens normale ademhaling is er sprake van een tonische activiteit om zo de zwaartekracht tegen te gaan en om het middenrif op de meest ideale lengte te houden voor het genereren van kracht. Wanneer de respiratoire load groter wordt (zoals we bijvoorbeeld zien bij inspanning, lage respiratoire compliantie, in sepsis en door intrinsieke PEEP) of wanneer de inspiratoire spiercapaciteit afneemt (door bijvoorbeeld spierzwakte), dan zullen de expiratoire spieren actief worden in de expiratoire fase van de ademhaling. Dit kan de inspiratoire spiercapaciteit bevorderen doordat het het EELV en de transpulmonale druk beide doet afnemen. Echter, net zoals de inspiratoire spieren, kan ook de expiratoire spierfunctie verzwakken. Er zijn bepaalde methoden die expiratoire spierfunctie kunnen bepalen in de kritisch zieke patient, zoals bijvoorbeeld het meten van de maagdruk of het verrichten van een echo van de spieren, alleen hun klinische implicatie moet eerst nog wel onderzocht worden.

Ook de expiratoire spieren spelen kunnen dus mogelijk een belangrijke rol spelen in patienten met spierzwakte of falen op respiratoir gebied. Dit laten we zien in **Hoofdstuk 4**, waarin we de inspiratoire en expiratoire spierfunctie en de respiratoire mechanica hebben geanalyseerd tijdens een 'spontaneous breathing trial' (SBT) in een heterogene groep kritische zieke patiënten. Het bleek dat patiënten die faalden bij het 'weanen' van de mechanische beademing hun expiratoire spierkracht vergrootte op het einde van de SBT, tot 24% van de totale respiratoire spierkracht, terwijl dit gelijk bleef in de patiënten die succesvol geëxtubeerd konden worden. Daarnaast was de neuromechanische efficiëntie lager in de groep die faalde in het weanen van de beademing. Dit suggereert dat de verzwakte kracht-genererende capaciteit van het middenrif ook een belangrijke rol lijkt te spelen in het falen van het weanen van mechanische beademing.

Ondanks de toegenomen beschikbaarheid van respiratoire monitoring tools, is het bepalen van de respiratoire spierkracht nog steeds geen onderdeel van de dagelijkse klinische praktijk. Om iets dagelijks te kunnen toepassen is het nodig dat de tool gemakkelijk toegepast kan worden aan het bed van de patiënt. In het tweede deel van deze thesis zullen we de betrouwbaarheid van twee indices evalueren die gemeten kunnen worden door een speciale neusmaag sonde. In **Hoofdstuk 5** onderzoeken we de herhaalbaarheid van de neuromechanische efficiëntie index (NME), gedefinieerd als het verschil in luchtwegdruk ( $\Delta P_{aw}$ ) gedeeld door het verschil in elektrische activiteit van het middenrif ( $\Delta E_{Adi}$ ) gemeten tijdens een eind-expiratoire occlusie

in 31 beademende Intensive Care patiënten. We lieten zien dat herhaaldelijke NME manoeuvres binnen een individuele patiënt een onacceptabele hoge variabiliteit had, tot 82,6%. Dit betekent dat één NME manoeuvre niet gebruikt kan worden om de druk die het middenrif genereert te kunnen schatten. Additionele analyses van de EAdi curve, om zo proberen te corrigeren voor niet-fysiologische patronen, leiden niet tot een verlaging van de variabiliteit. Wel bleek dat wanneer drie van de vijf occlusies met de laagste variabiliteit werden geselecteerd, dit de variabiliteit kon reduceren tot 29,8%. Naast de NME index, kan volgens de literatuur ook de 'patient-ventilator breath contribution (PVBC) index' gebruikt worden om de inspiratoire spierkracht te schatten. Deze index meet de relatieve bijdrage van de patiënt aan het totale teugvolume gegenereerd tijdens mechanische beademing, gebaseerd op de ratio van de elektrische activiteit van het middenrif en de luchtwegdruk tijdens teugen met en zonder ondersteuning. De resultaten in **Hoofdstuk 6** laten zien dat de methode om de PVBC te bepalen onbetrouwbaar is. Alleen wanneer we ons nieuwe algoritme, waarin de elektrische activiteit van het middenrif tussen teugen met en zonder ondersteuning werden gematcht, gebruikte was de betrouwbaarheid beter en kan de index potentieel wel gebruikt worden in de dagelijkse klinische praktijk. Echter dit algoritme is nogal complex en kan daardoor alleen gebruikt worden door de klinici als het ingebouwd wordt in de software van het beademingsapparaat.

In het derde deel van deze thesis bediscussieren we de strategieën om de ontwikkeling van disfunctie van het middenrif te voorkomen. De onderliggende oorzaak hiervan is echter multifactorieel, dus het vinden van één oplossing die het probleem kan verhelpen is lastig. Een van de opties is om de excessieve respiratoire spieractiviteit te reduceren, bijvoorbeeld door het bewerkstelligen van gedeeltelijke neuromusculaire blokkade door het toedienen van spierverslappers. **Hoofdstuk 7** geeft een overzicht van het mechanisme van hoe spierverslappers werken, wat verder gaat dan spierverslapping alleen. Spierverslappers oefenen hun neuromusculaire werking uit via interactie met de acetylcholine receptor (AChR) in de neuromusculaire spleet. Echter, deze receptoren zitten ook op andere weefsels en cellen en het is daardoor aannemelijk dat spierverslappers ook andere effecten uitoefenen dan alleen spierverslapping op zichzelf. Verschillende studies hebben laten zien dat niet-depolariserende spierverslappers bescherming kunnen bieden tegen beademings-geïnduceerde longschade door een direct, dosis-afhankelijke anti-inflammatoir effect. De meeste van deze studies zijn uitgevoerd met cisatracurium, terwijl wij vaker gebruik maken van andere spierverslappers zoals rocuronium en succinylcholine. In het laatste hoofdstuk van deze thesis (**Hoofdstuk 8**), laten we de immunomodulatoire effecten zien van drie bovengenoemde spierverslappers waarbij we perifere mononucleaire bloedcellen gebruiken van gezonde vrijwilligers.

We zagen dat deze spierverslappers zowel de productie van pro- als anti-inflammatoire cytokines, als ook de productie van vrije zuurstofradicalen doen verlagen. Deze data voorziet een alternatieve verklaring voor de geobserveerde positieve effecten van spierverslappers in beademde kritisch zieke patiënten.

## REFERENCES

1. De Jonghe, B., et al., *Respiratory weakness is associated with limb weakness and delayed weaning in critical illness*. Crit Care Med, 2007. **35**(9): p. 2007-15.
2. Adler, D., et al., *Does inspiratory muscle dysfunction predict readmission after intensive care unit discharge?* Am J Respir Crit Care Med, 2014. **190**(3): p. 347-50.
3. Goligher, E.C., et al., *Mechanical Ventilation-induced Diaphragm Atrophy Strongly Impacts Clinical Outcomes*. Am J Respir Crit Care Med, 2018. **197**(2): p. 204-213.
4. Levine, S., et al., *Rapid disuse atrophy of diaphragm fibers in mechanically ventilated humans*. N Engl J Med, 2008. **358**(13): p. 1327-35.
5. Jaber, S., et al., *Rapidly progressive diaphragmatic weakness and injury during mechanical ventilation in humans*. Am J Respir Crit Care Med, 2011. **183**(3): p. 364-71.
6. Hooijman, P.E., et al., *Diaphragm muscle fiber weakness and ubiquitin-proteasome activation in critically ill patients*. Am J Respir Crit Care Med, 2015. **191**(10): p. 1126-38.
7. Lindqvist, J., et al., *Positive End-Expiratory Pressure Ventilation Induces Longitudinal Atrophy in Diaphragm Fibers*. Am J Respir Crit Care Med, 2018. **198**(4): p. 472-485.
8. Narici, M., M. Franchi, and C. Maganaris, *Muscle structural assembly and functional consequences*. J Exp Biol, 2016. **219**(Pt 2): p. 276-84.
9. Hussain, S.N., et al., *Mechanical ventilation-induced diaphragm disuse in humans triggers autophagy*. Am J Respir Crit Care Med, 2010. **182**(11): p. 1377-86.
10. Matecki, S., et al., *Leaky ryanodine receptors contribute to diaphragmatic weakness during mechanical ventilation*. Proc Natl Acad Sci U S A, 2016. **113**(32): p. 9069-74.
11. van Hees, H.W., et al., *Plasma from septic shock patients induces loss of muscle protein*. Crit Care, 2011. **15**(5): p. R233.
12. Goligher, E.C., et al., *Evolution of Diaphragm Thickness during Mechanical Ventilation. Impact of Inspiratory Effort*. Am J Respir Crit Care Med, 2015. **192**(9): p. 1080-8.
13. Demoule, A., et al., *Diaphragm dysfunction on admission to the intensive care unit. Prevalence, risk factors, and prognostic impact-a prospective study*. Am J Respir Crit Care Med, 2013. **188**(2): p. 213-9.
14. Demoule, A., et al., *Patterns of diaphragm function in critically ill patients receiving prolonged mechanical ventilation: a prospective longitudinal study*. Ann Intensive Care, 2016. **6**(1): p. 75.
15. Supinski, G.S., P. Westgate, and L.A. Callahan, *Correlation of maximal inspiratory pressure to transdiaphragmatic twitch pressure in intensive care unit patients*. Crit Care, 2016. **20**: p. 77.
16. Colombo, D., et al., *Efficacy of ventilator waveforms observation in detecting patient-ventilator asynchrony*. Crit Care Med, 2011. **39**(11): p. 2452-7.
17. Doorduyn, J., et al., *Monitoring of the respiratory muscles in the critically ill*. Am J Respir Crit Care Med, 2013. **187**(1): p. 20-7.
18. Heunks, L.M., J. Doorduyn, and J.G. van der Hoeven, *Monitoring and preventing diaphragm injury*. Curr Opin Crit Care, 2015. **21**(1): p. 34-41.
19. de Vries, H., et al., *Assessing breathing effort in mechanical ventilation: physiology and clinical implications*. Ann Transl Med, 2018. **6**(19): p. 387.
20. Mauri, T., et al., *Esophageal and transpulmonary pressure in the clinical setting: meaning, usefulness and perspectives*. Intensive Care Med, 2016. **42**(9): p. 1360-73.
21. Beck, J., et al., *Electrical activity of the diaphragm during pressure support ventilation in acute respiratory failure*. Am J Respir Crit Care Med, 2001. **164**(3): p. 419-24.

22. Bellani, G., et al., *Estimation of patient's inspiratory effort from the electrical activity of the diaphragm*. Crit Care Med, 2013. **41**(6): p. 1483-91.
23. Liu, L., et al., *Neuroventilatory efficiency and extubation readiness in critically ill patients*. Crit Care, 2012. **16**(4): p. R143.
24. Liu, L., et al., *Assessment of patient-ventilator breath contribution during neurally adjusted ventilatory assist in patients with acute respiratory failure*. Crit Care, 2015. **19**: p. 43.
25. Bellani, G., et al., *The Ratio of Inspiratory Pressure Over Electrical Activity of the Diaphragm Remains Stable During ICU Stay and is not Related to Clinical Outcome*. Respir Care, 2016. **61**(4): p. 495-501.
26. Di Mussi, R., et al., *Impact of prolonged assisted ventilation on diaphragmatic efficiency: NAVA versus PSV*. Crit Care, 2016. **20**: p. 1.
27. Telias, I., F. Damiani, and L. Brochard, *The airway occlusion pressure (P0.1) to monitor respiratory drive during mechanical ventilation: increasing awareness of a not-so-new problem*. Intensive Care Med, 2018. **44**(9): p. 1532-1535.
28. Bertoni, M., et al., *A novel non-invasive method to detect excessively high respiratory effort and dynamic transpulmonary driving pressure during mechanical ventilation*. Crit Care, 2019. **23**(1): p. 346.
29. Maddocks, M., et al., *Neuromuscular electrical stimulation to improve exercise capacity in patients with severe COPD - Authors' reply*. Lancet Respir Med, 2016. **4**(4): p. e16.
30. Reynolds, S., et al., *Diaphragm Activation in Ventilated Patients Using a Novel Transvenous Phrenic Nerve Pacing Catheter*. Crit Care Med, 2017. **45**(7): p. e691-e694.
31. O'Rourke, J., et al., *Initial Assessment of the Percutaneous Electrical Phrenic Nerve Stimulation System in Patients on Mechanical Ventilation*. Crit Care Med, 2020. **48**(5): p. e362-e370.
32. Sotak, M., et al., *Phrenic nerve stimulation prevents diaphragm atrophy in patients with respiratory failure on mechanical ventilation*. BMC Pulm Med, 2021. **21**(1): p. 314.
33. Heunks, L. and C. Ottenheim, *Diaphragm-Protective Mechanical Ventilation to Improve Outcomes in ICU Patients?* Am J Respir Crit Care Med, 2018. **197**(2): p. 150-152.
34. Doorduyn, J., et al., *Partial Neuromuscular Blockade during Partial Ventilatory Support in Sedated Patients with High Tidal Volumes*. Am J Respir Crit Care Med, 2017. **195**(8): p. 1033-1042.
35. Annane, D., *What Is the Evidence for Harm of Neuromuscular Blockade and Corticosteroid Use in the Intensive Care Unit?* Semin Respir Crit Care Med, 2016. **37**(1): p. 51-6.
36. Bissett, B.M., et al., *Inspiratory muscle training to enhance recovery from mechanical ventilation: a randomised trial*. Thorax, 2016. **71**(9): p. 812-9.
37. Schellekens, W.J., et al., *Strategies to optimize respiratory muscle function in ICU patients*. Crit Care, 2016. **20**(1): p. 103.
38. van Hees, H.W., P.N. Dekhuijzen, and L.M. Heunks, *Levosimendan enhances force generation of diaphragm muscle from patients with chronic obstructive pulmonary disease*. Am J Respir Crit Care Med, 2009. **179**(1): p. 41-7.
39. Doorduyn, J., et al., *The calcium sensitizer levosimendan improves human diaphragm function*. Am J Respir Crit Care Med, 2012. **185**(1): p. 90-5.
40. Esteban, A., et al., *Characteristics and outcomes in adult patients receiving mechanical ventilation: a 28-day international study*. JAMA, 2002. **287**(3): p. 345-55.

41. Dres, M., et al., *Coexistence and Impact of Limb Muscle and Diaphragm Weakness at Time of Liberation from Mechanical Ventilation in Medical Intensive Care Unit Patients*. *Am J Respir Crit Care Med*, 2017. **195**(1): p. 57-66.
42. Dres, M., et al., *Critical illness-associated diaphragm weakness*. *Intensive Care Med*, 2017. **43**(10): p. 1441-1452.
43. Goligher, E.C., et al., *Measuring diaphragm thickness with ultrasound in mechanically ventilated patients: feasibility, reproducibility and validity*. *Intensive Care Med*, 2015. **41**(4): p. 734.
44. Reid, W.D., et al., *Diaphragm injury and myofibrillar structure induced by resistive loading*. *J Appl Physiol* (1985), 1994. **76**(1): p. 176-84.
45. Orozco-Levi, M., et al., *Injury of the human diaphragm associated with exertion and chronic obstructive pulmonary disease*. *Am J Respir Crit Care Med*, 2001. **164**(9): p. 1734-9.
46. Loring, S.H., J. Mead, and N.T. Griscom, *Dependence of diaphragmatic length on lung volume and thoracoabdominal configuration*. *J Appl Physiol* (1985), 1985. **59**(6): p. 1961-70.
47. Wait, J.L., et al., *Diaphragmatic thickness-lung volume relationship in vivo*. *J Appl Physiol* (1985), 1989. **67**(4): p. 1560-8.
48. Wait, J.L., D. Staworn, and D.C. Poole, *Diaphragm thickness heterogeneity at functional residual capacity and total lung capacity*. *J Appl Physiol* (1985), 1995. **78**(3): p. 1030-6.
49. Gauthier, A.P., et al., *Three-dimensional reconstruction of the in vivo human diaphragm shape at different lung volumes*. *J Appl Physiol* (1985), 1994. **76**(2): p. 495-506.
50. Grassino, A., et al., *Mechanics of the human diaphragm during voluntary contraction: statics*. *J Appl Physiol Respir Environ Exerc Physiol*, 1978. **44**(6): p. 829-39.
51. Similowski, T., et al., *Contractile properties of the human diaphragm during chronic hyperinflation*. *N Engl J Med*, 1991. **325**(13): p. 917-23.
52. Hooijman, P.E., et al., *Diaphragm fiber strength is reduced in critically ill patients and restored by a troponin activator*. *Am J Respir Crit Care Med*, 2014. **189**(7): p. 863-5.
53. van den Berg, M., et al., *Diaphragm Atrophy and Weakness in the Absence of Mitochondrial Dysfunction in the Critically Ill*. *Am J Respir Crit Care Med*, 2017. **196**(12): p. 1544-1558.
54. Chapman, B., et al., *Estimation of lung volume in infants by echo planar imaging and total body plethysmography*. *Arch Dis Child*, 1990. **65**(2): p. 168-70.
55. Baydur, A., et al., *A simple method for assessing the validity of the esophageal balloon technique*. *Am Rev Respir Dis*, 1982. **126**(5): p. 788-91.
56. Barwing, J., et al., *Evaluation of the catheter positioning for neurally adjusted ventilatory assist*. *Intensive Care Med*, 2009. **35**(10): p. 1809-14.
57. McGill, S., D. Jucker, and P. Kropf, *Appropriately placed surface EMG electrodes reflect deep muscle activity (psoas, quadratus lumborum, abdominal wall) in the lumbar spine*. *J Biomech*, 1996. **29**(11): p. 1503-7.
58. Brown, S.H. and S.M. McGill, *A comparison of ultrasound and electromyography measures of force and activation to examine the mechanics of abdominal wall contraction*. *Clin Biomech (Bristol, Avon)*, 2010. **25**(2): p. 115-23.
59. Mills, G.H., et al., *Tracheal tube pressure change during magnetic stimulation of the phrenic nerves as an indicator of diaphragm strength on the intensive care unit*. *Br J Anaesth*, 2001. **87**(6): p. 876-84.
60. Luo, Y.M., et al., *Reproducibility of twitch and sniff transdiaphragmatic pressures*. *Respir Physiol Neurobiol*, 2002. **132**(3): p. 301-6.
61. Sinderby, C.A., et al., *Enhancement of signal quality in esophageal recordings of diaphragm EMG*. *J Appl Physiol* (1985), 1997. **82**(4): p. 1370-7.

62. Sinderby, C., L. Lindstrom, and A.E. Grassino, *Automatic assessment of electromyogram quality*. J Appl Physiol (1985), 1995. **79**(5): p. 1803-15.
63. Sinderby, C., et al., *Voluntary activation of the human diaphragm in health and disease*. J Appl Physiol (1985), 1998. **85**(6): p. 2146-58.
64. Doorduyn, J., et al., *Respiratory Muscle Effort during Expiration in Successful and Failed Weaning from Mechanical Ventilation*. Anesthesiology, 2018. **129**(3): p. 490-501.
65. Lessard, M.R., F. Lofaso, and L. Brochard, *Expiratory muscle activity increases intrinsic positive end-expiratory pressure independently of dynamic hyperinflation in mechanically ventilated patients*. Am J Respir Crit Care Med, 1995. **151**(2 Pt 1): p. 562-9.
66. Vogiatzis, I., et al., *Patterns of dynamic hyperinflation during exercise and recovery in patients with severe chronic obstructive pulmonary disease*. Thorax, 2005. **60**(9): p. 723-9.
67. Parthasarathy, S., et al., *Sternomastoid, rib cage, and expiratory muscle activity during weaning failure*. J Appl Physiol (1985), 2007. **103**(1): p. 140-7.
68. Jansen, D., et al., *Estimation of the diaphragm neuromuscular efficiency index in mechanically ventilated critically ill patients*. Crit Care, 2018. **22**(1): p. 238.
69. Oppersma, E., et al., *Functional assessment of the diaphragm by speckle tracking ultrasound during inspiratory loading*. J Appl Physiol (1985), 2017. **123**(5): p. 1063-1070.
70. Oppersma, E., et al., *The effect of metabolic alkalosis on the ventilatory response in healthy subjects*. Respir Physiol Neurobiol, 2018. **249**: p. 47-53.
71. Petroll, W.M., H. Knight, and D.F. Rochester, *Effect of lower rib cage expansion and diaphragm shortening on the zone of apposition*. J Appl Physiol (1985), 1990. **68**(2): p. 484-8.
72. Sassoon, C.S., et al., *Positive end-expiratory airway pressure does not aggravate ventilator-induced diaphragmatic dysfunction in rabbits*. Crit Care, 2014. **18**(5): p. 494.
73. Soilemezi, E., et al., *Effects of continuous positive airway pressure on diaphragmatic kinetics and breathing pattern in healthy individuals*. Respirology, 2016. **21**(7): p. 1262-9.
74. Beck, J., et al., *Effects of lung volume on diaphragm EMG signal strength during voluntary contractions*. J Appl Physiol (1985), 1998. **85**(3): p. 1123-34.
75. Farkas, G.A. and C. Roussos, *Diaphragm in emphysematous hamsters: sarcomere adaptability*. J Appl Physiol Respir Environ Exerc Physiol, 1983. **54**(6): p. 1635-40.
76. Oliven, A., G.S. Supinski, and S.G. Kelsen, *Functional adaptation of diaphragm to chronic hyperinflation in emphysematous hamsters*. J Appl Physiol (1985), 1986. **60**(1): p. 225-31.
77. Paiva, M., et al., *Mechanical implications of in vivo human diaphragm shape*. J Appl Physiol (1985), 1992. **72**(4): p. 1407-12.
78. Sieck, G.C., et al., *Mechanical properties of respiratory muscles*. Compr Physiol, 2013. **3**(4): p. 1553-67.
79. Whitelaw, W.A., *Shape and size of the human diaphragm in vivo*. J Appl Physiol (1985), 1987. **62**(1): p. 180-6.
80. Kim, M.J., et al., *Mechanics of the canine diaphragm*. J Appl Physiol, 1976. **41**(3): p. 369-82.
81. Shi, Z.H., et al., *Expiratory muscle dysfunction in critically ill patients: towards improved understanding*. Intensive Care Med, 2019. **45**(8): p. 1061-1071.
82. Bishop, B., *Reflex Control of Abdominal Muscles during Positive-Pressure Breathing*. J Appl Physiol, 1964. **19**: p. 224-32.
83. Russell, J.A. and B. Bishop, *Vagal afferents essential for abdominal muscle activity during lung inflation in cats*. J Appl Physiol, 1976. **41**(3): p. 310-5.
84. Laghi, F., et al., *Inhibition of central activation of the diaphragm: a mechanism of weaning failure*. J Appl Physiol (1985), 2020. **129**(2): p. 366-376.



85. Laghi, F., et al., *Diaphragmatic neuromechanical coupling and mechanisms of hypercapnia during inspiratory loading*. *Respir Physiol Neurobiol*, 2014. **198**: p. 32-41.
86. Lenherr, N., et al., *Leaks during multiple-breath washout: characterisation and influence on outcomes*. *ERJ Open Res*, 2018. **4**(1).
87. Cluzel, P., et al., *Diaphragm and chest wall: assessment of the inspiratory pump with MR imaging-preliminary observations*. *Radiology*, 2000. **215**(2): p. 574-83.
88. Mogalle, K., et al., *Quantification of Diaphragm Mechanics in Pompe Disease Using Dynamic 3D MRI*. *PLoS One*, 2016. **11**(7): p. e0158912.
89. De Troyer, A. and A.M. Boriek, *Mechanics of the respiratory muscles*. *Compr Physiol*, 2011. **1**(3): p. 1273-300.
90. Schepens, T., et al., *Diaphragm-protective mechanical ventilation*. *Curr Opin Crit Care*, 2019. **25**(1): p. 77-85.
91. Jonkman, A.H., D. Jansen, and L.M. Heunks, *Novel insights in ICU-acquired respiratory muscle dysfunction: implications for clinical care*. *Crit Care*, 2017. **21**(1): p. 64.
92. De Troyer, A., et al., *Triangularis sterni muscle use in supine humans*. *J Appl Physiol* (1985), 1987. **62**(3): p. 919-25.
93. Wilson, T.A., et al., *Respiratory effects of the external and internal intercostal muscles in humans*. *J Physiol*, 2001. **530**(Pt 2): p. 319-30.
94. De Troyer, A. and A. Legrand, *Mechanical advantage of the canine triangularis sterni*. *J Appl Physiol* (1985), 1998. **84**(2): p. 562-8.
95. De Troyer, A., P.A. Kirkwood, and T.A. Wilson, *Respiratory action of the intercostal muscles*. *Physiol Rev*, 2005. **85**(2): p. 717-56.
96. De Troyer, A., et al., *Transversus abdominis muscle function in humans*. *J Appl Physiol* (1985), 1990. **68**(3): p. 1010-6.
97. Abe, T., et al., *Differential respiratory activity of four abdominal muscles in humans*. *J Appl Physiol* (1985), 1996. **80**(4): p. 1379-89.
98. De Troyer, A., *Mechanical role of the abdominal muscles in relation to posture*. *Respir Physiol*, 1983. **53**(3): p. 341-53.
99. Loring, S.H. and J. Mead, *Abdominal muscle use during quiet breathing and hyperpnea in uninformed subjects*. *J Appl Physiol Respir Environ Exerc Physiol*, 1982. **52**(3): p. 700-4.
100. Damiani, F., et al., *Prevalence of Reverse Triggering Assessed by Electrical Activity of the Diaphragm in the First 48 Hours of Mechanical Ventilation*. *American Journal of Respiratory and Critical Care Medicine*, 2018. **197**.
101. Aliverti, A., et al., *Human respiratory muscle actions and control during exercise*. *J Appl Physiol* (1985), 1997. **83**(4): p. 1256-69.
102. Laghi, F., et al., *Is weaning failure caused by low-frequency fatigue of the diaphragm?* *Am J Respir Crit Care Med*, 2003. **167**(2): p. 120-7.
103. Suzuki, J., et al., *Assessment of abdominal muscle contractility, strength, and fatigue*. *Am J Respir Crit Care Med*, 1999. **159**(4 Pt 1): p. 1052-60.
104. Smith, J. and F. Bellemare, *Effect of lung volume on in vivo contraction characteristics of human diaphragm*. *J Appl Physiol* (1985), 1987. **62**(5): p. 1893-900.
105. Grimby, G., M. Goldman, and J. Mead, *Respiratory muscle action inferred from rib cage and abdominal V-P partitioning*. *J Appl Physiol*, 1976. **41**(5 Pt. 1): p. 739-51.
106. Derenne, J.P., P.T. Macklem, and C. Roussos, *Respiratory Muscles - Mechanics, Control, and Pathophysiology*.2. *American Review of Respiratory Disease*, 1978. **118**(2): p. 373-390.

107. Dodd, D.S., T. Brancatisano, and L.A. Engel, *Chest Wall Mechanics during Exercise in Patients with Severe Chronic Air-Flow Obstruction*. American Review of Respiratory Disease, 1984. **129**(1): p. 33-38.
108. Wolfson, D.A., et al., *Effects of an Increase in End-Expiratory Volume on the Pattern of Thoracoabdominal Movement*. Respiration Physiology, 1983. **53**(3): p. 273-283.
109. McCool, F.D., *Global physiology and pathophysiology of cough: ACCP evidence-based clinical practice guidelines*. Chest, 2006. **129**(1 Suppl): p. 48S-53S.
110. Langlands, J., *The dynamics of cough in health and in chronic bronchitis*. Thorax, 1967. **22**(1): p. 88-96.
111. Arora, N.S. and T.J. Gal, *Cough dynamics during progressive expiratory muscle weakness in healthy curarized subjects*. J Appl Physiol Respir Environ Exerc Physiol, 1981. **51**(2): p. 494-8.
112. Kravitz, R.M., *Airway clearance in Duchenne muscular dystrophy*. Pediatrics, 2009. **123** Suppl 4: p. S231-5.
113. Slutsky, A.S., *Lung injury caused by mechanical ventilation*. Chest, 1999. **116**(1 Suppl): p. 9S-15S.
114. Muscedere, J.G., et al., *Tidal ventilation at low airway pressures can augment lung injury*. Am J Respir Crit Care Med, 1994. **149**(5): p. 1327-34.
115. Talmor, D., et al., *Esophageal and transpulmonary pressures in acute respiratory failure*. Crit Care Med, 2006. **34**(5): p. 1389-94.
116. Tsuchida, S., et al., *Atelectasis causes alveolar injury in nonatelectatic lung regions*. Am J Respir Crit Care Med, 2006. **174**(3): p. 279-89.
117. Guervilly, C., et al., *Effects of neuromuscular blockers on transpulmonary pressures in moderate to severe acute respiratory distress syndrome*. Intensive Care Med, 2017. **43**(3): p. 408-418.
118. Pellegrini, M., et al., *The Diaphragm Acts as a Brake during Expiration to Prevent Lung Collapse*. Am J Respir Crit Care Med, 2017. **195**(12): p. 1608-1616.
119. Junhasavasdikul, D., et al., *Expiratory Flow Limitation During Mechanical Ventilation*. Chest, 2018. **154**(4): p. 948-962.
120. Mead, J., et al., *Significance of the relationship between lung recoil and maximum expiratory flow*. J Appl Physiol, 1967. **22**(1): p. 95-108.
121. Kafi, S.A., et al., *Expiratory flow limitation during exercise in COPD: detection by manual compression of the abdominal wall*. European Respiratory Journal, 2002. **19**(5): p. 919-927.
122. Zakynthinos, S.G., et al., *Contribution of expiratory muscle pressure to dynamic intrinsic positive end-expiratory pressure: validation using the Campbell diagram*. Am J Respir Crit Care Med, 2000. **162**(5): p. 1633-40.
123. Vallverdu, I., et al., *Clinical characteristics, respiratory functional parameters, and outcome of a two-hour T-piece trial in patients weaning from mechanical ventilation*. Am J Respir Crit Care Med, 1998. **158**(6): p. 1855-62.
124. Zeggwagh, A.A., et al., *Weaning from mechanical ventilation: a model for extubation*. Intensive Care Med, 1999. **25**(10): p. 1077-83.
125. Su, W.L., et al., *Involuntary cough strength and extubation outcomes for patients in an ICU*. Chest, 2010. **137**(4): p. 777-82.
126. Savi, A., et al., *Weaning predictors do not predict extubation failure in simple-to-wean patients*. J Crit Care, 2012. **27**(2): p. 221 e1-8.
127. Silva, C.S., et al., *Low mechanical ventilation times and reintubation rates associated with a specific weaning protocol in an intensive care unit setting: a retrospective study*. Clinics (Sao Paulo), 2012. **67**(9): p. 995-1000.
128. Kutchak, F.M., et al., *Reflex cough PEF as a predictor of successful extubation in neurological patients*. J Bras Pneumol, 2015. **41**(4): p. 358-64.

129. Lai, C.C., et al., *Establishing predictors for successfully planned endotracheal extubation*. Medicine (Baltimore), 2016. **95**(41): p. e4852.
130. Chao, C.M., et al., *Establishing failure predictors for the planned extubation of overweight and obese patients*. Plos One, 2017. **12**(8).
131. Hsieh, M.H., et al., *An Artificial Neural Network Model for Predicting Successful Extubation in Intensive Care Units*. Journal of Clinical Medicine, 2018. **7**(9).
132. Green, M., et al., *Tests of respiratory muscle strength*. American Journal of Respiratory and Critical Care Medicine, 2002. **166**(4): p. 528-547.
133. Savi, A., et al., *Weaning predictors do not predict extubation failure in simple-to-wean patients*. Journal of Critical Care, 2012. **27**(2).
134. Friedrich, O., et al., *The Sick and the Weak: Neuropathies/Myopathies in the Critically Ill*. Physiological Reviews, 2015. **95**(3): p. 1025-1109.
135. Lanone, S., et al., *Diaphragmatic fatigue during sepsis and septic shock*. Intensive Care Medicine, 2005. **31**(12): p. 1611-1617.
136. Lanone, S., et al., *Muscular contractile failure in septic patients - Role of the inducible nitric oxide synthase pathway*. American Journal of Respiratory and Critical Care Medicine, 2000. **162**(6): p. 2308-2315.
137. Lanone, S., et al., *Sepsis is associated with reciprocal expressional modifications of constitutive nitric oxide synthase (NOS) in human skeletal muscle: Down-regulation of NOS1 and up-regulation of NOS3*. Critical Care Medicine, 2001. **29**(9): p. 1720-1725.
138. Petrof, B.J. and S.N. Hussain, *Ventilator-induced diaphragmatic dysfunction: what have we learned?* Curr Opin Crit Care, 2016. **22**(1): p. 67-72.
139. Aliverti, A., et al., *Chest wall mechanics during pressure support ventilation*. Crit Care, 2006. **10**(2): p. R54.
140. Malbrain, M.L., et al., *The role of abdominal compliance, the neglected parameter in critically ill patients - a consensus review of 16. Part 1: definitions and pathophysiology*. Anaesthesiol Intensive Ther, 2014. **46**(5): p. 392-405.
141. Laghi, F. and M.J. Tobin, *Disorders of the respiratory muscles*. Am J Respir Crit Care Med, 2003. **168**(1): p. 10-48.
142. Tobin, M.J., F. Laghi, and A. Jubran, *Narrative review: ventilator-induced respiratory muscle weakness*. Ann Intern Med, 2010. **153**(4): p. 240-5.
143. Man, W.D., et al., *Cough gastric pressure and maximum expiratory mouth pressure in humans*. Am J Respir Crit Care Med, 2003. **168**(6): p. 714-7.
144. Rooban, N., et al., *Comparing intra-abdominal pressures in different body positions via a urinary catheter and nasogastric tube: a pilot study*. Ann Intensive Care, 2012. **2 Suppl 1**: p. S11.
145. Norisue, Y., et al., *Increase in intra-abdominal pressure during airway suctioning-induced cough after a successful spontaneous breathing trial is associated with extubation outcome*. Ann Intensive Care, 2018. **8**(1): p. 61.
146. Appendini, L., et al., *Physiologic effects of positive end-expiratory pressure and mask pressure support during exacerbations of chronic obstructive pulmonary disease*. Am J Respir Crit Care Med, 1994. **149**(5): p. 1069-76.
147. Parthasarathy, S., A. Jubran, and M.J. Tobin, *Cycling of inspiratory and expiratory muscle groups with the ventilator in airflow limitation*. Am J Respir Crit Care Med, 1998. **158**(5 Pt 1): p. 1471-8.
148. Jubran, A., W.B. Van de Graaff, and M.J. Tobin, *Variability of patient-ventilator interaction with pressure support ventilation in patients with chronic obstructive pulmonary disease*. Am J Respir Crit Care Med, 1995. **152**(1): p. 129-36.

149. Polkey, M.I., et al., *Functional magnetic stimulation of the abdominal muscles in humans*. Am J Respir Crit Care Med, 1999. **160**(2): p. 513-22.
150. Hamnegard, C.H., et al., *Diaphragm fatigue following maximal ventilation in man*. Eur Respir J, 1996. **9**(2): p. 241-7.
151. Kyrrousis, D., et al., *Abdominal muscle fatigue after maximal ventilation in humans*. J Appl Physiol (1985), 1996. **81**(4): p. 1477-83.
152. Bai, T.R., B.J. Rabinovitch, and R.L. Pardy, *Near-maximal voluntary hyperpnea and ventilatory muscle function*. J Appl Physiol Respir Environ Exerc Physiol, 1984. **57**(6): p. 1742-8.
153. Kyrrousis, D., et al., *Respiratory muscle activity in patients with COPD walking to exhaustion with and without pressure support*. Eur Respir J, 2000. **15**(4): p. 649-55.
154. Cabello, B. and J. Mancebo, *Work of breathing*. Intensive Care Med, 2006. **32**(9): p. 1311-4.
155. Vassilakopoulos, T., *Understanding wasted/ineffective efforts in mechanically ventilated COPD patients using the Campbell diagram*. Intensive Care Med, 2008. **34**(7): p. 1336-9.
156. Ninane, V., et al., *Abdominal muscle use during breathing in patients with chronic airflow obstruction*. Am Rev Respir Dis, 1992. **146**(1): p. 16-21.
157. Condessa, R.L., et al., *Inspiratory muscle training did not accelerate weaning from mechanical ventilation but did improve tidal volume and maximal respiratory pressures: a randomised trial*. J Physiother, 2013. **59**(2): p. 101-7.
158. Fregonezi, G., et al., *Muscle impairment in neuromuscular disease using an expiratory/inspiratory pressure ratio*. Respir Care, 2015. **60**(4): p. 533-9.
159. Gobert, F., et al., *Predicting Extubation Outcome by Cough Peak Flow Measured Using a Built-in Ventilator Flow Meter*. Respir Care, 2017. **62**(12): p. 1505-1519.
160. Matamis, D., et al., *Sonographic evaluation of the diaphragm in critically ill patients. Technique and clinical applications*. Intensive Care Med, 2013. **39**(5): p. 801-10.
161. McMeeken, J.M., et al., *The relationship between EMG and change in thickness of transversus abdominis*. Clin Biomech (Bristol, Avon), 2004. **19**(4): p. 337-42.
162. Misuri, G., et al., *In vivo ultrasound assessment of respiratory function of abdominal muscles in normal subjects*. Eur Respir J, 1997. **10**(12): p. 2861-7.
163. Rankin, G., M. Stokes, and D.J. Newham, *Abdominal muscle size and symmetry in normal subjects*. Muscle Nerve, 2006. **34**(3): p. 320-6.
164. Tahan, N., et al., *Measurement of superficial and deep abdominal muscle thickness: an ultrasonography study*. J Physiol Anthropol, 2016. **35**(1): p. 17.
165. Beduneau, G., et al., *Epidemiology of Weaning Outcome according to a New Definition. The WIND Study*. Am J Respir Crit Care Med, 2017. **195**(6): p. 772-783.
166. Penuelas, O., et al., *Characteristics and outcomes of ventilated patients according to time to liberation from mechanical ventilation*. Am J Respir Crit Care Med, 2011. **184**(4): p. 430-7.
167. Funk, G.C., et al., *Incidence and outcome of weaning from mechanical ventilation according to new categories*. Eur Respir J, 2010. **35**(1): p. 88-94.
168. Boles, J.M., et al., *Weaning from mechanical ventilation*. Eur Respir J, 2007. **29**(5): p. 1033-56.
169. Doorduyn, J., J.G. van der Hoeven, and L.M. Heunks, *The differential diagnosis for failure to wean from mechanical ventilation*. Curr Opin Anaesthesiol, 2016. **29**(2): p. 150-7.
170. Heunks, L.M. and J.G. van der Hoeven, *Clinical review: the ABC of weaning failure--a structured approach*. Crit Care, 2010. **14**(6): p. 245.

171. Hooijman, P.E., et al., *Diaphragm Muscle Fiber Weakness and Ubiquitin-Proteasome Activation in Critically Ill Patients*. American Journal of Respiratory and Critical Care Medicine, 2015. **191**(10): p. 1126-1138.
172. Hermans, G., et al., *Increased duration of mechanical ventilation is associated with decreased diaphragmatic force: a prospective observational study*. Crit Care, 2010. **14**(4): p. R127.
173. DiNino, E., et al., *Diaphragm ultrasound as a predictor of successful extubation from mechanical ventilation*. Thorax, 2014. **69**(5): p. 423-7.
174. Dres, M., et al., *Diaphragm electromyographic activity as a predictor of weaning failure*. Intensive Care Med, 2012. **38**(12): p. 2017-25.
175. Vassilakopoulos, T., S. Zakynthinos, and C. Roussos, *Respiratory muscles and weaning failure*. Eur Respir J, 1996. **9**(11): p. 2383-400.
176. Tobin, M.J., F. Laghi, and L. Brochard, *Role of the respiratory muscles in acute respiratory failure of COPD: lessons from weaning failure*. J Appl Physiol (1985), 2009. **107**(3): p. 962-70.
177. Kyroussis, D., et al., *Effect of maximum ventilation on abdominal muscle relaxation rate*. Thorax, 1996. **51**(5): p. 510-515.
178. Emeriaud, G., et al., *Diaphragm electrical activity during expiration in mechanically ventilated infants*. Pediatric Research, 2006. **59**(5): p. 705-710.
179. Allo, J.C., et al., *Influence of neurally adjusted ventilatory assist and positive end-expiratory pressure on breathing pattern in rabbits with acute lung injury*. Critical Care Medicine, 2006. **34**(12): p. 2997-3004.
180. Easton, P.A., et al., *Postinspiratory activity of costal and crural diaphragm*. Journal of Applied Physiology, 1999. **87**(2): p. 582-589.
181. Meessen, N.E.L., et al., *Continuous Negative Airway Pressure Increases Tonic Activity in Diaphragm and Intercostal Muscles in Humans*. Journal of Applied Physiology, 1994. **77**(3): p. 1256-1262.
182. Muller, N., A.C. Bryan, and N. Zamel, *Tonic Inspiratory Muscle-Activity as a Cause of Hyper-Inflation in Histamine-Induced Asthma*. Journal of Applied Physiology, 1980. **49**(5): p. 869-874.
183. Muller, N., et al., *Diaphragmatic Muscle Tone*. Journal of Applied Physiology, 1979. **47**(2): p. 279-284.
184. Doorduyn, J., et al., *Assisted Ventilation in Ards Patients: Lung-Distending Pressure and Patient-Ventilator Interaction*. Intensive Care Medicine, 2014. **40**: p. S156-S156.
185. Doorduyn, J., et al., *Assessment of dead-space ventilation in patients with acute respiratory distress syndrome: a prospective observational study*. Critical Care, 2016. **20**.
186. Doorduyn, J., et al., *Automated patient-ventilator interaction analysis during neurally adjusted non-invasive ventilation and pressure support ventilation in chronic obstructive pulmonary disease*. Critical Care, 2014. **18**(5).
187. Doorduyn, J., et al., *The Calcium Sensitizer Levosimendan Improves Human Diaphragm Function*. American Journal of Respiratory and Critical Care Medicine, 2012. **185**(1): p. 90-95.
188. Beck, J., et al., *Influence of bipolar esophageal electrode positioning on measurements of human crural diaphragm electromyogram*. Journal of Applied Physiology, 1996. **81**(3): p. 1434-1449.
189. Jubran, A. and M.J. Tobin, *Pathophysiologic basis of acute respiratory distress in patients who fail a trial of weaning from mechanical ventilation*. Am J Respir Crit Care Med, 1997. **155**(3): p. 906-15.
190. Sassoon, C.S., et al., *Pressure-time product during continuous positive airway pressure, pressure support ventilation, and T-piece during weaning from mechanical ventilation*. Am Rev Respir Dis, 1991. **143**(3): p. 469-75.
191. Fleury, B., et al., *Work of breathing in patients with chronic obstructive pulmonary disease in acute respiratory failure*. Am Rev Respir Dis, 1985. **131**(6): p. 822-7.

192. Frank, N.R., J. Mead, and B.G. Ferris, Jr., *The mechanical behavior of the lungs in healthy elderly persons*. J Clin Invest, 1957. **36**(12): p. 1680-7.
193. Field, S., S. Sanci, and A. Grassino, *Respiratory muscle oxygen consumption estimated by the diaphragm pressure-time index*. J Appl Physiol Respir Environ Exerc Physiol, 1984. **57**(1): p. 44-51.
194. Rochester, D.F. and G. Bettini, *Diaphragmatic blood flow and energy expenditure in the dog. Effects of inspiratory airflow resistance and hypercapnia*. J Clin Invest, 1976. **57**(3): p. 661-72.
195. Kayser, B., et al., *Respiratory effort sensation during exercise with induced expiratory-flow limitation in healthy humans*. J Appl Physiol (1985), 1997. **83**(3): p. 936-47.
196. Yan, S., et al., *Expiratory muscle pressure and breathing mechanics in chronic obstructive pulmonary disease*. Eur Respir J, 2000. **16**(4): p. 684-90.
197. Jaber, S., et al., *Clinical review: Ventilator-induced diaphragmatic dysfunction - human studies confirm animal model findings!* Critical Care, 2011. **15**(2).
198. Supinski, G.S. and L.A. Callahan, *Diaphragm weakness in mechanically ventilated critically ill patients*. Crit Care, 2013. **17**(3): p. R120.
199. Ebihara, S., et al., *Mechanical ventilation protects against diaphragm injury in sepsis: interaction of oxidative and mechanical stresses*. Am J Respir Crit Care Med, 2002. **165**(2): p. 221-8.
200. Akoumianaki, E., et al., *The application of esophageal pressure measurement in patients with respiratory failure*. Am J Respir Crit Care Med, 2014. **189**(5): p. 520-31.
201. Grasselli, G., et al., *Assessment of patient-ventilator breath contribution during neurally adjusted ventilatory assist*. Intensive Care Med, 2012. **38**(7): p. 1224-32.
202. Grams, S.T., et al., *Unidirectional Expiratory Valve Method to Assess Maximal Inspiratory Pressure in Individuals without Artificial Airway*. PLoS One, 2015. **10**(9): p. e0137825.
203. Vassilakopoulos, T., S. Zakynthinos, and C. Roussos, *The tension-time index and the frequency/tidal volume ratio are the major pathophysiologic determinants of weaning failure and success*. Am J Respir Crit Care Med, 1998. **158**(2): p. 378-85.
204. Bland, J.M. and D.G. Altman, *Measuring agreement in method comparison studies*. Stat Methods Med Res, 1999. **8**(2): p. 135-60.
205. Bland, J.M. and D.G. Altman, *Calculating correlation coefficients with repeated observations: Part 1--Correlation within subjects*. BMJ, 1995. **310**(6977): p. 446.
206. Bland, J.M. and D.G. Altman, *Calculating correlation coefficients with repeated observations: Part 2--Correlation between subjects*. BMJ, 1995. **310**(6980): p. 633.
207. Bellemare, F. and A. Grassino, *Effect of pressure and timing of contraction on human diaphragm fatigue*. J Appl Physiol Respir Environ Exerc Physiol, 1982. **53**(5): p. 1190-5.
208. Beck, J., et al., *Crural diaphragm activation during dynamic contractions at various inspiratory flow rates*. J Appl Physiol (1985), 1998. **85**(2): p. 451-8.
209. Bland, J.M. and D.G. Altman, *Correlation, regression, and repeated data*. BMJ, 1994. **308**(6933): p. 896.
210. Medin, D.L., et al., *Validation of continuous thermodilution cardiac output in critically ill patients with analysis of systematic errors*. J Crit Care, 1998. **13**(4): p. 184-9.
211. Watson, A.C., et al., *Measurement of twitch transdiaphragmatic, esophageal, and endotracheal tube pressure with bilateral anterolateral magnetic phrenic nerve stimulation in patients in the intensive care unit*. Crit Care Med, 2001. **29**(7): p. 1325-31.
212. Buscher, H., et al., *Assessment of diaphragmatic function with cervical magnetic stimulation in critically ill patients*. Anaesth Intensive Care, 2005. **33**(4): p. 483-91.
213. Baydur, A., E.J. Cha, and C.S. Sassoon, *Validation of esophageal balloon technique at different lung volumes and postures*. J Appl Physiol (1985), 1987. **62**(1): p. 315-21.



214. Roze, H., et al., *Neuro-ventilatory efficiency during weaning from mechanical ventilation using neurally adjusted ventilatory assist*. Br J Anaesth, 2013. **111**(6): p. 955-60.
215. Bartlett, J.W. and C. Frost, *Reliability, repeatability and reproducibility: analysis of measurement errors in continuous variables*. Ultrasound Obstet Gynecol, 2008. **31**(4): p. 466-75.
216. Shrout, P.E. and J.L. Fleiss, *Intraclass correlations: uses in assessing rater reliability*. Psychol Bull, 1979. **86**(2): p. 420-8.
217. Koo, T.K. and M.Y. Li, *A Guideline of Selecting and Reporting Intraclass Correlation Coefficients for Reliability Research*. J Chiropr Med, 2016. **15**(2): p. 155-63.
218. MacGregor-Fors, I. and M.E. Payton, *Contrasting Diversity Values: Statistical Inferences Based on Overlapping Confidence Intervals*. Plos One, 2013. **8**(2).
219. Sinderby, C., *Neurally adjusted ventilatory assist (NAVA)*. Minerva Anesthesiol, 2002. **68**(5): p. 378-80.
220. Bellani, G., et al., *Epidemiology, Patterns of Care, and Mortality for Patients With Acute Respiratory Distress Syndrome in Intensive Care Units in 50 Countries*. JAMA, 2016. **315**(8): p. 788-800.
221. Gainnier, M., et al., *Effect of neuromuscular blocking agents on gas exchange in patients presenting with acute respiratory distress syndrome*. Crit Care Med, 2004. **32**(1): p. 113-9.
222. Forel, J.M., et al., *Neuromuscular blocking agents decrease inflammatory response in patients presenting with acute respiratory distress syndrome*. Crit Care Med, 2006. **34**(11): p. 2749-57.
223. Papazian, L., et al., *Neuromuscular blockers in early acute respiratory distress syndrome*. N Engl J Med, 2010. **363**(12): p. 1107-16.
224. Slutsky, A.S., *Neuromuscular blocking agents in ARDS*. N Engl J Med, 2010. **363**(12): p. 1176-80.
225. Bennett, S. and W.E. Hurford, *When should sedation or neuromuscular blockade be used during mechanical ventilation?* Respir Care, 2011. **56**(2): p. 168-76; discussion 176-80.
226. Albuquerque, E.X., et al., *Mammalian nicotinic acetylcholine receptors: from structure to function*. Physiol Rev, 2009. **89**(1): p. 73-120.
227. Murray, M.J., et al., *Clinical Practice Guidelines for Sustained Neuromuscular Blockade in the Adult Critically Ill Patient*. Crit Care Med, 2016. **44**(11): p. 2079-2103.
228. Hunter, J.M., *New neuromuscular blocking drugs*. N Engl J Med, 1995. **332**(25): p. 1691-9.
229. Eglén, R.M., *Overview of muscarinic receptor subtypes*. Handb Exp Pharmacol, 2012(208): p. 3-28.
230. Fanelli, V., et al., *Neuromuscular Blocking Agent Cisatracurium Attenuates Lung Injury by Inhibition of Nicotinic Acetylcholine Receptor- $\alpha$ 1*. Anesthesiology, 2016. **124**(1): p. 132-40.
231. Sottile, P.D., D. Albers, and M.M. Moss, *Neuromuscular blockade is associated with the attenuation of biomarkers of epithelial and endothelial injury in patients with moderate-to-severe acute respiratory distress syndrome*. Crit Care, 2018. **22**(1): p. 63.
232. Brower, R.G., et al., *Ventilation with lower tidal volumes as compared with traditional tidal volumes for acute lung injury and the acute respiratory distress syndrome*. New England Journal of Medicine, 2000. **342**(18): p. 1301-1308.
233. National Heart, L., et al., *Early Neuromuscular Blockade in the Acute Respiratory Distress Syndrome*. N Engl J Med, 2019. **380**(21): p. 1997-2008.
234. Jansen, D., H. de Vries, and L.M.A. Heunks, *Acetylcholine receptor antagonists in acute respiratory distress syndrome: much more than muscle relaxants*. Crit Care, 2018. **22**(1): p. 132.
235. Abraham, E., et al., *Urokinase-type plasminogen activator potentiates lipopolysaccharide-induced neutrophil activation*. J Immunol, 2003. **170**(11): p. 5644-51.
236. Jonsson, M., et al., *Distinct pharmacologic properties of neuromuscular blocking agents on human neuronal nicotinic acetylcholine receptors: a possible explanation for the train-of-four fade*. Anesthesiology, 2006. **105**(3): p. 521-33.

237. Tracey, K.J., *The inflammatory reflex*. Nature, 2002. **420**(6917): p. 853-9.
238. Craige, S.M., S. Kant, and J.F. Keaney, Jr., *Reactive oxygen species in endothelial function - from disease to adaptation*. Circ J, 2015. **79**(6): p. 1145-55.
239. Jeong, J.S., et al., *Antioxidant effect of muscle relaxants (vecuronium, rocuronium) on the rabbit abdominal aortic endothelial damage induced by reactive oxygen species*. Korean J Anesthesiol, 2013. **65**(6): p. 552-8.
240. Poulard, T., et al., *Poor Correlation between Diaphragm Thickening Fraction and Transdiaphragmatic Pressure in Mechanically Ventilated Patients and Healthy Subjects*. Anesthesiology, 2022. **136**(1): p. 162-175.
241. Amato, M.B., et al., *Driving pressure and survival in the acute respiratory distress syndrome*. N Engl J Med, 2015. **372**(8): p. 747-55.
242. Bellani, G., et al., *Do spontaneous and mechanical breathing have similar effects on average transpulmonary and alveolar pressure? A clinical crossover study*. Crit Care, 2016. **20**(1): p. 142.



## RESEARCH DATA MANAGEMENT

### Ethics and privacy

Five chapters in this thesis are based on the results of medical-scientific research with human participants. The studies described in chapter 2, 4 and 8 were subject to the Medical Research Involving Human Subjects Act (WMO) and were conducted in accordance with the ICH-GCP guidelines (Good Clinical Practice). The institutional research ethical committee of the VUMC (chapter 2) and Radboudumc (chapter 4 and 8) have given approval to conduct these studies (file numbers: ethics ref. 2017.590; approval number 2010-058; CMO2299 2010/104). Informed consent was obtained from research participants. For chapter 5 and 6 the institutional ethical committee of the Radboudumc approved the study protocols and informed consent was waived due to the non-invasive nature of the study and negligible risks. Technical and organizational measures were followed to safeguard the availability, integrity and confidentiality of the data (these measures include the use of independent monitoring, pseudonymization, access authorization and secure data storage).

### Data collection and storage

Data for chapter 2, 4, 5 and 6 was collected through breath-by-breath analysis by Matlab (Matlab, R2018b; Mathworks, USA) and electronic Case Report Forms (eCRF) using CASTOR EDC. From here data were exported to SPSS (SPSS Inc., Chicago, Illinois, USA) and Graphpad (GraphPad Software, Inc., USA). Pseudonymized data were stored in encrypted Excel files on the department server and in Castor EDC and are only accessible by project members working at the Radboudumc / VUMC.

### Availability of data

All studies are published open access. The data will be archived for 15 years after termination of the study. Reusing the data for future research is only possible after a renewed permission by the participants. The anonymous datasets that were used for analysis are available from the corresponding author upon reasonable request.

## BIOGRAFIE



Diana Jansen werd geboren op 20 juli 1988 te Bladel. Na het behalen van haar VWO diploma aan het Pius X College te Bladel ging ze op kamers in Nijmegen om Geneeskunde te gaan studeren aan de Radboud Universiteit. Eind 2013 behaalde ze haar Master en ging aan de slag als ANIOS op de Intensive Care, eerst in het TweeSteden ziekenhuis in Tilburg en later in het vertrouwde Radboudumc in Nijmegen. Daar had ze aangegeven dat het haar leuk leek om de kliniek met

wetenschap te combineren en kwam zo in contact met prof. dr. Leo M.A. Heunks, expert op het gebied van beademing. Vanaf toen is haar enthousiasme voor wetenschap alleen maar toegenomen en besloot ze om in 2017 met haar promotie-traject te starten. Daarbij heeft ze zich voornamelijk gericht op klinische studies die het effect van beademing op de middenrifspier onderzochten en hoe je deze functie kunt monitoren en/of herstellen.

Omdat ze de kliniek niet volledig wilde verlaten, heeft ze het promotietraject gecombineerd met de opleiding Anesthesiologie. Inmiddels is ze afgestudeerd en met veel plezier werkzaam als anesthesioloog in de maatschap Anesthesiologie in het Elisabeth-Tweesteden ziekenhuis in Tilburg. En is haar ambitie om ook daar het doen van onderzoek meer van de grond te krijgen.

## PUBLICATION LIST

- D. Jansen** et al., Influenza A or B virus infection 2012-2013: incidence, characteristics and outcome in critically ill patients in two Dutch intensive care units. *Neth J Crit Care* – vol 18 – No 4 – Oct 2014.
- D. Jansen** et al., Tubular Injury Biomarkers to Detect Gentamicin- Induced Acute Kidney Injury in the Neonatal Intensive Care Unit. *Am J Perinatol* 2016;33:180–187.
- W.J.M. Schellekens, **D. Jansen**, M.J. Dorrestijn and L.M.A. Heunks, 'Recommended reading from Radboud University Medical Centre fellow – Diaphragmatic dysfunction in patients with ICU-acquired weakness and its impact on extubation failure'. *Am J Resp Crit Care Med*, Vol 195, Is 2, pp 258-260, Jan 15, 2017.
- A.H. Jonkman, **D. Jansen** and L.M.A. Heunks, chapter in 'Annual Update in Intensive Care 2017' entitled: 'Novel insights in ICU-acquired respiratory muscle dysfunction: implications for clinical care', dual publication in *Critical Care*. *Crit Care*. 2017 Mar 21;21(1):64.
- D. Jansen**, H. de Vries and L.M.A. Heunks, Acetylcholine receptor antagonists in acute respiratory distress syndrome: much more than muscle relaxants. *Crit Care*. 2018 May 22;22(1):132.
- J. Doorduyn, L.H. Roesthuis, **D. Jansen** et al., Respiratory muscle effort during expiration in successful and failed weaning from mechanical ventilation. *Anesthesiology*. 2018 Sep;129(3):490-501.
- D. Jansen**, A.H. Jonkman, L.H. Roesthuis et al., Estimation of the diaphragm neuromuscular efficiency index in mechanically ventilated critically ill patients. *Crit Care*. 2018 Sep 27;22(1):238.
- A.H. Jonkman, **D. Jansen**, S. Gadgil et al., Monitoring patient-ventilator breath contribution in the critically ill during neurally adjusted ventilatory assist: reliability and improved algorithms for bedside use. *J Appl Physiol*, 2019 Jul 1;127(1):264-271.
- Z.H. Shi, A.H. Jonkman, H. de Vries, **D. Jansen** et al., Expiratory muscle dysfunction in critically ill patients: towards improved understanding. *Intensive Care Med*. 2019 Aug;45(8):1061-1071
- D. Jansen**, A.H. Jonkman, H. de Vries et al., Positive end-expiratory pressure affects geometry and function of the human diaphragm. *J Appl Physiol*, 2021 Sept 2; 131:1328-1339.
- D. Jansen**, R. Bremer, G.J. Noordergraaf, Life-Saving Improvements after Implementation of Trauma Systems: Is it Good Enough and Can it also Work for you?. *Clin Surg*. 2021; 6: 3330.

## DANKWOORD

Ik zei vroeger altijd 'Nee, ik ga echt nooit promoveren, dat is niks voor mij!', maar dat liep toch anders dan verwacht... Als ANIOS op de Intensive Care wilde ik er graag iets bij doen, waarop ik het advies kreeg om eens bij Leo binnen te lopen want hij had vast nog een leuk onderwerp voor een onderzoek. Enkele maanden later lag mijn eerste onderzoeksprotocol bij de CMO en mocht ik samen met Suvarna aan de slag; binnen en buiten werktijd metingen doen bij beademde patiënten, om vervolgens urenlang alles met de hand te analyseren. Menig student zou al lang afgehaakt zijn, maar bij mij werd hier het zaadje geplant. Maar data aan de hand van printscreens van de beademingsmonitor analyseren was natuurlijk alles behalve professioneel dus we kregen al snel hulp van de technisch geneeskundige onder ons, Lianne en Annemijn. Ik raakte steeds enthousiaster en het woord 'promoveren' viel steeds vaker. Er was alleen nog wel een dingetje, want ondertussen was bekend dat ik was aangenomen voor de opleiding Anesthesie in het Radboudumc en Leo als intensivist in het VUmc in Amsterdam ging werken. Maar na goedkeuringen aan beide kanten was het officieel: ik ging dan toch promoveren!

Ondanks dat het soms (of stiekem best wel vaak) heel hard werken was om beide functies te combineren, had ik het niet anders willen doen. Maar dit alles was me niet gelukt zonder jou **Prof. Dr. Leo Heunks** als mijn promotor. Jij bent echt een voorbeeld voor mij **Leo**. Altijd enthousiast, en kritisch op het juiste moment. Het beste voor hebben met de patiënt, maar ook met ons als promovendi. Me vrij laten om te stoeien met de data, en sturing geven indien dit nodig was. Nooit te beroerd om tijd vrij te maken voor overleg, met vele mails over en weer op de meest onchristelijke tijdstippen. Jouw bevoegenheid werkt enorm aanstekelijk! En ik realiseerde me pas dat dit niet perse de standaard was toen ik op de verplichte bijeenkomsten van andere PhD studenten hoorde hoe anders het contact met hun promotor was. Ik ben dan ook enorm blij en trots op dat ik bij jou heb mogen promoveren. Ik heb super veel geleerd, en ook al was ik soms ongeduldig, door jou leerde ik inzien dat de aanhouder uiteindelijk wint. Ontzettend bedankt voor alles!

En het onderzoek had ik nooit kunnen combineren met de opleiding Anesthesie als ik niet de vrijheid en het vertrouwen had gekregen vanuit jullie **Prof. Dr. Gert-Jan Scheffer** en **dr. Christiaan Keijzer**. Vanaf het begin af aan hebben jullie geloofd in mijn kunnen, ook al twijfelde ik er soms zelf aan. En hoewel de term 'persoonlijk opleidingsplan' in die tijd vaak vooral mooie woorden waren, hebben jullie er ook echt werk van gemaakt **Gert-Jan** en **Christiaan**. Altijd bereid om met me mee te denken, te kijken hoe ik het doen van onderzoek kon laten passen met de kliniek.

En natuurlijk stond officieel de vorming tot 'een volwaardige anesthesioloog' voorop, maar dat nam niet weg dat ik me niet verder mocht ontwikkelen; of het nu ging om het bezoeken van een congres, het volgen van een cursus persoonlijk leiderschap of de verdieping 'Urgentie-geneeskunde', alles was mogelijk. Hierdoor ben ik enorm gegroeid, als jonge dokter, maar ook als persoon. Dank jullie wel voor die onvoorwaardelijke steun!

**Dr, Lucas van Eijck.** Je sloot pas relatief laat als co-promotor aan bij mijn onderzoekstraject **Lucas**, maar dat wil niet zeggen dat ik je daardoor minder waardeer. Het is fijn om iemand om je heen te hebben die zelf nog niet zo lang geleden gepromoveerd is, en daardoor net wat beter snapt in welke schuitje je zit. Altijd bereid om te helpen en vol met goede tips, heel erg bedankt!

We waren allebei ANIOS op de IC, en wat hebben wij samen veel uren door gebracht voor de beademingsmachine en achter de computer **Suvarna Gadgil**. Printscreens maken, analyses doen, eerst met de hand gewoon op papier, en toen toch alles nog maar eens over gedaan zodat we het digitaal konden bijhouden. Het heeft even geduurd, maar uiteindelijk is het onderzoek enkele jaren later dan toch gepubliceerd. Na onze tijd op de IC zijn we allebei aangenomen voor de opleiding Anesthesie, weliswaar in een andere stad, maar contact hebben we altijd gehouden. Samen studeren, bij jou of mij aan de keukentafel, en één keer zijn we er zelfs voor naar Londen gegaan. Je bruisende energie en super attente karakter is echt uniek. Dankjewel voor wie je bent!

**Annemijn Jonkman**, ik weet niet zo goed waar ik moet beginnen. Maar zonder jou had ik geen van deze onderzoeken kunnen uitvoeren zoals ze zijn uitgevoerd. We waren een gouden koppel, ik met een meer klinische blik, en jij met een technische, en zo hebben we super veel van elkaar geleerd. Oneindig veel geduld moeten hebben met de analyses van de NME en PVBC, maar uiteindelijk toch gelukt omdat jij de ruis van de signalen wist te halen met je eigen geschreven algoritme. Voor mij nog steeds één grote abracadabra maar respect en vol lof voor jouw kunde. Daarnaast een hele leuke tijd gehad in Amsterdam, waar we samen alle metingen rondom de PEEP studie hebben gedaan. Een geoliede machine. Met vaak in de weekenden nog de metingen onder de MRI, maar daar maakten we dan maar gewoon een feestje van, met aansluitend een lekkere lunch bij Loetje als beloning. Dankjewel voor je altijd luisterende oor, de vele congresbezoekjes met aansluitend etentjes & borrels, voor je onuitputtelijke energie t.a.v. onderzoek doen waardoor ik ook zelf een tandje harder ging lopen. Heel veel succes gewenst in Rotterdam, maar ik heb er alle vertrouwen in dat je daar een hele mooie onderzoekslijn gaat opzetten!

Gelukkig had ik ook in Nijmegen altijd twee technisch geneeskundige in de buurt die ik kon raadplegen als ik er niet uit kwam met de metingen of analyses. Fijn dat ik gewoon even bij jullie kon lopen **Jonne Doorduyn**, en **Lisanne Roesthuis**. **Jonne** daarnaast heel erg bedankt voor je hulp en feedback op veel van mijn stukken. En **Lisanne**, bedankt voor je hulp bij de metingen en analyses van de NME.

En ook vanuit de hoek van de biomedische wetenschappen en immunologie heb ik hulp gekregen. Leuk om eens vanuit een andere invalshoek naar een onderwerp te leren kijken. Bedankt **Matthijs Kox** voor het mee denken over de opzet en de analyses van de NMBA studie. En zonder jou **Jelle Gerretsen** waren de analyses van de cytokines en ROS in het lab waarschijnlijk één grote flop geworden.

**Prof. Dr. Peter Pickkers** kende ik al van mijn allereerste wetenschapsstage tijdens de studie Geneeskunde. Dat was heel bijzonder, want ik mocht onderzoek doen op de neonatale ICU, waar ik urine van de neonaatjes verzamelde om te onderzoeken op tubulaire schademarkers. Jaren later lag de vriezer er nog vol mee, want je wist nooit of je het nog kon gebruiken haha. Ik was dan ook blij dat jij mijn mentor wilde zijn. Gelukkig was er weinig te bespreken met zo'n top team om me heen, maar dan werd het gewoon even gezellig bijkletsen, iets wat op jouw naam geschreven staat. Dankjewel voor alles, en ook dat ik tijdens de NMBA studie hulp heb gekregen van jouw subdivisie op de IC.

**Prof. Dr. Hans van der Hoeven**, de IC in Nijmegen stond mede namens jouw aanwezigheid hoog aangeschreven en ik was dan ook heel blij dat ik daar als ANIOS mocht beginnen. Ik heb enorm veel bewondering voor jouw ontoreikende kennis, altijd up-to-date van de laatste vernieuwingen binnen de gezondheidszorg en de meest recente literatuur. Je kon geen studie aanhalen of je had hem gelezen en wist de samenvatting en kritische punten van het onderzoek zonder problemen te benoemen. Maar desondanks altijd benaderbaar, welwillend om ons te leren, en dat is altijd zo gebleven. Ook toen ik als AIOS Anesthesiologie terug kwam en in het fellow-rooster mee mocht draaien. Heel erg bedankt daarvoor. En daarnaast ook bedankt dat ik op jouw IC een heel groot deel van mijn onderzoek heb mogen uitvoeren. Een team van verpleegkundigen, research verpleegkundigen, arts-assistenten en medisch specialisten die altijd bereid waren om te helpen en ook het nut van onderzoek doen in zag. Heel erg fijn om daar onderdeel van uit te hebben mogen maken!

Tijdens mijn opleiding ben ik negen maanden naar het VUmc in Amsterdam gegaan voor het doen van onderzoek. Vanuit het dorp waar ik woon naar de grote stad,

waarbij ik er al snel achter kwam dat ik beter maar heel vroeg in de auto of trein kon zitten wilde ik niet te lang onderweg zijn. Dus ik heb vele zonsopkomsten en -ondergangen vanuit de auto bewonderd, maar dat was het dubbel en dwars waard. Dankjewel Armand Girbes, dat ik bij jou op de IC mocht komen voor mijn onderzoeken. De planning was eigenlijk om erheen te gaan voor de inclusie van de Relax-studie, echter ging de aanvraag bij de medisch ethische commissie wat moeizamer dan aanvankelijk gepland. Maar daar werd al snel iets op bedacht want er waren ook plannen om de effecten van PEEP op het middenrif te onderzoeken en die goedkeuring kwam wat sneller van de grond. De inclusie ging als een speer en we raakten als team goed op elkaar ingespeeld tijdens de fysiologische metingen. Mijn dank ik groot voor jullie hulp **Heder de Vries, Myrthe Wennen, Judith Elshof** en **Maud Hoofs**. Met daarnaast hele waardevolle hulp van **Tim Marcus** bij het opstellen van het uitgebreide MRI-protocol en de uitvoering van de uitzonderlijk nauwkeurige MRI metingen, ook in de avond en weekenduren. **Heder**, daarnaast bedankt voor je gezelligheid op de kamer, altijd wat aan de late kant aanwezig, maar dat maakte je dubbel en dwars goed met je tomeloze enthousiasme. Altijd kritisch bij de discussie over de analyses, de juiste vragen stellend, maar dat hield ons wel scherp. Zelf inmiddels ook bijna gepromoveerd en onderweg naar het worden van longarts-intensivist. Veel succes gewenst, en ik weet zeker dat ze een goede arts / wetenschapper aan je hebben! **Sander Rozemeijer**, jij bent echt een bijzonder persoon. Ook al had je niks met het diafragma onderzoek van doen, toch zat je bij ons op de kamer. En dat was ontzettend fijn. Altijd vragen hoe het ging, hoe het weekend was en wat je dwars zat. En je bent geen opgever, je studie kwam wat lastig van de grond maar toch bleef je ervoor gaan, dat siert je. Inmiddels ook in opleiding bij de Anesthesiologie, heel veel succes gewenst en wie weet zien we elkaar nog ooit ergens op een congres.

**Prof. Dr. Coen Ottenheijm**, wat heb ik veel van je kunnen leren over de fysiologie van het diafragma. Fascinerend wat jij allemaal in het lab heb onderzocht op microscopisch gebied. Dat bracht ons op het idee om de PEEP studie te gaan doen. Kijken of wat jij in het rattenmodel had gevonden ook optrad bij onze gezonde vrijwilligers. We konden natuurlijk geen biopten afnemen maar met behulp van de MRI beelden en de uitkomsten van de fysiologische metingen hebben we wel de basis kunnen leggen en aan kunnen tonen dat de longitudinale atrofie zeer waarschijnlijk ook bij ons als mens optreedt. Daarnaast heel erg bedankt voor je input bij de wekelijkse overleggen.

Al deze onderzoeken, inclusies en uitkomsten had ik nooit kunnen doen / bereiken als ik niet de onvoorwaardelijke steun had gekregen van alle verpleegkundige,

arts-assistenten, medisch specialisten, ondersteunend personeel, research verpleegkundige. En niet te vergeten, van alle patiënten en/of families die hebben ingestemd met het doen van het onderzoek. En alle gezonde vrijwilligers die zich bloot wilde stellen aan onze handelingen. Ontzettend bedankt daarvoor!

En daarnaast dank aan alle leden van de manuscript commissie, voor jullie bereidheid om mijn proefschrift aandachtig te bestuderen en tijd vrij te maken om deze dag om mijn verdediging waar te kunnen maken.

Daarnaast wil ik nog een paar mensen in mijn nabije omgeving bedanken.

Allereerst **Amy van den Berg**, mede AIOS Anesthesiologie met daarnaast een hele mooie hobby. Heel erg leuk dat jij met mij wilde nadenken over de cover en ik ben super blij met het resultaat!

De opleiding Anesthesie combineren met het promotie traject vergde de nodige inspanning, met vele avonden en weekenden die daaraan besteed werden. Dat werd niet altijd helemaal begrepen, want 'waarom werk je al die uren zonder dat je er voor betaald krijgt?' Maar of jullie het nu wel of niet begrepen, de onvoorwaardelijke steun was er altijd vanuit jullie dames van GZM. Als afleiding van het harde werken hebben we hele mooie jaren samen gehad (en nog steeds); stappen, etentjes, vakanties, puzzel- en spelletjesavonden, borrels en gewoon bijkletsen zoals alleen dames dat kunnen. En ook al heb ik het nooit als zodanig benoemd, toch was het een welkome afwisseling met de volle dagen in het ziekenhuis / thuis aan de laptop en alles wat er thuis speelde. Dus heel erg bedankt daarvoor **Wout, Adams, Nien, Roest, Sas, Britt, Vera en Stone**.

De geneeskunde opleiding heb ik samen met jullie doorgebracht **Anne, Anne, Eefje, Elke en Katrien** (ook wel bekend als AADEEK), en het was heel fijn om die basis te hebben. Allemaal een hele andere kant op gegaan na de opleiding, maar dat maakt het juist leuk. Van een dokter die al vanaf het begin van de opleiding riep dat ze geen dokter wilde worden, maar toch als eerste gespecialiseerd was en de beste is voor haar patiënten. Tot aan een superspecialisatie tot kinderneuroloog, en alles daartussen. Een paar jaar terug hebben we ons 15-jarig jubileum gevierd met een weekendje weg in onze vertrouwde stad Nijmegen. En ook nu zien we elkaar nog heel regelmatig om bij te kletsen. Als mede dokters snapten jullie een heel stuk beter waarom ik toch al die uren in het werk stopte en voelde ik ook de steun als ik het even niet meer zag zitten. Dankjewel voor de enorme fijne tijd die we gehad hebben en nog steeds hebben.



De opleiding Anesthesie zijn we met zijn vieren gestart, **Rachel, Tess, Rianne** en ik. Het klikte meteen heel goed, dus het idee was al snel ontstaan om een potje te maken. Iedere maand geld lappen, zodat we aan het einde van onze opleiding naar de Librije konden gaan. Dat was echt top. En ondanks dat we inmiddels allemaal afgestudeerd zijn is er ééntje nog steeds chronisch blut. Dus dat potje is blijven bestaan en we gaan nog steeds regelmatig een hapje eten om even bij te kletsen. Super bedankt voor de steun die ik van jullie heb gehad tijdens de opleiding. Ik had me geen beter groepje kunnen wensen!

En als laatste wil ik toch wel mijn zus bedanken, **Ilona**. Van grote kleine zus, tot proefpersoon, ze ondergaat het allemaal, met af en toe wat horde en stoten (lees: braakneigingen bij het inbrengen van de catheters voor het onderzoek), maar toch zette je door want je wilde zo graag mee doen en mij helpen. En dat is kenmerkend voor jou als persoon. Altijd vertrouwen hebben in de ander, de ander willen helpen, soms ten koste van jezelf. Maar toch is die onvoorwaardelijke liefde heel erg fijn! Bedankt voor wie je bent!

En nu ben ik vast nog een hele hoop namen vergeten, en dat ligt niet aan jullie, maar aan mijn geheugen ;) dus voor alle mensen die in de zaal zitten, die een bijdrage hebben geleverd en niet hier in dit boekje vermeld staan, toch heel erg bedankt voor jullie komst en steun! En dan komt aan mijn promotie nu echte een einde. Ik heb ontzettend genoten van de reis, veel geleerd en ik had het voor geen goud willen missen!

Liefs, Diana





**Radboudumc**  
university medical center

**Radboud University**

